2012-08-10

A Novel Communication Mechanism Between the Presynapse and Postsynapse Through Exosomes: A Dissertation

Ceren Korkut
University of Massachusetts Medical School

A NOVEL COMMUNICATION MECHANISM BETWEEN THE PRESYNAPSE AND POSTSYNAPSE THROUGH EXOSOMES

A Dissertation Presented

by

Ceren Korkut

Submitted to the Faculty

University of Massachusetts Graduate School of Biomedical Sciences, Worcester

in partial fulfillment of the requirements for the degree of

DOCTOR OF PHILOSOPHY

August 10, 2012

Neuroscience

A NOVEL COMMUNICATION MECHANISM BETWEEN THE PRESYNAPSE AND POSTSYNAPSE THROUGH EXOSOMES

A Dissertation Presented
By
Ceren Korkut
The signatures of the Dissertation Defense Committee signify completion and approval as to style and content of the Dissertation

---

Vivian Budnik, Ph.D. Thesis Advisor

Mark J. Alkema, Ph.D. Member of Committee

Mary Munson, Ph.D. Member of Committee

Motojiro Yoshihara, Ph.D. Member of Committee

Paul Garrity, Ph.D. Member of Committee

The signature of the Chair of the Committee signifies that the written dissertation meets the requirements of the Dissertation Committee.

Marc Freeman, Ph.D. Chair of Committee

The signature of the Dean of the Graduate School of Biomedical Sciences signifies that the student has met all graduation requirements of the school.

Anthony Carruthers, Ph.D.,
Dean of the Graduate School of Biomedical Sciences

Program in Neuroscience
August 10, 2012

ACKNOWLEDGEMENTS

It would have not been possible to finish my doctoral training without the help and support of a long list of kind people. First and foremost, I would like to express my most sincere gratitude to my advisor Dr. Vivian Budnik for her continuous guidance and generous support throughout my doctoral career. I would like to thank the present and former members of the Budnik lab including Dr. Preethi Ramachandran, Dr. James Ashley, Dr. Kate Koles, Romina Barria, John Nunnari, Yihang Li, Dr. Cassandra Brewer and Norberto Gherbesi for invaluable help with my projects and scientific discussions. I would like to give special thanks to Dr. Bulent Ataman for his support during the initial stages of my doctoral career. I also thank Dr. Motojiro Yoshihara for stimulating scientific discussions and various suggestions. I would like to extend my gratitude to the rest of my committee members Dr. Marc Freeman, Dr. Mary Munson, Dr. Mark Alkema, and Dr. Paul Garrity for their time and input about my graduate studies. Moreover, I would like to thank the faculty of Neurobiology Department at UMass Medical School as well as Dr. Deniz Erturk-Hasdemir for her generous help.

Finally, I would like to express my deep gratitude to my beloved husband Erman Korkut. Without his love, encouragement and patience, I would not have been able to pursue my degree. I also thank my parents Sule Tezer and Kemal Tezer as well as my sister Irem Tezer for their huge support and encouragement at every step of my life. Additionally, I would like to thank the rest of my supportive family and all my friends, especially Tuba Bas, Esra Korkut, Ozge Tasdemir, Aysegul Demirtas and Esra Gokce.

ABSTRACT

The minimal element of the nervous system, the synapse, is a plastic structure that has the ability to change in response to various internal and external factors. This property of the synapse underlies complex behaviors such as learning and memory. However, the exact molecular and cellular mechanisms involved in this process are not fully understood. To understand the mechanisms that regulate synapse development and plasticity I took advantage of a powerful model system, the *Drosophila* larval neuromuscular junction (NMJ). In this system, both anterograde and retrograde signaling pathways critical for coordinated synapse development and plasticity have been documented.

An anterograde WNT/Wingless (Wg) signaling pathway plays a crucial role in both developmental and activity-dependent synaptic plasticity at the NMJ. Presynaptic motor neuron terminals secrete highly hydrophobic Wg, which travels to relatively distant postsynaptic sites where it activates a signal transduction pathway required for postsynaptic development. In the first half of my thesis I unraveled a previously unrecognized cellular mechanism by which Wg is shuttled to postsynaptic sites. In this mechanism Wg rides on secreted microvesicles or exosomes that contain a dedicated WNT secretion factor, the WNT-binding transmembrane protein, Evenness Interrupted/Wntless/Sprinter (Evi/Wls/Srt). To our knowledge, this was the first *in vivo* study demonstrating that neurons release exosomes, which are involved in trans-synaptic communication. Moreover, this was the first study showing that hydrophobic

WNT signals are transported to the extracellular space on exosomes to reach WNT-receptor containing target cells.

Retrograde signals are also critical during development and plasticity of synaptic connections. These signals function to adjust the activity of presynaptic cells according to postsynaptic cell outputs, to maintain synaptic function within a dynamic range. However, the mechanisms that trigger the release of retrograde signals and the role of presynaptic cells in this signaling event are not clear. In the second half of my thesis, I provided evidence that a crucial component of retrograde signaling at the fly NMJ, Synaptotagmin-4 (Syt4), is transmitted to the postsynaptic cell through anterograde delivery of Syt4 via exosomes. *Drosophila* Syt4 is known to reside on postsynaptic vesicles at the NMJ and function as a calcium sensor to release a retrograde signal upon synaptic activity. This event is required for coordinated maturation of the presynaptic terminal. We demonstrated that retrograde Syt4 function in postsynaptic muscle is required for activity-dependent presynaptic growth. However, surprisingly, Syt4 protein was not synthesized in postsynaptic muscles. Instead, Syt4 was produced in motorneurons and transferred to postsynaptic muscle cells via exosome secretion by presynaptic cells. The above study provided evidence for a presynaptic control of postsynaptic retrograde signaling through exosomal transfer of an essential retrograde signaling component.

In summary, this body of work reveals a novel mechanism of *trans*-synaptic communication through exosomes. While intercellular communication through exosomes had been demonstrated during antigen presentation in the

immune system, our studies were the first to substantiate this mode of communication in the nervous system. Thus, these studies provide a significantly deeper and novel understanding of the mechanisms underlying synapse development and plasticity.

TABLE OF CONTENTS

Page

LIST OF FIGURES

LIST OF NOMENCLATURE

BDNF- Bone-derived Neurotrophic Factor

BMP – Bone Morphogenetic Protein

Brp – Bruchpilot

cAMP – Cyclic Adenosine Monophosphate

ChR2 – Channelrhodopsin2

CNS – Central nervous system

DFz2 – *Drosophila* Frizzled-2

dGRIP – *Drosophila* homolog of Glutamate-Receptor-Interacting Protein

DLG – Discs-large

DRL-Derailed

DVL-Disheveled

Eag – Ether a go-go

ESCRT- Endosomal Sorting Complex Required for Transport

EJP – Excitatory Junctional Potential

EM- Electron Microscopy

Evi- Evenness Interrupted, aka Wntless (Wls)

FasII – Fasciclin II

FNI – Frizzled Nuclear Import pathway

GFP – Green Fluorescent Protein

GluR – AMPA-type glutamate receptor

GPI – Glycosylphosphatidylinositol

GSK3β- Glycogen Synthase Kinase 3 beta

HRP- Horseradish Peroxidase

Hrs- Hepatocyte Growth Factor (HGF) 1-regulated tyrosine kinase substrate

JNK- JUN N-terminal kinase

LTD – Long Term Depression

LTP – Long Term Potentiation

LRP- Low Density Lipoprotein Receptor-related Protein

MAP1B – Microtubule Associated Protein 1B

mEJP – Miniature Excitatory Junctional Potential

MHC- Myosin Heavy Chain

MT – Microtubule

MVB- Multivesicular Body

Myr-mRFP- Myrisylated monomeric red fluorescent protein

NGF- Nerve Growth Factor

NLS- Nuclear Localization Signal

NMJ – Neuromuscular Junction

NpHR- Halorhodopsin from *N. pharaonis*

PDZ – Postsynaptic Density-95/Discs-large/Zona Ocludens

PKC – Protein Kinase C

PNS – Peripheral Nervous System

RFP – Red Fluorescent Protein

RNAi – RNA Interference

RT-PCR- Reverse transcription- polymerase chain reaction

S2- *Drosophila* Schneider-2 cells

Sgg – Shaggy, *Drosophila* homolog of GSK3-β

SSR – Subsynaptic Reticulum

SNARE – Soluble NSF attachment receptor

Syt4 – Synaptotagmin 4

TGF-β – Transforming Growth Factor β

Wg – Wingless (*Drosophila* WNT-1)

WNT- Wingless-Int-1

CHAPTER 1

INTRODUCTION

Part of the following chapter is reprinted from a *Nature Reviews in Neuroscience* review (Korkut, C. and Budnik, V. (2009). WNTs tune up the neuromuscular junction. *Nat Rev Neurosci.* 10(9): 627-634.)

Neural circuits in the nervous system consist of highly specific neuronal connections, which are the basis for sensory, motor and cognitive abilities. The single unit of this complex network is the synapse, where communication between a neuron and its target cell takes place. Both simple and complex behaviors such as learning and memory depend on the ability of synapses within relevant circuits to change structurally and functionally upon various internal and external factors. This phenomenon is called synaptic plasticity. This flexibility of synaptic connections is pivotal for the adaptation of an organism to a changing environment. Although the term ‘’plasticity’’ in neuroscience was coined over a century ago, the exact underlying molecular and cellular mechanisms are still a matter of intense investigation.

William James in his *Principles of Psychology* was the first to link brain plasticity to behavior in 1890 (James, 1890). However, the pioneering neuroscientist, Ramon y Cajal established the first real conceptual foundation for neural plasticity and its association with learning (Berlucchi and Buchtel, 2009). Cajal proposed that the nervous system was composed of individual neurons that are separated by specialized tiny spaces. This hypothesis became to known as the ‘’Neuron Doctrine’’ (Cajal, 1906; De Felipe, 2002). Cajal also showed that regenerative plasticity took place in central nervous system (CNS) neurons by demonstrating the ability of these neurons to grow new axons after injury. Prior to this, regenerative plasticity had only been described in peripheral nervous system (PNS) neurons (De Felipe, 2002). The findings of the ‘’father of modern neuroscience’’ led neuroscientists to investigate synaptic plasticity as well as the

mechanisms underlying this phenomenon further.

Several decades later, in 1949, the first attempt to explain the biological mechanisms underlying synaptic plasticity came fro m Donald Hebb, who postulated that “when axon of cell A is near enough to excite a cell B and repeatedly and persistently takes part in firing it, some growth process or metabolic change takes place in one or both cells such that A’s efficiency as one of the cells firing B is increased” (Hebb, 1949). The firing of two neurons not only increases the strength of their synapses but also results in morphological changes at the synapses. The Hebbian rule ‘’neurons that fire together wire together’’ (Brown and Milner, 2003; Hebb, 1949) has been a foundation for understanding the formation of neural networks and how these networks control behavior.

Bliss and Lomo presented supporting evidence to the Hebbian theory with the discovery of the phenomenon of Long Term Potentiation (LTP) in 1973 (Bliss and Lomo, 1973). Briefly, upon high frequency stimulation of presynaptic neurons, a dramatic increase in the excitatory postsynaptic potential as well as a decrease in the threshold to fire an action potential takes place and these changes last from a few hours to days, depending on the stimulation paradigm used. The phenomenon of LTP is thought to be the cellular model for synapse strengthening and memory formation. In addition to functional changes such as alterations in presynaptic neurotransmitter release and postsynaptic receptor clustering, LTP also induces structural changes at the synapse including an increase in both postsynaptic spine size and number (Lang et al., 2004;

Leenders and Sheng, 2005). A specific type of glutamate receptors, known as N-Methyl-D-Aspartate (NMDA) receptor has been demonstrated to be required for LTP and therefore critical for synaptic plasticity (Collingridge et al., 1983). These postsynaptic NMDA receptors function as ‘’coincidence detectors’’ that couple two simultaneous events: (1) the release of glutamate by the presynaptic cell; (2) the depolarization of the postsynaptic cell membrane induced by glutamate gating of a second class of glutamate receptor, AMPA receptors. This event serves to relieve a Mg^{++} block of NMDA receptors at resting potentials (Bourne and Nicoll, 1993). Opening of NMDA receptors allow calcium influx into the postsynaptic cell. Subsequently, the increased intracellular calcium concentration triggers signal transduction pathways such as the activation of Calcium/Calmodulin Kinase II (CaMKII) and cyclic adenosine monophosphate (cAMP) pathways. These pathways then lead to both short-term changes, including local receptor phosphorylation, and long-term changes through regulation of gene transcription and new protein synthesis (Alberini et al., 1995; Lynch et al., 1983; Malenka et al., 1988). One piece of evidence for the association between memory formation and LTP was demonstrated in a study where blocking NMDA receptors in rodents inhibited spatial memory formation (Morris et al., 1986). However, it is clear that LTP is not the entire story, as other forms of memory are not affected by defective LTP (Lynch, 2004).

In contrast to synaptic strengthening by LTP, synaptic depression is thought to occur through a phenomenon called Long Term Depression (LTD), which results from low frequency stimulation for long periods (Ito and Kano,

1982). Consequently, the postsynaptic cell generates a decreased response and spine size and number are reduced. LTP and LTD have been studied profoundly in mammalian models, such as hippocampal slices. However, simpler model organisms provide the ability to study mechanisms underlying synaptic plasticity in the context of intact organisms.

The sea slug *Aplysia californica* has been an excellent model organism to study long-term plasticity. Using the simple ‘’gill and siphon withdrawal reflex’’ of *Aplysia* as a behavioral output*,* important synaptic processes like sensitization, facilitation and habituation have been characterized (Pittenger and Kandel, 2003). In addition to *Aplysia*, the fruit fly *Drosophila melanogaster* has been an invaluable model to study long-term behavioral plasticity using mushroom body neurons, which are implicated in olfactory memory, as a model system (De Belle and Heisenberg, 1994; Heisenberg et al., 1985). Although combined with the powerful genetic approaches possible in flies this has been a highly successful model, a fine analysis of structural changes at the level of single synapses has been more difficult, due to their small size.

In my thesis research, I used the *Drosophila* larval neuromuscular junction (NMJ), a prime model to understand the molecular and cellular mechanisms of synaptic plasticity at identified synapses.

The *Drosophila* Larval Neuromuscular Junction: A model to study synapse development, plasticity and function

The fruit fly *Drosophila melanogaster* larval neuromuscular junction (NMJ) is a powerful *in vivo* model system to study a wide number of neuroscientific processes relevant to synapse biology, such as neurotransmitter release, ion channel function, synapse physiology, axon pathfinding and molecular mechanisms of synapse formation, development and plasticity (Ruiz-Canada and Budnik, 2006). The highly conserved mechanisms and molecules involved in these neurobiological processes across species makes the findings using this model highly relevant for all organisms.

In addition to the advantages of using *Drosophila,* such as its short life cycle and the availability of powerful genetic tools, the easy accessibility of the large NMJ synapses has made it a popular system. The NMJ model provides the ability to study synapses at single cell resolution, which is quite challenging to achieve within brain tissue. Individual motorneurons innervate postsynaptic muscle cells in a very stereotypic fashion, which allows researchers to observe and compare differences in the same synapse of multiple animals. This is in contrast to central synapses in the brain, where billions of synaptic connections are formed. Moreover, the cuticle of fruit fly larva is both transparent and thin; therefore, synaptic proteins can be easily visualized both as live and fixed preparations using microscopy techniques. Live imaging of fluorophore tagged molecules through the cuticle of intact larvae allows for observing changes over a significant time span during larval development (Koon and Budnik, 2012; Parnas

et al., 2001; Zito et al., 1999).

Another reason why the *Drosophila* larval NMJ has been used extensively is the numerous similarities between excitatory synapses of the vertebrate central nervous system and the fly NMJ. First, both synapses are mainly glutamatergic, meaning that they use glutamate as the main neurotransmitter (Jan and Jan, 1976a). Secondly, similar to central synapses of vertebrates, the larval NMJ is highly plastic. During the 4 days of larval development muscle cells increase nearly 100-fold in size and motorneuron terminals undergo rapid and continuous growth to maintain muscle control (Gorczyca et al., 1993; Keshishian et al., 1993; Schuster et al., 1996) (Fig 1.1). This form of developmental plasticity has allowed researchers to study genetic mechanisms underlying synaptic plasticity, such as activity-dependent synaptic bouton growth (Budnik et al., 1990; Zhong et al., 1992). Other forms of acute and experience dependent plasticity are also observed in this system (Ataman et al., 2008; Koon et al., 2011). Moreover, many of the synaptic proteins and molecular mechanisms are conserved between synapses of the *Drosophila* NMJ and vertebrate central synapses. For instance, the *Drosophila* homolog of vertebrate scaffolding protein PSD-95 (Postsynaptic Density-95/Discs-Large/Zona Occludens) is DLG (Discs-Large) and both proteins function to cluster cell adhesion molecules and ion channels at synaptic sites (Kim et al., 1995; Tejedor et al., 1997; Thomas et al., 1997; Zito et al., 1997).

As mentioned above, *Drosophila melanogaster* has a short life cycle, where a fertilized egg takes roughly 10 days to develop into an adult. Embryonic

development is completed in about a day at room temperature, resulting larval hatching. Next is the larval stage (L1, L2, L3), which takes about 4 days and the worm-like larva extensively feeds and grows in size. This rapid development of the fruit fly allows researchers to obtain results in a short period of time. In *Drosophila*, sophisticated genetic manipulation, such as generating mutants, designing RNAi or transgenic constructs is easily done (Fjose et al., 2001). Moreover, a wide variety of genetic tools including multiple collections of *Drosophila* mutants, chromosomal deficiencies, genetic markers, and transgenic RNAi lines spanning the whole genome are readily available to researchers (Grumbling G, 2006). Furthermore, using the GAL4/UAS (Brand and Perrimon, 1993), the LexA/lexAop (Lai and Lee, 2006), the GAL80 (McGuire et al., 2004), and the Q system (Potter et al., 2010) , one can either express or knock down genes of interest in a tissue-specific pattern with temporal control. These systems allow bypassing early developmental stages, rescuing mutant phenotypes as well as determining the cell types and developmental stages at which the protein of interest functions. Genome sequencing of *Drosophila* as well as decades of studies on fruit fly genes have shown a high degree of conservation between fly and mammalian genes; therefore studying mammalian gene homologs in *Drosophila* provides insight in potential function of genes in mammals. The genome of *Drosophila melanogaster* is simpler than mammalian genomes, where genetic redundancy is a common issue. While there are multiple isoforms of most genes in mammals, *Drosophila* has the advantage of having a single isoform in most cases. This makes the fruit fly a powerful model

organism to study gene function *in vivo.* Relatively recently, *Drosophila* has been used as a disease model, as many human disease genes have homologs in the fruit fly and the disruption of these genes often mimics the phenotypes observed in patients. Specifically, the larval NMJ is becoming a popular model to study the pathogenesis of neurodegenerative and neuromuscular diseases such as muscular atrophy, myotonic dystrophy and Amyotrophic lateral sclerosis (ALS) (Lloyd and Taylor, 2010).

General anatomy of the *Drosophila* larval NMJ

The *Drosophila* larva consists of 30 skeletal, supercontractile body wall muscles per abdominal hemisegment from A1 to A7 (Figure 1.1). These muscles are easily identifiable upon dissection of the animal and are aligned in a highly stereotypic fashion (Figure 1.1). Each hemisegment of the body wall muscles is innervated by approximately 36 motorneurons, whose cell bodies are found in the ventral ganglion and whose axons project to the muscles through the segmental nerves (Figure 1.2A) (Landgraf et al., 1997; Landgraf and Thor, 2006). At the larval stage, motor neuron terminals form varicosities, which are called synaptic boutons. These boutons are separated by neurites and form branched arbors, which appear as the classic ‘‘beads on a string’’ (Figure 1.2 B and C and 1.3C) (Prokop, 2006). Depending on their size, shape, neurotransmitter content, postsynaptic specializations and electrophysiological properties, synaptic boutons are divided into three types; type I, which is further classified into type 1b (big) and type 1s (small), type II and type III (Anderson et al., 1988; Atwood et al., 1993; Gorczyca et al., 1993; Jia et al., 1993; Johansen et al., 1989; Monastirioti

et al., 1995). Type I bouton innervations are found in all muscles in roughly one motorneuron to one muscle ratio and these boutons release glutamate, the primary excitatory neurotransmitter at the larval NMJ. Moreover, larval locomotion depends mainly on type I boutons, as they are the main source of stimulus input for muscle contraction (Prokop, 2006). The other types of boutons, type II and type III, are thought to be modulatory. In addition to glutamate, type II synapses contain the biogenic amine octopamine (Monastirioti et al., 1995) and type III synapses contain a variety of neuropeptides (Cantera and Nassel, 1992; Gorczyca et al., 1993). In my studies, I used the best-studied type I synapses on muscles 6-7 of segment A3, as they show a highly stereotypic innervation, morphology and synapse number.

At the ultrastructural level, a typical type Ib synaptic bouton contains mitochondria, endosomes and a significant number of neurotransmitter vesicles of 30-40 nm. Many of these vesicles cluster at specialized domains of presynaptic membrane, called active zones (Figure 1.3A and B). These active zones are the neurotransmitter release sites and they appear as T-bar shaped electron dense (presumably due to high protein content) structures using electron microscopy (Figure 1.3B) (Atwood et al., 1993; Jia et al., 1993). The readily releasable synaptic vesicles containing glutamate are located on these T-bars at the active zone. At synapses the presynaptic membrane is tightly apposed to the postsynaptic membrane being separated by a synaptic cleft 15-20nm wide (Figure 1.3B) (Jia et al., 1993). Active zones are directly apposed to high-density glutamate receptor (GluR) clusters, which give an electron dense appearance to

this postsynaptic membrane. However, this postsynaptic density (PSD) is not as prominent as the PSDs established by central neurons. In addition to PSDs, the muscle membrane surrounding the synaptic boutons forms a specialized muscle membrane that surrounds individual synaptic boutons forming convoluted invaginations and becoming structured as multiple layers. This complex postsynaptic structure is called the subsynaptic reticulum (SSR) (Figure 1.3A). The SSR membrane folds increase the surface of the postsynaptic muscle membrane region. Although glutamate receptors (GluR) are just localized on the postsynaptic membrane directly apposed to the active zones (Ataman et al., 2006b), many molecules such as K^+ channels, cell adhesion proteins, signal receptors and scaffolding proteins are localized throughout the membrane layers of the SSR (Ataman et al., 2006b). Nevertheless, the exact physiological function of SSR is not clear.

Anterograde and Retrograde Signaling at the *Drosophila* Neuromuscular Junction

Synapse formation, development and function depend on effective communication between presynaptic and postsynaptic cells. Both developmental and activity-dependent plasticity of synapses require bi-directional signaling that allows for coordinated development of synaptic structures and functioning of the pre- and postsynapse. One direction of communication is anterograde signaling, which allows the presynaptic cell to signal to the postsynaptic cell through synaptic transmission, the secretion of signaling molecules, and cell adhesion proteins (Packard et al., 2003). Another form of communication at synapses is

called retrograde signaling, in which the target postsynaptic cell influences the presynaptic neuron (Keshishian and Kim, 2004). Both anterograde and retrograde *trans*-synaptic signals activate signal transduction pathways at the *Drosophila* larval NMJ (Packard et al., 2003). WNT/Wingless signaling is the primary anterograde pathway involved in synapse development and plasticity at the fly NMJ (see next section for details), although this pathway has also some influence on retrograde signaling (Korkut and Budnik, 2009; Speese and Budnik, 2007). On the other hand, retrograde signaling is mediated mainly by TGF-β (Transforming Growth Factor- β) signaling. The ligand Glass bottom boat (Gbb) is secreted from the postsynaptic muscles and binds to its TGF-β/BMP (Bone Morphogenetic Protein) type II receptor, Wishful Thinking (Wit), and type I receptor, Thickveins (Tkv) or Saxophone (Sax) on the presynaptic cell membrane (Marques, 2005). Binding of Gbb to its receptors on the motorneuron membrane activates either a LIM Kinase-1 to stabilize synapses (Eaton and Davis, 2005) or a canonical BMP pathway. In this canonical pathway, activation of the receptors leads to the phosphorylation of a Smad, the transcription factor Mothers against decapentaplegic (Mad). Phosphorylated Mad associates with the co-Smad Medea and this complex is translocated into the motorneuron nucleus to regulate transcription (Marques, 2005). TGF-β signaling in motorneurons is crucial for expansion of the NMJ and disruption of this retrograde pathway results in decreased NMJ growth and reduced neurotransmission (Keshishian and Kim, 2004). A putative E3 ubiquitin ligase, Highwire, has been shown to be a negative regulator of the BMP pathway through its binding to Medea (McCabe et al.,

2004). In addition, Highwire also functions to regulate a MAP kinase kinase kinase (MAPKKK) homolog, Wallenda, suggesting that the MAPK pathway plays a role in NMJ growth and branching (Collins CA, 2006).

Relatively recently, a member of the Synaptotagmin family, Synaptotagmin-4 (Syt4), has been shown to mediate retrograde signaling at the *Drosophila* embryonic neuromuscular junction (Yoshihara et al., 2005). Syt4 functions in postsynaptic muscle cells and acts as a calcium sensor on postsynaptic vesicles to release an unknown *trans*-synaptic retrograde signal upon high frequency stimulation of the presynaptic cell (Yoshihara et al., 2005). This retrograde signaling has been suggested to activate a cyclic adenosine monophosphate (cAMP)-dependent protein kinase pathway in the presynapse, which stimulates presynaptic growth (Yoshihara et al., 2005). In addition to embryonic neuromuscular junctions, it has been suggested that Syt4 also localizes to postsynaptic vesicles and regulates retrograde signaling at the larval NMJ (Barber et al., 2009).

The WNT Signaling Pathway

Since this doctoral dissertation revolves around WNT signaling, this signaling mechanism is described in more detail below. WNT signaling has crucial functions in a variety of developmental processes and adult tissue homeostasis in all metazoan organisms studied to date. The cellular events controlled by WNTs range from cell proliferation, cell fate decisions and stem cell maintenance to providing positional information to cells for tissue polarity

(Siegfried and Perrimon, 1994). WNT family proteins are highly conserved secreted lipid-modified glycoproteins, that can act as morphogens (Mikels and Nusse, 2006). The name “WNT” is an amalgram of *Drosophila* Wingless, which was identified as a segment polarity gene and mouse Int-1, which was identified as a proto-oncogene (Nusse and Varmus, 1982; Rijsewijk, 1987). Abnormal WNT signaling results in a number of diseases including cancer and degenerative diseases in humans (Logan and Nusse, 2004).

In the nervous system, misregulation of the WNT pathway is linked to conditions such as Alzheimer’s disease, Huntington’s disease, schizophrenia and bipolar disorder (Caricasole et al., 2005; De Ferrari and Inestrosa, 2000; Gould and Manji, 2002; Inestrosa et al., 2002; Johnson and Rajamannan, 2006), which suggests that members of this family have a role in postmitotic neurons. Indeed, studies of the nervous system have uncovered roles for WNTs in axon pathfinding, dendritic development, synaptogenesis, synapse maturation and plasticity (Salinas and Zou, 2008; Speese and Budnik, 2007). Particularly intriguing are a series of recent studies that implicate WNTs in the development of NMJs across species ranging from worms to mammals (Song and Balice-Gordon, 2008; Speese and Budnik, 2007). These studies are unraveling a role for WNTs in neurotransmitter receptor clustering and the organization of presynaptic and postsynaptic specializations.

The WNT family is composed of multiple family members, including 5 in worms, 7 in flies, 15 in zebrafish, and 19 in mice and humans. Adding to this diversity is the presence of a myriad of typical WNT receptors, known as Frizzled

receptors, which include 3 in worms, 5 in flies, 12 in fish and 11 in mammals, as well as nonconventional receptors such as Derailed (DRL) — a member of the RYK (related toreceptor tyrosine kinase) subfamily of receptor tyrosine kinases and ROR2 (receptor tyrosine kinase-like orphan receptor 2). This complexity of WNT signaling is further heightened by the activation of at least five different WNT transduction pathways, which trigger various cellular processes (Speese and Budnik, 2007; Widelitz, 2005) (Figure 1.4).

Canonical WNT signaling is the best-characterized pathway, in which WNT binding to Frizzled receptors activates the scaffolding protein Dishevelled (DVL), which disassembles a so-called ‘destruction complex’ formed by glycogen synthase kinase 3β (GSK3β), Axin and adenomatous polyposis coli (APC) — a complex that normally leads to the degradation of β-catenin (Figure 1.4.A). WNT binding to Frizzled disrupts the destruction complex, and this results in cytoplasmic stabilization of β-catenin and its import into the nucleus, where it regulates gene expression through association with lymphoid enhancer factor/T cell factor (LEF/TCF) transcription factors (Wodarz and Nusse, 1998). In this pathway, Frizzled collaborates with a co-receptor, LRP5/6 of the low-density lipoprotein receptor related protein (LRP) family. This pathway is antagonized by the secreted protein Dickkopf1 (DKK1) and secreted Frizzled related proteins (SFRPs) (van Amerongen and Nusse, 2009).

In WNT divergent canonical pathway, DVL binds to microtubules and regulates GSK3β-dependent phosphorylation of microtubule- associated proteins (MAPs), such as MAP1B, Tau, MAP2 (Ciani et al., 2004; Lucas et al., 1998), and

the related *Drosophila* protein Futsch (Gogel et al., 2006) (Figure 1.4.B). Inhibition of GSK3β upon activation of the WNT divergent canonical pathway, thus enhances microtubule stability.

WNT planar cell polarity pathway involves activation of DVL, which turns on the small GTPases RHOA or RAC1 and the JUN N-terminal kinase (JNK) to regulate actin and microtubule cytoskeletons (van Amerongen and Nusse, 2009) (Figure 1.4.C).

WNT calcium pathway is a fourth signaling pathway, in which DVL activation induces an elevation in the levels of intracellular Ca^{++} and activation of protein kinase C (PKC) and calcium/ calmodulin-dependent protein kinase II (CaMKII) (Figure 1.4.D). This results in the nuclear import of the transcription factor nuclear-factor of activated T cells (NFAT), which regulates gene expression (Li et al., 2005).

Frizzled nuclear import (FNI) pathway is an alternative transduction pathway, in which WNT receptors themselves are internalized, cleaved and imported into the nucleus (Speese and Budnik, 2007) (Zhong, 2008) (Figure 1.4.E). Trafficking of the DFrizzled-2 (DFz2) receptor towards the nucleus depends on its binding partner GRIP (7-PDZ-domain glutamate-receptor binding protein). This mechanism has been substantiated at the *Drosophila* NMJ (Mathew et al., 2005), as well as during the development of cortical neurons in mammals (Lyu et al., 2008).

The first hint that WNTs function in synapse development emerged from studies of the developing cerebellum, which suggested that WNT7a operated in a

retrograde manner to enhance presynaptic differentiation (Salinas and Zou, 2008) (Lucas and Salinas, 1997). A similar retrograde role for WNT3, involving the divergent canonical pathway was also demonstrated in sensory neurons and motor neurons (Krylova et al., 2002). WNT7b has also been involved in dendrite development in the hippocampus, probably through the activation of canonical and non-canonical WNT pathways (Salinas and Zou, 2008) (Rosso et al., 2005). Recent studies have extended WNT function to the development of the NMJ in both vertebrate and invertebrate organisms.

Although WNTs have been long thought of as regulators of cell fate, they are also involved in crucial aspects of synaptic development in the nervous system. Particularly compelling are studies of the neuromuscular junction in nematodes, insects, fish and mammals. These studies place WNTs as major determinants of synapse differentiation and neurotransmitter receptor clustering.

WNT Signaling at the *Drosophila* Neuromuscular Junction

The role of WNTs in invertebrate synapses was recognized by the finding that Wingless (Wg, also known as WNT-1) and its receptor DFz-2 were present at the *Drosophila* larval NMJ (Packard et al., 2002). Through the use of a temperature sensitive *wg* mutant (wg^{ts}), which allowed for a temporal block of Wg secretion, thus bypassing early roles of Wg in embryogenesis, as well as various molecular manipulations, it was shown that Wg was released by presynaptic boutons, but probably not by muscles. Blocking Wg release during larval growth, led to a decrease in synaptic bouton number and to changes in bouton morphology, that

were rescued by restoring Wg in the motor neurons (Packard et al., 2002). By contrast, increasing the levels of Wg in motor neurons led to synaptic bouton overgrowth. In *wg*^{ts} mutants, presynaptic boutons had abnormal postsynaptic Discs large (DLG), a PSD95 family member, and GluR localization. Most strikingly, a subset of boutons ('ghost boutons') were filled with synaptic vesicles, but were devoid of active zones, postsynaptic specializations and mitochondria, which suggests that Wg has central roles during synapse differentiation (Ataman et al., 2006a; Packard et al., 2002). The mutants also had disruptions in the presynaptic microtubule cytoskeleton, as demonstrated by examining the microtubule-associated protein 1b (MAP1b)-related protein Futsch, which has been shown to be phosphorylated by GSK3β (Gogel et al., 2006). Interfering with DFz2 function in the muscle alone resulted in similar synaptic growth and morphology defects (Packard et al., 2002), suggesting that Wg activates both anterograde and retrograde signaling (Figure 1.5).

The search for the transduction cascade activated by Wg at the *Drosophila* NMJ led to the finding of a previously unrecognized alternative WNT pathway in larval muscles, the FNI pathway (Mathew et al., 2005) (Figures 1.4 and 1.5), in which a fragment of the DFz2 receptor itself is cleaved and imported into the nucleus. The importance of DFz2 cleavage was demonstrated by *dfz2* mutant rescue experiments, which showed that although expressing a full-length DFz2 transgene in muscles rescued the defects in bouton number, expressing a transgene lacking the cleavage site did not. Notably, expressing the DFz2-C fragment did not bypass the requirement for Wg signaling, raising the possibility

that DFz2-C is modified in a Wg-dependent fashion before nuclear import (Mathew et al., 2005). The FNI pathway was also shown to depend on the *Drosophila* homologue of GRIP (7-PDZ-domain glutamate-receptor binding protein), which interacts directly with the carboxy-terminal PDZ binding sequence of DFz2, and which is required to traffic the receptor from the synapse to the nucleus (Ataman et al., 2006a) (Figure 1.5). Although in mammals GRIP also seems to be crucial for postsynaptic development of neurons in culture (Hoogenraad et al., 2005), an association between GRIP and WNT pathways has not been as yet established in mammals. A similar mechanism involving cleavage and import has been implicated in establishing communication between the cell surface and the nucleus by several other receptors, including Notch, eGFR (epidermal growth-factor receptor) and the voltage-gated calcium channel ($Ca_v1.2$) (Baron et al., 2002; Gomez-Ospina et al., 2006; Lin et al., 2001).

Recently synaptic Wg signaling was also shown to underlie activity-dependent remodeling of the NMJ (Ataman et al., 2008). Wg secretion was enhanced by activity and this was correlated to rapid activity-dependent NMJ growth. Spaced stimulation, by potassium induced depolarization, motor nerve stimulation or light activation of neuronally expressed channelrhodopsin-2 (ChR2) induced the formation of dynamic filopodia-like extensions (synaptopods) and ghost boutons, as well as a potentiation of spontaneous neurotransmitter release 2 hours after the stimulation began. This was blocked by low extracellular calcium and by genetic manipulations that blocked action potentials or neurotransmitter release. Live imaging of ghost boutons from live non-dissected

preparations demonstrated that they could acquire GluRs and active zones, and thus represent synaptic bouton intermediates. Although ghost boutons were also observed in non-stimulated larvae, albeit at very low frequency, the activity-induced formation of ghost boutons required four to five cycles of spaced simulation and was blocked by transcriptional and translational inhibitors. This is akin to long-term behavioural and physiological plasticity, which also requires spaced training and/or stimulation and new protein synthesis (Barco et al., 2006).

Given that disrupting the FNI pathway leads to poor bouton proliferation and the formation of ghost boutons, it was speculated that this transduction pathway might be involved in the acute activity-dependent synaptic growth. Indeed, heterozygous *wg* mutants suppressed the activity-dependent synaptic growth, which was rescued by restoring Wg in motor neurons. Importantly, over-expressing Wg in motor neurons bypassed some of the requirements for spaced stimulation in the formation of ghost boutons, whereas wild-type larvae required four to five cycles of spaced stimulations, Wg over-expressing larvae required only three. As expected, activity also regulated the FNI pathway in the muscle cell. Spaced stimulation or chronic increase in activity through the use of mutations in potassium-channel subunits, *eag Sh* increased DFz2-C in the nucleus. This increase could be prevented by decreasing *wg* gene dosage in the *eag Sh* mutant background. Conversely, manipulations that blocked motor neuron action potentials or neurotransmitter release decreased levels of DFz2-C in the nucleus.

In the presynaptic compartment, WNT signalling was found to involve the

regulation of GSK3β activity, as GSK3β inhibition was required in motor neurons for activity-dependent synaptic growth (Figure 1.5). Whereas over-expressing GSK3β in motor neurons prevented bouton growth, expressing a GSK3β dominant-negative form bypassed activity requirements, as was observed by Wg over-expression in motor neurons. Thus, Wg release in an activity-dependent manner activates bi-directional pathways in the presynaptic and postsynaptic cell, with a divergent canonical pathway being activated in motor neurons and presumably regulating the presynaptic cytoskeleton, and the FNI pathway activated in muscles presumably to regulate the development of the postsynaptic apparatus. The bi-directional activation of alternative pathways represents a mechanism to precisely match the development of presynaptic and postsynaptic structures, a crucial process during synapse development. Whether such a bi-directional signaling mechanism could also operate at the vertebrate NMJ is still unclear.

Further evidence that Wg activated a divergent canonical pathway in motor neurons was provided by the finding that GSK3β over-expression, like mutations in *wg*, also disrupted the presynaptic microtubule cytoskeleton (Miech et al., 2008). However, it has also been suggested that GSK3β functions through AP1 by regulating the JUN N-terminal kinase (JNK) pathway (Franciscovich et al., 2008). It was further found that Arrow (also known as LRP5/6) and DVL but not the β-catenin homologue Armadillo were present at the NMJ (Miech et al., 2008). Mutations in *arrow* mimicked the *wg* mutant phenotypes at the presynaptic terminal. However, Arrow seemed to have both presynaptic and postsynaptic

functions as some phenotypes were rescued by expressing an Arrow transgene in either presynaptic or postsynaptic cell. Disruption of DVL in neurons, by expressing a dominant- negative transgene mimicked the phenotypes resulting from disrupting Wg and Arrow. However, no such effect was found on disrupting the function of the TCF homologue Pangolin or Armadillo, suggesting that presynaptic development is not regulated by the canonical pathway, but rather by the divergent canonical pathway (Figure 1.5). However, the involvement of JNK (Franciscovich et al., 2008), an enzyme of the planar cell polarity pathway, suggests additional complexity on the pathways involved.

Besides Wg, WNT5 and its atypical receptor Derailed (DRL) also function as positive regulators of NMJ development (Liebl et al., 2008) (Figure 1.5). DRL is present at the NMJ and *drl* mutants have a significant reduction in synaptic bouton number. In addition, in *wnt5* mutants, the density of active zones was decreased, although they remained unaffected in *drl* mutants, suggesting DRL-independent functions of WNT5. Functional defects in *wnt5* mutants included a reduction in the amplitude of evoked excitatory junctional currents (eJCs), as well as the frequency of spontaneous miniature eJCs (meJCs) similar to the defects in *gsk3β* (Franciscovich et al., 2008). However, both inhibition and overexpression of GSK3β led to a reduction in the amplitude of eJCs. WNT5 seemed to function in part in an anterograde manner, as over-expressing WNT5 in motor neurons suppressed the *drl* phenotype and DRL was required in muscle for normal NMJ growth. Further, expressing WNT5 in neurons but not in muscles, rescued the reduced synaptic bouton number of the *wnt5* mutant, and over-

expressing WNT5 in motor neurons led to synaptic overgrowth. However, the active zone phenotype was restored either by neuronal or muscle WNT5 expression, suggesting a potential retrograde function. Thus, more than one WNT pathway can function in parallel to positively regulate synapse development.

While the signaling cascades activated by WNT proteins have been studied in detail, how WNTs are secreted to the extracellular space and transported to the target cell membrane is not exactly clear. WNT proteins are highly hydrophobic glycoproteins that are posttranslationally lipid-modified at two different sites. The first lipid modification is a saturated acyl chain, palmitate; the second is a mono-unsaturated acyl chain, palmitoleate (Harterink and Korswagen, 2012). These lipid modifications are required for both secretion and the signaling activity of the protein (Harterink and Korswagen, 2012). An important question in the field has been: how are these hydrophobic WNT proteins released to the hydrophilic extracellular space and travel long distances to signal target cells? The fact that WNTs are lipid-modified hydrophobic proteins suggests that they are associated with lipid membranes. Several potential mechanisms have been suggested for the movement of WNTs in the extracellular milieu: (1) lateral diffusion through binding to heparan sulfate proteoglycans (Baeg et al., 2001); (2) formation of soluble micelles containing WNTs (Port and Basler, 2010); (3) travel on extracellular membrane fragments called argosomes (Greco et al., 2001); (4) travel on lipoprotein particles (Panakova et al., 2005); and (5) planar transcytosis, in which WNTs are

repeatedly endocytosed and resecreted through neighbouring cells (Coudreuse et al., 2006). However, the exact mechanism and the molecular details that allow WNTs to be transported intercellularly have been elusive.

It has recently become clear that the trafficking and secretion of WNT proteins are highly regulated and specialized processes. The discovery of the WNT binding protein Evenness Interrupted/Wntless/Sprinter (Evi/Wls/Srt) revealed the presence of a dedicated secretion machinery, where the type II multipass transmembrane protein, Evi, is specifically required for WNT secretion in epithelial cells of *Drosophila* wing imaginal discs and human cultured cells (Banziger et al., 2006; Bartscherer et al., 2006; Goodman et al., 2006). Moreover, this evolutionarily conserved Evi protein has been shown to be a WNT cargo receptor that functions in trafficking WNTs from the Golgi compartment to the plasma membrane of the secreting cell. It has been also suggested that Evi is recycled from the plasma membrane back to the Golgi through the retromer complex (Belenkaya et al., 2008; Franch-Marro et al., 2008; Pan et al., 2008; Port et al., 2008; Yang et al., 2008).

In the second chapter of my thesis, I will present evidence for a previously unknown cellular mechanism by which secreted WNT/Wingless signals are transported from presynaptic motorneurons to postsynaptic muscle cells, by riding on Evi-containing extracellular vesicles. In addition to the function of Evi in Wg secretion and extracellular transport, we provide compelling evidence that Evi also plays a role in the signal-receiving postsynaptic muscle cell to target DGRIP, a DFz2-interacting protein, to postsynaptic sites.

A further study led by Dr. Kate Koles, a postdoctoral fellow in the Budnik lab, has provided compelling evidence that the Evi-containing extracellular vesicles correspond to exosomes, using multiple methods such as mass spectrometry, western blot analysis and electron microscopy (Koles et al., 2012). Both of these above studies are unique in the sense that they provide a function for exosomes *in vivo* in the nervous system for the first time.

Exosomes

In pluricellular organisms, intercellular communication takes place through secretion of soluble extracellular molecules such as proteins and short peptides, which interact with receptors in the target cell. Recently, a novel cell-to-cell communication mechanism was identified through the release of membrane vesicles to the extracellular space. These extracellular vesicles contain numerous proteins including transmembrane proteins, lipids, and nucleic acids (Thery, 2011). Although initially they were considered solely as a means to discard cellular debris, they are now being recognized as signal carriers, as they have been shown to affect the recipient cells, such as the activation of signal transduction pathways (Record et al., 2011). There are multiple types of membrane vesicles that are secreted from cells, however, the best studied among them are the ‘’exosomes’’ (Thery et al., 2009).

Exosomes were first described about three decades ago (Harding et al., 1983; Pan et al., 1985; Trams et al., 1981). However, their significance and function as vehicles for intercellular signaling has just beginning to emerge over

the past few years. Exosomes are 50-100nm membrane-limited vesicles that originate from intracellular multivesicular compartments and are secreted to the extracellular space through the exocytic fusion of multivesicular bodies (MVBs) with the plasma membrane of the cell (Thery et al., 2009). MVBs are well known membrane limited compartments, which are intermediates between early endosomes or the *trans*-Golgi network and lysosomes in the degradation pathway (Futter et al., 1996). However, it has become increasingly clear that they are alternatively directed to the plasma membrane instead of the lysosomes for exosome release (Johnstone et al., 1991). It is not yet clear how these distinct fates of MVBs are regulated. Moreover, exosomes have been demonstrated to be secreted both constitutively and upon induction. Although, the exact mechanisms regulating exosome release is unknown (Raposo et al., 1997; Savina et al., 2003), some components of the release machinery are beginning to be identified (Koles et al., 2012).

The protein and lipid content of exosomes vary depending on the type of cells they are secreted from. The proteins found at exosomes are mostly derived from the plasma membrane, endosomes, cytosol, Golgi and even the nucleus of the originating cell. However, they rarely derive from mitochodria or endoplasmic reticulum. The proteins contained in exosomes include cell adhesion molecules, cytoskeletal proteins, membrane trafficking proteins, signaling molecules, proteins involved in MVB formation, tetraspanins, heat shock proteins, metabolic enzymes and proteins involved in transcription and protein synthesis (Record et al., 2011). The lipid composition of exosomes also depends on the cell type.

However, a common feature of exosomes regardless of their origin is their enrichment with sphingomyelins (Subra et al., 2007). Other lipids found in exosomes include cholesterol, phosphatidylcholine, phosphatidylserine, phosphatidylethanolamine, lysophosphatidylcholine, and diglyceride (Laulagnier et al., 2004). In addition, lipid rafts have been shown to be present in exosomes (de Gassart et al., 2003).

Exosomes are well studied in immune cells and tumors. The first study that demonstrated a function for exosomes reported that B cells of the immune system communicate with T cells through exosomes for antigen presentation (Raposo et al., 1996b). Exosomes released by B-lymphocytes contain major histocompatibility class (MHC) II- antigen peptide complexes and they participate on the presentation of these complexes to specific T-cells. Subsequently, dendritic cells of the immune system were also demonstrated to secrete exosomes to induce antitumor immune responses in mice (Zitvogel et al., 1998). These early studies formed the basis for the view of exosomes as signaling entities. A key discovery in the field happened in 2007 when exosomes were demonstrated to contain mRNA and microRNA. Moreover, RNA transported by exosomes was translated in the recipient cells, suggesting that the transported RNA was biologically active (Valadi et al., 2007). The specific roles of exosomes depend on the original cell type they are secreted from. In contrast to exosomes of the immune system, exosomes in the nervous system have been rarely studied. A potential role of exosomes in the nervous system emerged when a study showed that cultured cortical neurons from rats secrete exosomes to the

culture media (Faure et al., 2006). Subsequent studies reported that exosomes are released by both embryonic neurons as well as fully differentiated cortical and hippocampal neurons in culture (Chivet et al., 2012; Lachenal et al., 2011). Furthermore, secretion of exosomes has been shown to be modulated by calcium influx and glutamatergic synaptic activity in cultured neurons, suggesting an exosome function in synaptic physiology (Lachenal et al., 2011). However, the function of exosomes *in vivo* in the nervous system had remained unclear, until our work in 2009, where we demonstrated that larval NMJs are likely to release exosomes for the presentation of Wg to postsynaptic DFrizzled2 receptors (Korkut et al., 2009).

In the third chapter of my thesis, I will present evidence for a presynaptic control of postsynaptic retrograde signaling through the exosomal transfer of an essential retrograde signaling component, Syt4. I will demonstrate that retrograde Syt4 function in the postsynaptic muscle is required for activity-dependent presynaptic growth as well as potentiation of spontaneous neurotransmitter release, and that this function depends on exosomal release of Syt4 by presynaptic terminals.

In conclusion, my thesis unravels a novel cellular mechanism for *trans*-synaptic communication through release of exosomes from presynaptic terminals. First, the extracellular transport of the synaptogenic WNT/Wingless signal is aided by exosomes through its binding to Evi. Second, exosomes are critical for presynaptic regulation of postsynaptic retrograde signaling through Syt4 release. These studies unequivocally show that signaling through exosomes

is crucial for both activity-dependent and developmental synaptic plasticity in the nervous system.

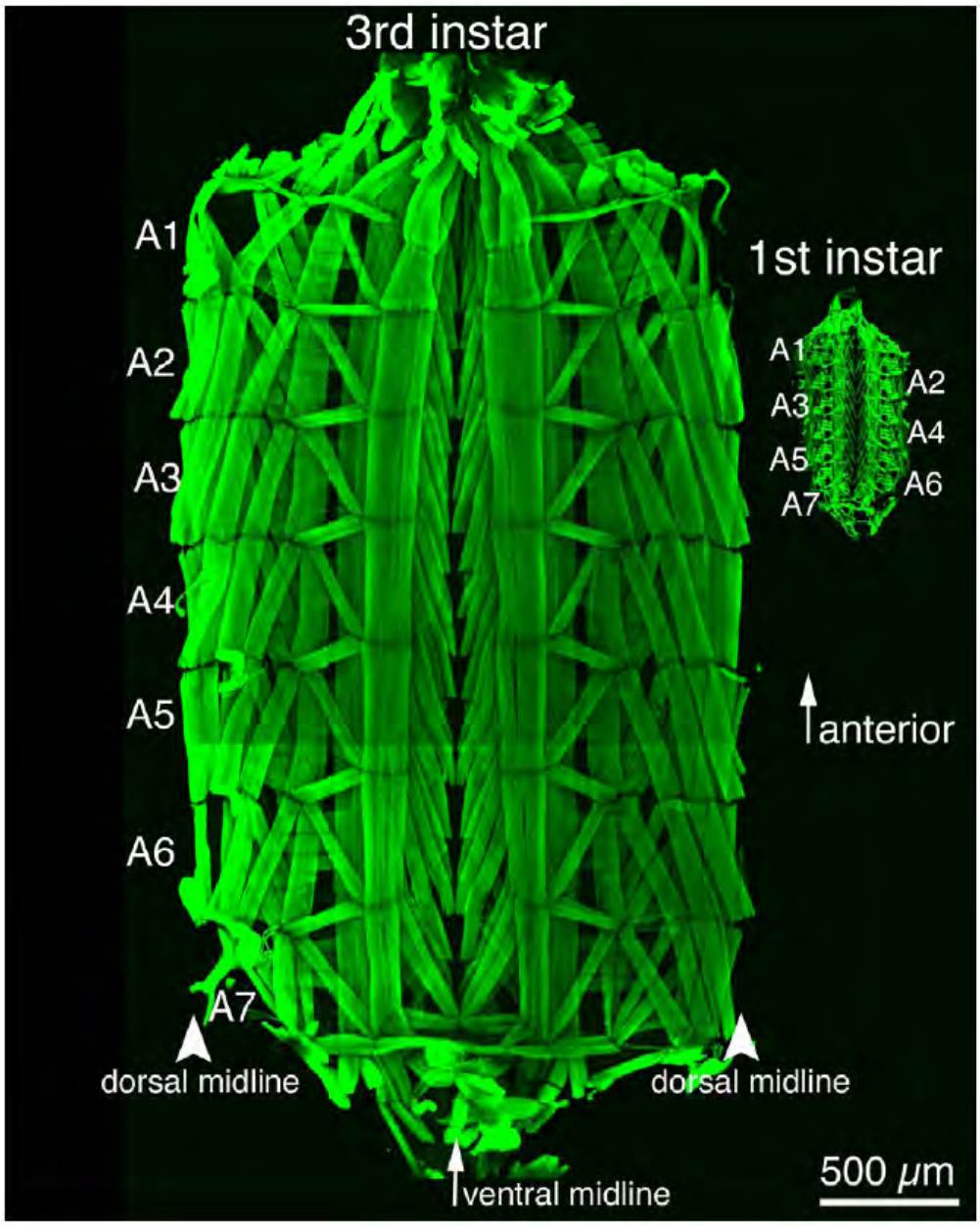

Figure 1.1. (Adapted from (Gorczyca, 2006) **Body wall muscles of the *Drosophila melanogaster* larva**. Third instar wandering stage (left) and first instar (right) larval body wall muscles preparations labeled with FITC-conjugated phalloidin. During development, the number of muscles does not increase, but the size of each muscle can increase up to 100 fold. Abdominal segments 1-7 are labeled as A1 to A7. Up is anterior.

A

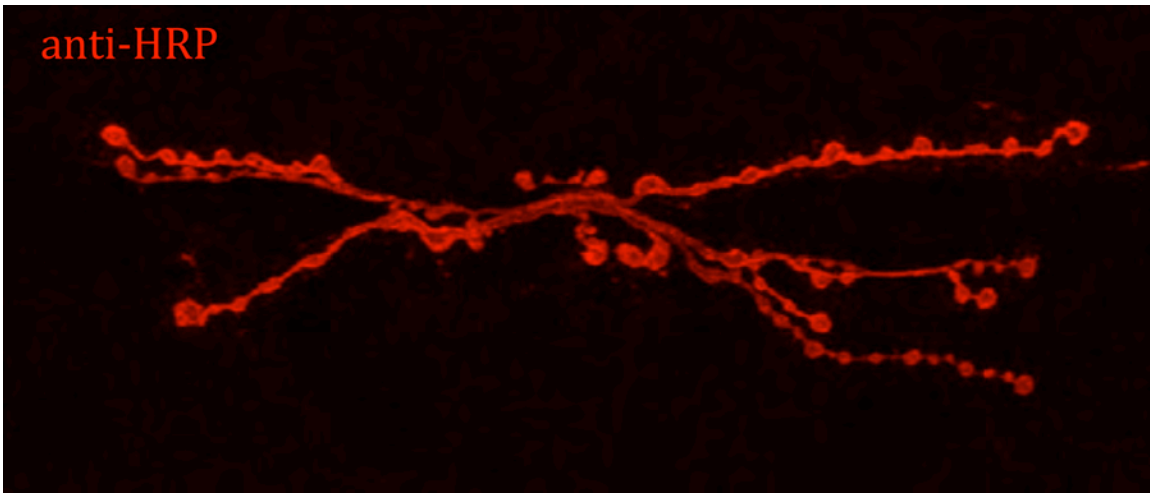

B

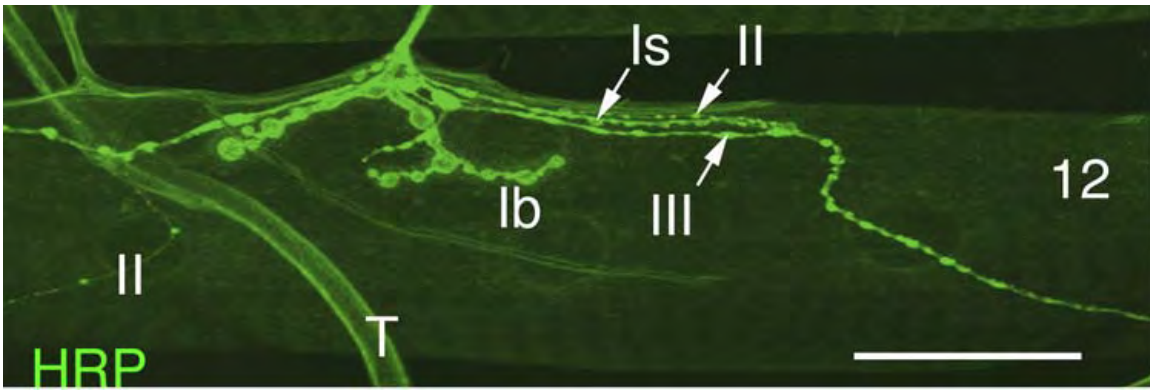

C

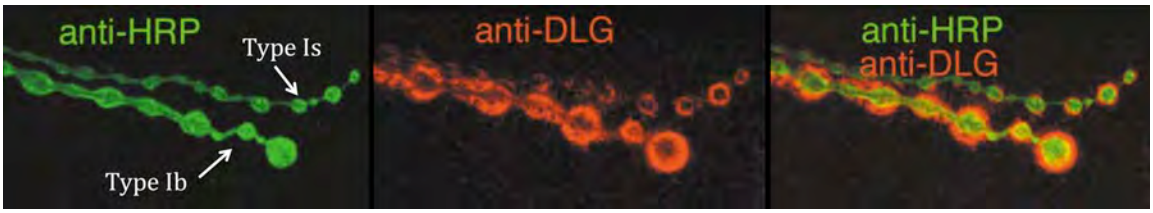

Figure 1.2. (Adapted from (Gorczyca, 2006) and (Packard et al., 2002)

Anatomical structure of the *Drosophila* larval neuromuscular junction.

(A) Confocal image of a third instar larval NMJ innervated in muscles 6-7. ‘’Beads on a string’’-like synaptic boutons are labeled with a presynaptic marker, anti- HRP (red) (Gorczyca, 2006).

(B) Body wall muscle 12 innervated by type Ib, type Is, type II and type III, labeles with anti-horseradish peroxidase (anti-HRP) (Gorczyca, 2006).

(C) Type Ib and type Is boutons stained with antibodies against HRP (green) and the scaffolding protein DLG (red), a postsynaptic marker.

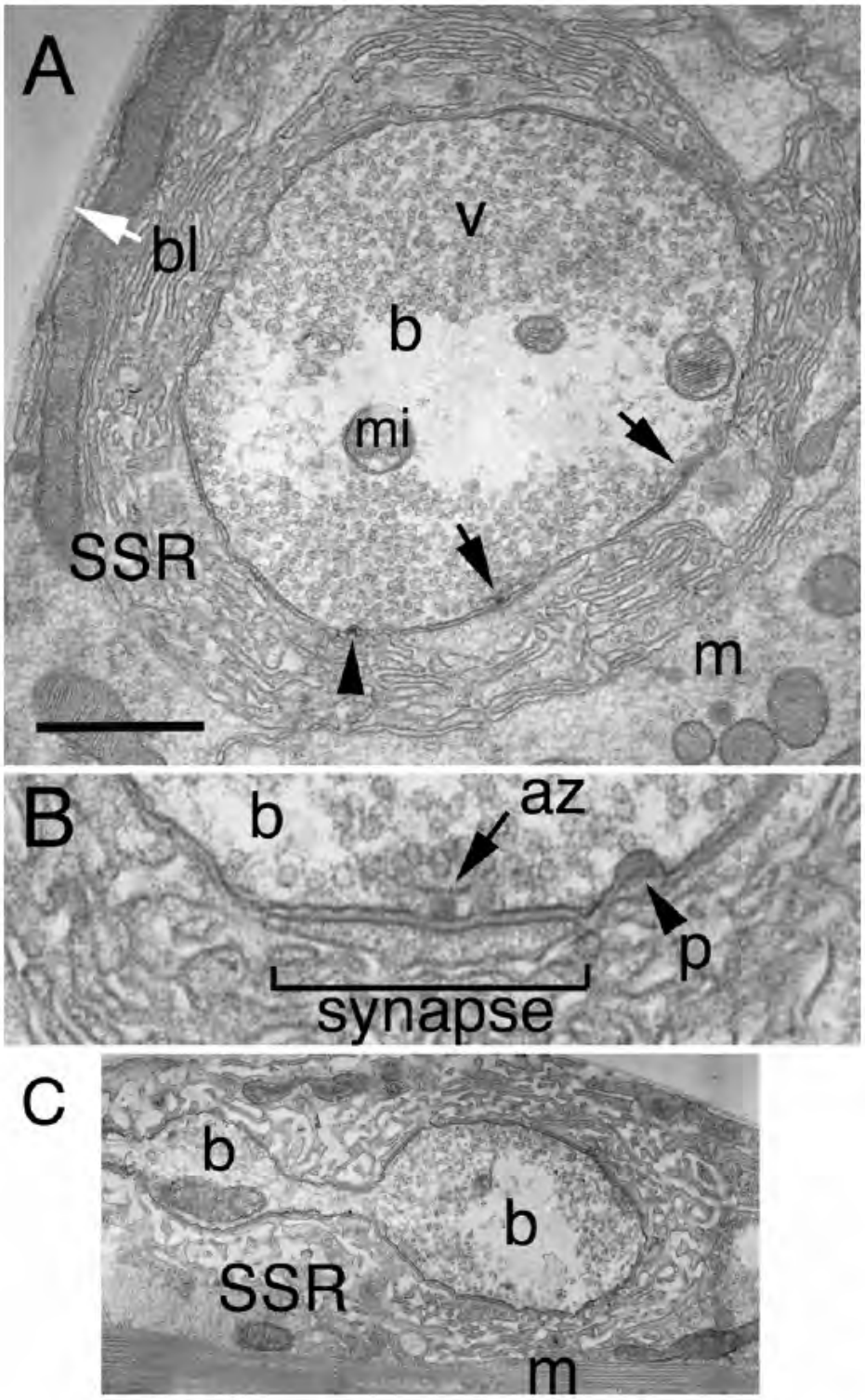

Figure 1.3. (Adapted from (Gorczyca, 2006) **Ultrastructural view of Type 1b synaptic boutons.**

(A) Midline cross section through a type Ib bouton. b = bouton, v = vesicles, mi =mitochondria, bl (white arrow) = basal lamina, SSR = subsynaptic reticulum, m = muscle. Arrows point to T-bar active zones. Arrowhead denotes an endocytic coated pit. (B) High magnification view of a synaptic area, showing a T-bar active zone, and a coated pit (p). (C) Longitudinal cross section through a type Ib NMJ showing two boutons (b) joined by a neurite process. Calibration bar is 0.8 µm in A, 0.3 µm in B, and 2.5 µm in C.

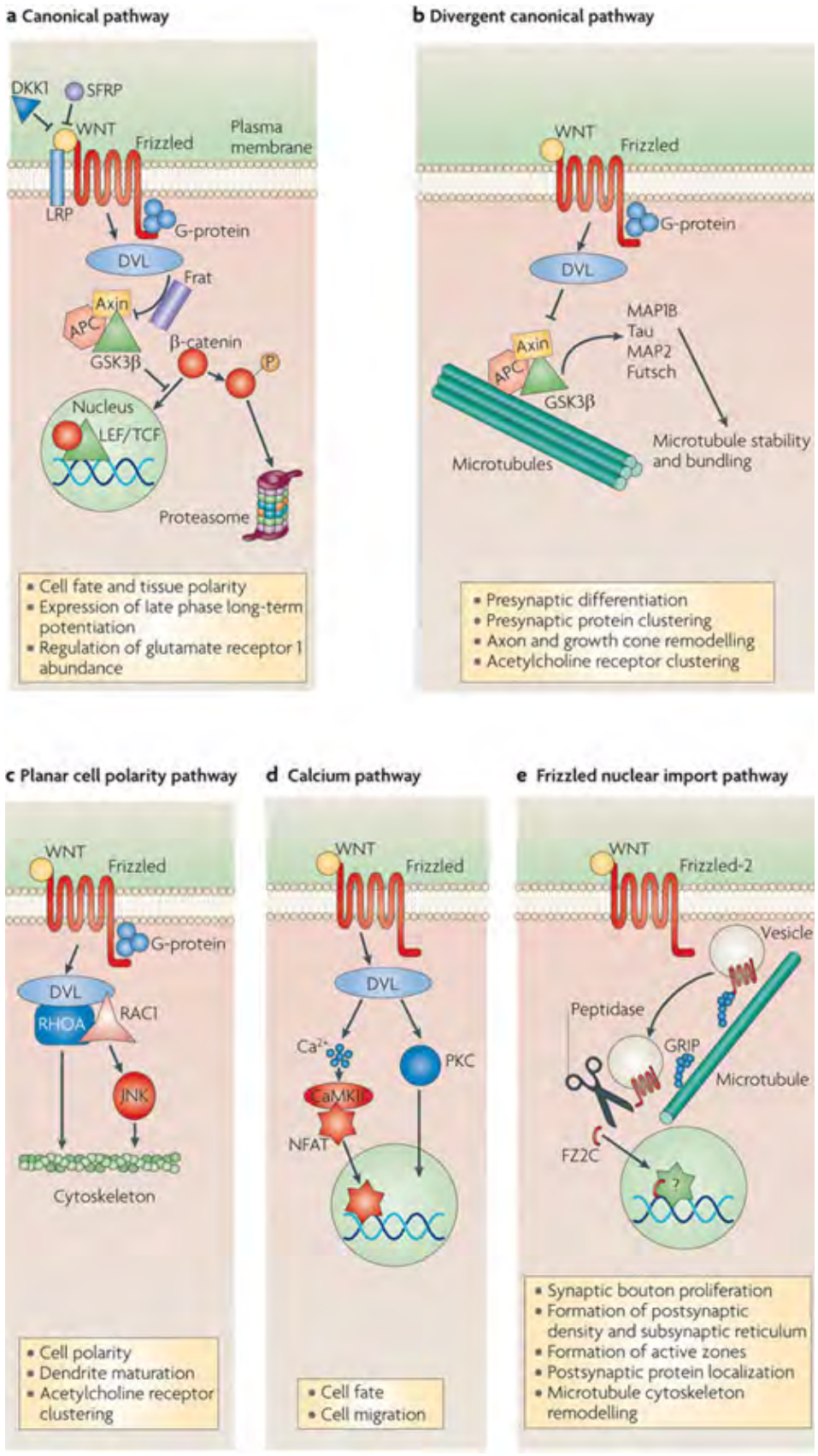
a Canonical pathway
DKK1
SFRP
WNT
Frizzled
Plasma membrane
LRP
G-protein
DVL
Frat
Axin
APC
β-catenin
GSK3β
P
Nucleus
LEF/TCF
Proteasome
• Cell fate and tissue polarity
• Expression of late phase long-term potentiation
• Regulation of glutamate receptor 1 abundance
b Divergent canonical pathway
WNT
Frizzled
G-protein
DVL
MAP1B
Tau
MAP2
Futsch
Axin
APC
GSK3β
Microtubules
Microtubule stability and bundling
• Presynaptic differentiation
• Presynaptic protein clustering
• Axon and growth cone remodelling
• Acetylcholine receptor clustering
c Planar cell polarity pathway
WNT
Frizzled
G-protein
DVL
RHOA
RAC1
JNK
Cytoskeleton
• Cell polarity
• Dendrite maturation
• Acetylcholine receptor clustering
d Calcium pathway
WNT
Frizzled
DVL
Ca2+
PKC
CaMKII
NFAT
• Cell fate
• Cell migration
e Frizzled nuclear import pathway
WNT
Frizzled-2
Vesicle
Peptidase
GRIP
Microtubule
FZ2C
?
• Synaptic bouton proliferation
• Formation of postsynaptic density and subsynaptic reticulum
• Formation of active zones
• Postsynaptic protein localization
• Microtubule cytoskeleton remodelling

Figure 1.4. Adapted from (Korkut and Budnik, 2009) **WNT Signaling Pathways. (A)** Canonical pathway, **(B)** Divergent canonical pathway, **(C)** Planar cell polarity pathway, **(D)** WNT calcium pathway, **(E)** Frizzled nuclear import (FNI) pathway.

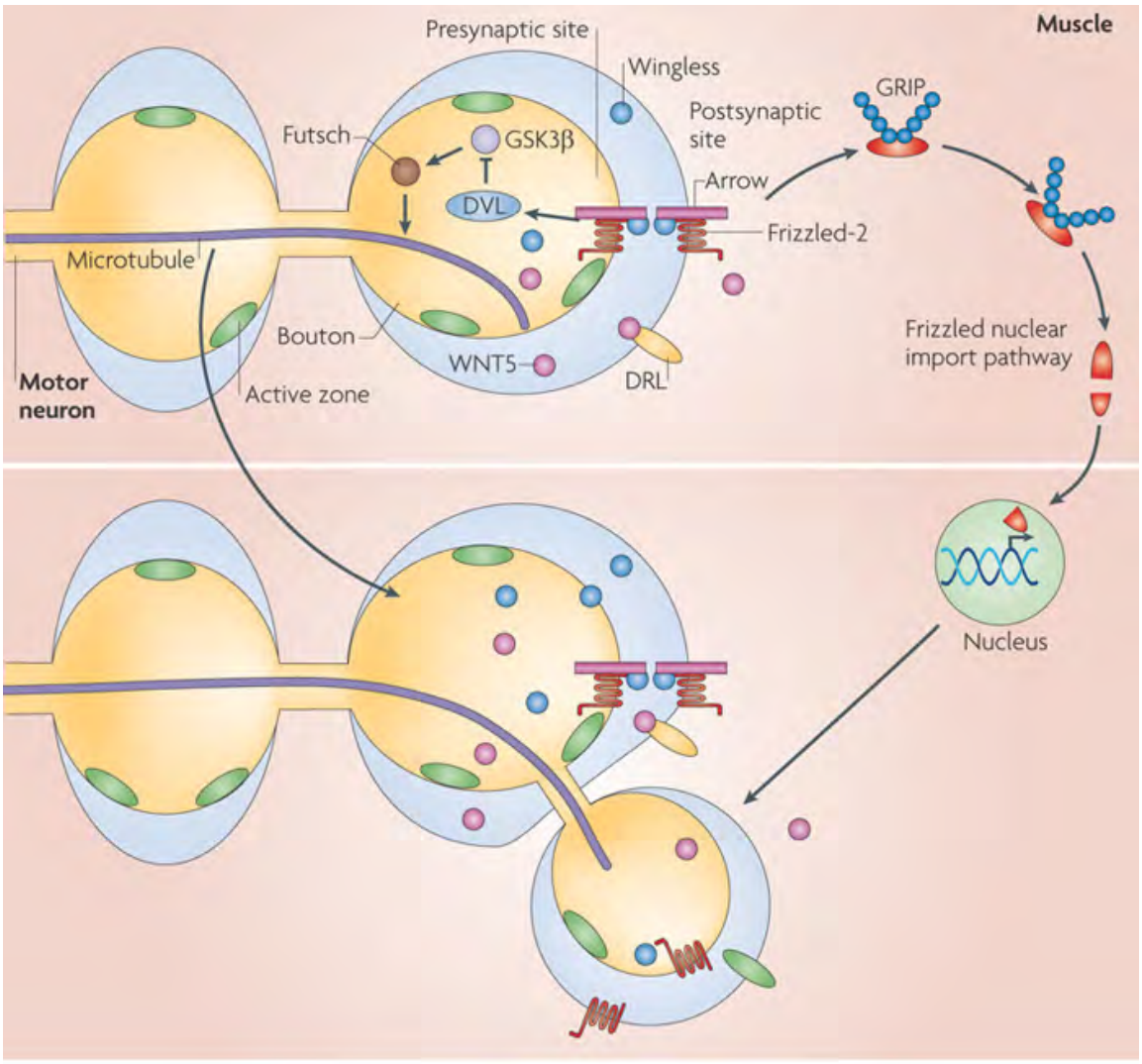

Figure 1.5. (Adapted from Korkut and Budnik, 2009) **Role of WNTs during *Drosophila* larval neuromuscular junction development**

Wingless (Wg) secreted from presynaptic motor neuron endings, binds to DFrizzled-2 (DFz2) and coreceptor Arrow, which are localized presynaptically and postsynaptically. In the presynaptic cell, Wg activates a divergent canonical pathway, involving DVL (Dishevelled) activation, inhibition of GSK3β (glycogen synthase kinase 3β) activity and the regulation of the microtubule cytoskeleton through Futsch. In the postsynaptic cell, Wg activates the FNI pathway, which involves the cleavage and nuclear import of DFz2. GRIP (7-PDZ-domain

glutamate-receptor binding protein) is required for the trafficking of receptors from the postsynaptic membrane towards the nucleus. WNT5 is also released from the presynaptic boutons and binds to its receptor Derailed (DRL) on the postsynaptic membrane to regulate synaptic bouton growth.

CHAPTER 2

TRANS-SYNAPTIC TRANSMISSION OF VESICULAR WNT SIGNALS THROUGH EVI/WNTLESS

The following chapter is reprinted from a *Cell* article (Korkut, C., Ataman, B., Ramachandran, P., Ashley, J., Barria, R., Gherbesi, N., and Budnik, V. (2009). Trans-synaptic transmission of vesicular WNT signals through Evi/Wntless. *Cell* 139, 393-404).

ABSTRACT

WNTs play pivotal roles during development and in the mature nervous system. However, the mechanism by which WNTs traffic between cells has remained elusive. Here we demonstrate a mechanism of WNT transmission through release of exosome-like vesicles containing the WNT-binding protein Evenness Interrupted/Wntless/Sprinter (Evi/Wls/Srt). We show that at the *Drosophila* larval neuromuscular junction (NMJ), presynaptic vesicular release of Evi is required for the secretion of the WNT, Wingless (Wg). We also show that Evi acts cell- autonomously in the postsynaptic WNT-receiving cell to target dGRIP, a Wg-receptor-interacting protein, to postsynaptic sites. Upon Evi loss of function, dGRIP is not properly targeted to synaptic sites, interfering with postsynaptic WNT signal transduction. These findings uncover a previously unknown cellular mechanism by which a secreted WNT is transported across synapses by Evi-containing vesicles and reveal trafficking functions of Evi in both the WNT-producing and the WNT-receiving cells.

INTRODUCTION

Members of the WNT family of morphogens orchestrate a myriad of developmental processes in all metazoan organisms studied to date (Siegfried and Perrimon, 1994). These include the establishment of cell identity during pattern formation, control of cell proliferation and migration, and cytoskeletal remodeling. WNTs are also known to coordinate major aspects of the nervous system from early development to adult function, in which they regulate neural

stem cell proliferation, axon pathfinding, synapse differentiation and plasticity, as well as learning (Ataman et al., 2008) (Salinas and Zou, 2008) (Speese and Budnik, 2007) (Zhao et al., 2005). Not surprisingly, alterations in WNT signaling in humans have been linked to a number of cognitive disorders, such as schizophrenia and Alzheimer's disease (De Ferrari and Moon, 2006).

WNTs activate a variety of intracellular signal transduction pathways that regulate gene expression and cytoskeletal organization events (Gordon and Nusse, 2006) (Salinas and Zou, 2008). The best understood signaling pathway is the canonical WNT pathway, in which WNT ligands bind to the Frizzled (Fz) family of serpentine receptors. Receptor activation in turn stabilizes cytoplasmic β-catenin, which enters the nucleus and regulates gene expression. In a divergent canonical pathway, GSK3- β operates through a nongenomic mechanism, by phosphorylating microtubule-associated proteins, thereby regulating microtubule stability. Alternative signal transduction mechanisms activated by WNT ligands include the planar cell polarity (PCP) pathway and the WNT/Ca^{2+} pathway. Recent studies at the *Drosophila* neuromuscular junction (NMJ) and in the developing mammalian nervous system have uncovered a novel transduction mechanism in which WNT receptors themselves are cleaved and translocated into the nucleus (Lyu et al., 2008) (Mathew et al., 2005). These nonexclusive transduction cascades provide alternative mechanisms for cells to regulate diverse processes in different spatiotemporal contexts.

Whereas considerable progress has been made in elucidating the signaling pathways activated by WNTs, much less is known about how WNTs

are secreted and transported to distant locales. At the *Drosophila* imaginal wing disc, the WNT-1 homolog Wingless (Wg) is secreted by a discrete row of Wg-producing cells. Secreted Wg forms a long-range gradient expanding many cell diameters away from the source of Wg secretion (Neumann and Cohen, 1997). The mechanisms by which Wg is transported from its site of secretion to distant target cells have remained poorly understood. WNT proteins are highly hydrophobic and tightly associated to cell membranes owing to palmitoyl modifications essential for biological activity (Willert et al., 2003). Thus, unescorted WNT molecules are not easily diffusible in the extracellular milieu. Several mechanisms have been proposed to explain the movement of WNT molecules from their site of secretion, including their association with glycosaminoglycan-modified proteins at the extracellular matrix (Baeg et al., 2001), the formation of exosome-like vesicles called argosomes (Greco et al., 2001), extracellular lipoprotein particles (Panakova et al., 2005), transcytosis (Coudreuse et al., 2006), or a combination of the above. However, the exact mechanism employed during intercellular WNT transport has remained elusive.

Recent studies have identified a type II multipass transmembrane protein called Evenness Interrupted/Wntless/Sprinter (Evi/Wls/Srt), which appears to be specifically required in vivo for WNT secretion in epithelial cells of flies and human cultured cells (Banziger et al., 2006); (Bartscherer et al., 2006); (Goodman et al., 2006). In the wing epithelium of *Drosophila*, Wg cannot be secreted from the *evi* mutant cells, and this leads to the accumulation of Wg within these cells. In contrast, the secretion of other morphogens, such as

Hedgehog (Hh), remains unaffected, suggesting that Evi is dedicated to the secretion of WNT proteins. Further analysis has suggested that Evi functions as a WNT cargo receptor during trafficking from the Golgi to the plasma membrane and is recycled back to the Golgi through the retromer complex (Belenkaya et al., 2008); (Franch-Marro et al., 2008); (Pan et al., 2008); (Port et al., 2008); (Yang et al., 2008).

In the nervous system, WNTs are released by pre- or postsynaptic cells and function in either a retrograde or anterograde manner (Salinas and Zou, 2008); (Speese and Budnik, 2007). Similar to other cell types, the mechanisms by which WNTs are transported between synaptic compartments are principally unexplored. Considering that WNT-1 is released from synapses in an activity-dependent manner (Ataman et al., 2008), and the substantial short- and long-term effects of WNT signaling on neurons, elucidating the mechanisms by which WNT secretion/transport is regulated in the nervous system remains an important problem.

Here we have addressed this key question by using the glutamatergic synapses of the *Drosophila* larval NMJ, where WNT-1/Wg is secreted from motorneurons. We report that Evi is localized at these synapses and its function is indispensable for proper Wg secretion and signaling. We also demonstrate a novel mechanism for transport of the Wg signal across the synapse through the release of Evi-containing exosome-like vesicles. Further, we show that Evi is required for the proper trafficking of the Wg receptor DFrizzled-2 (DFz2), through actions that involve the DFz2-interacting protein dGRIP, a PDZ protein required

for the transport of internalized DFz2 vesicles toward the nucleus (Ataman et al., 2006a); (Mathew et al., 2005).

RESULTS

Evi Is Required for Wg Secretion at the Neuromuscular Junction

Previous studies have suggested that Evi is required for Wg secretion in non- neuronal cells (Banziger et al., 2006); (Bartscherer et al., 2006). Because Wg is secreted from motorneurons at the fly NMJ (Ataman et al., 2008); (Packard et al., 2002), we first examined the distribution of Wg at the NMJ of *evi* null mutants, which survive to the third instar larval stage (Bartscherer et al., 2006). We found that secreted Wg levels were substantially reduced at postsynaptic muscles in *evi* mutants (Figures 2.1A, 2.1C, and 2.1E). However, this reduction was not limited to the postsynaptic compartment but was also observed in the presynaptic boutons as determined by volumetric quantifications of the Wg signal inside the presynaptic bouton demarcated by anti-HRP staining (Figures 2.1A, 2.1C, and 2.1E). A similar decrease was observed when Evi was downregulated using Evi-RNAi expressed in neurons using the elav-Gal4 driver (Figures S2.1A and S2.1B). These results could indicate that Evi might be required for the stability or synthesis of Wg in motorneurons. However, we did not observe any changes in Wg levels in the nervous system (Figure 2.1F). Thus, at the NMJ, Evi is required for the transport and/or secretion of Wg in presynaptic terminals. A prediction of this hypothesis is that Wg should accumulate in the cell bodies or axons of motorneurons in *evi* mutants. We found that there was a substantial

increase in Wg immunoreactivity levels in motorneuron cell bodies and longitudinal axons within the neuropil (Figures S2.1C–S2.1E).

The above model was further tested by rescue experiments. Expressing an Evi-GFP transgene in the motorneurons of *evi* mutants, by using the Gal4 driver C380, completely rescued the low levels of Wg in both the pre- and postsynaptic compartments (Figures 2.1B and 2.1E). Notably, however, expression of the Evi-GFP transgene in postsynaptic muscles, by using the Gal4 strain BG487, did not (Figures 2.1D and 2.1E). Thus, Evi is required in motorneurons for normal Wg transport and/or secretion.

We also observed that mutations in *evi* mimicked synaptic phenotypes previously observed in mutations affecting Wg signaling (Ataman et al., 2006a); (Mathew et al., 2005); (Packard et al., 2002). As muscle fibers grow in size, the *Drosophila* larval NMJ continuously expands by adding new synaptic boutons. This expansion is critically dependent on Wg signaling (Packard et al., 2002). Wg appears to be secreted by motorneurons, and suppressing Wg secretion substantially reduces synaptic bouton proliferation. Further, in *wg* mutants many boutons are misshapen, and some remain in an undifferentiated state (ghost boutons), lacking active zones and postsynaptic apparatus. Conversely, increasing Wg secretion by overexpressing Wg in motorneurons enhances formation of synaptic boutons. In the presynaptic cell Wg activates a divergent canonical pathway that regulates microtubules (Ataman et al., 2008); (Franco et al., 2004); (Miech et al., 2008). In the postsynaptic muscle cell Wg initiates an atypical pathway in which the DFz2 receptor itself is cleaved and a fragment

imported to the nucleus (Ataman et al., 2006a);(Ataman et al., 2008); (Mathew et al., 2005). In *evi* mutants the total number of synaptic boutons was decreased by over 50%, without any change in muscle size, and the boutons had an aberrant morphology being large and deformed (Figures 2.2A–2.2E and S2.2). In addition, *evi* NMJs had a significantly higher number of ghost boutons (Figures 2.2D, arrows and 2.2F). The decrease in bouton number was only partially rescued by expressing Evi in either the pre or postsynaptic cell (Figure 2.2E). However, it was completely rescued by simultaneously expressing Evi in both cells (Figure 2.2E). In the case of ghost boutons, expressing the Evi transgene in motorneurons or in both motorneurons and muscles completely rescued the abnormal increase in ghost boutons in *evi* mutants (Figure 2.2F). Expressing Evi in muscles using the weaker Gal4 driver BG487-Gal4 did not rescue the increase in ghost boutons, but this phenotype was completely rescued by using the stronger muscle Gal4 driver C57-Gal4 (Figure 2.2F). Thus, although Evi is required only in motorneurons for proper Wg transport and/or secretion, Evi is needed both in neurons and muscles for normal synaptic growth.

The similarity in the synaptic phenotypes between *evi* and *wg* mutants at the NMJ, together with previous evidence suggesting that both proteins establish biochemical interactions (Banziger et al., 2006), raised the question of whether there were genetic interactions between *evi* and *wg* during NMJ growth. This was addressed by analysis of transheterozygotes. The number of boutons was normal in heterozygotes, but there was a supra-additive reduction in the number of boutons in the transheterozygotes (expected decrease in bouton number by

simple additivity in *wg/+; evi/+* is 14.2% versus 27% observed in *wg/+; evi/+* transheterozygotes; Figure 2.2G), suggesting that *evi* and *wg* genetically interact during synaptic bouton proliferation.

Evi Is Localized Both Pre- and Postsynaptically and Is Transferred *Trans*-synaptically from the Pre to the Postsynaptic Compartment

To examine the synaptic localization of Evi, we generated two antibodies directed to a predicted either extracellular (Evi-Nex) or intracellular (Evi-Cin) region of the Evi protein (Figures 2.3A, S2.3A, and S2.3B). Both antibodies strongly labeled the NMJ in similar patterns (Figures 2.3B and 2.3C). This immunoreactivity was specific, as it was severely decreased in *evi* mutants (Figures 2.3D and 2.3E). Immunoreactive Evi label was observed both in pre- and postsynaptic compartments at the NMJ, as determined by double labeling with anti-HRP, which defines the boundary of the presynaptic compartment. However, Evi was particularly enriched at the postsynaptic junctional region (Figures 2.3B and 2.3C), the same region occupied by secreted Wg and its receptor DFz2 at the NMJ (Packard et al., 2002). In this region Evi immunoreactivity was present in a punctate pattern presumably reflecting vesicular structures (Figures 2.3B and 2.3C).

The rescue experiments suggested that Evi functions both pre- and postsynaptically during synaptic bouton proliferation, but that it is required solely presynaptically for Wg transport and/or secretion. To further determine the requirement of Evi in the pre- and postsynaptic side, we expressed Evi-RNAi with

the cell-specific Gal4 drivers. Surprisingly, expressing Evi-RNAi in the motorneurons (Evi-RNAi-pre) not only led to a reduction in Evi immunoreactivity inside presynaptic terminals but also substantially reduced the label at the postsynaptic region (Figures 2.3F and 2.3I). The observation that presynaptic knockdown of Evi has a *trans*-synaptic effect on Evi levels in muscle was quite unexpected. Such a phenomenon is not observed when knocking down other well-known synaptic proteins such as dGRIP (Ataman et al., 2006a) or spectrin (Pielage et al., 2005). This observation was also not due to a leaky Gal4 driver, as C380-Gal4 expresses Gal4 in motorneurons and not in muscles (Budnik et al., 1996); (Sanyal et al., 2003). Further, expressing a nuclear LacZ (UAS-LacZNLS) with C380-Gal4 resulted in strong labeling of neuronal but not muscle nuclei (Figures S2.3D and S2.3E), and expressing myristylated- mRFP (myr-mRFP) usingC380-Gal4 did not result in postsynaptic myr-mRFP signal (Figure S2.3C). These observations suggest that postsynaptic Evi is at least partly derived from the presynaptic motorneurons. The possibility that Evi could be transferred from the pre- to the postsynaptic compartment was tested by expressing Evi-GFP in motorneurons (Evi-GFP-pre). Notably, GFP was observed both in presynaptic boutons as well as at the postsynaptic junctional region (Figure 2.3G), supporting the notion that Evi could be transferred from pre- to postsynaptic compartments. This transfer was unlikely to result from Evi overexpression, as when the Evi-GFP transgene was expressed presynaptically in an *evi* mutant background, at levels similar to endogenous levels (Figure S2.3F), a similar distribution of the GFP label in the postsynaptic side was observed (Figures 2.3H and S2.3F). This

transfer of presynaptic Evi was also clearly observed *in vivo* in samples expressing myr-mRFP and Evi-GFP in motorneurons and imaged live (Figure S2.3C).

Given that Wg is secreted by presynaptic boutons and that Evi is required for normal Wg secretion, we next examined if presynaptically derived Evi colocalized with endogenous secreted Wg observed at postsynaptic sites. For these experiments we expressed Evi-GFP in motorneurons and examined both the Wg and Evi-GFP labels at the postsynaptic compartment. We found that there was substantial colocalization between Wg and Evi-GFP distal to the bouton rim, right outside the HRP label (Figure 2.3J), consistent with the idea that secreted Evi vesicles contain Wg.

In contrast to the expression of Evi-RNAi in motorneurons, expressing Evi-RNAi in the muscles (Evi-RNAi-post), although significantly reducing the levels of Evi protein in the postsynaptic compartment, did not change the levels of Evi in presynaptic boutons (Figures 2.3K and 2.3I). These results demonstrate that Evi is expressed by both motorneurons and muscles, but that there is a unidirectional transfer of Evi from presynaptic boutons to the postsynaptic region.

Considering that Evi is a multipass transmembrane protein, two possible scenarios might account for the above transfer of Evi from the pre- to the postsynaptic region. One possibility is that an extracellular region of Evi is cleaved, as is the case for other membrane receptors (Selkoe et al., 1996) (Figure 2.3N). However, this possibility is highly unlikely, as in the Evi-GFP transgene the GFP tag is fused to the intracellular C-terminal region of Evi, and

thus the transfer must include the intracellular domain. An alternative possibility is that the entire Evi protein could be transported in the form of a vesicle from the pre- to the postsynaptic compartment (Figure 2.3O), as has been previously suggested with argosomes, vesicular structures that can transport Wg from cell to cell (Greco et al., 2001). To address this possibility, we took advantage of the Evi-Nex antibody, which recognizes an epitope localized at the first extracellular loop of Evi (Figure 2.3A; red region in Figures 2.3N and 2.3O), and which is separated from the C-terminal GFP tag by seven transmembrane domains. For these experiments, we expressed Evi-GFP in motorneurons in an *evi* null mutant background and determined whether the postsynaptic GFP signal colocalized with the Evi-Nex and Evi-Cin immunoreactivity. We found that anti-Evi-Nex and anti-Evi-Cin immunoreactivities were exactly colocalized with Evi-GFP at the postsynaptic region (Figures 2.3L, 2.3M, S2.3G, and S2.3H). Thus, these results support the notion that intact Evi is transferred across the synapse likely in a vesicle.

We also examined *Drosophila* Schneider-2 (S2) cells transfected with the Evi-GFP construct. We found that untransfected S2 cells in contact with Evi-GFP-transfected cells often contained Evi-GFP-positive puncta within their cytoplasm (Figure 2.4A, arrowheads). To verify that this was due to transfer of Evi-GFP from transfected to nontransfected cells, Evi-untransfected cells were separately transfected with mCherry and mixed with the Evi-GFP-transfected cells. Again, we found that mCherry-positive (Evi-untransfected) cells had GFP puncta within their cytoplasm (Figure 2.4B), suggesting that Evi-transfected cells

transferred Evi to nearby cells. We also found that Evi-GFP puncta were observed in the medium, suggesting the secretion of Evi vesicles into the medium (Figure 2.4A, arrow). To determine if the Evi vesicles that were transferred to adjacent cells contained Wg, we cotransfected S2 cells with Evi-GFP and Wg. We found that the Evi vesicles transferred to adjacent cells or to the medium contained Wg (Figures 2.4C and 2.4D, arrowhead). Interestingly, in these double transfected cells Wg localized to varicosities within filopodia (arrows in Figure 2.4D). These filopodia were also present in untransfected cells as seen with phalloidin staining to label endogenous F-actin (Figure S2.4C). Two other membrane proteins, DFz2 and rCD2-mRFP, which also become localized to filopodia, were not observed to be secreted (Figures S2.4A and S2.4B). We also carried out a western blot analysis of the S2 cells and the culture medium. We found that indeed the culture medium contained full-length Evi protein, suggesting that Evi was secreted to the medium (Figure 2.4E). The above observation was directly visualized by time-lapse imaging of the Evi-GFP fluorescence. We found that Evi-GFP puncta trafficked within highly dynamic filopodia-like structures in the S2 cells and that some of these puncta were secreted to the media in a time frame of several minutes (Figure 2.4F). Thus, release and transcellular transfer of Evi vesicles to adjacent cells is a common biological mechanism utilized by both neuronal and non-neuronal cells.

Evi Is Present in Multiple Compartments at the Neuromuscular Junction

To determine the subcellular localization of Evi within pre- and postsynaptic compartments we next carried out immunoelectron microscopy studies with the Evi antibodies. For these experiments 1.4 nm gold-conjugated secondary antibodies followed by silver intensification were used to mark sites of Evi-antibody binding using the pre-embedding technique. Consistent with our immunofluorescence studies, Evi was found to be localized in several pre- and postsynaptic structures.

At the postsynaptic junctional region, Evi was found within the subsynaptic reticulum (SSR), a system of muscle-derived membrane folds that completely surrounds synaptic boutons (Figure 2.5A; the presynaptic bouton highlighted in pink overlay). Within the SSR, silver-intensified gold particles were observed in close association with the membrane folds (Figure 2.5E, arrows). Notably, gold particles were also found inside approximately 200 nm in diameter membranous vesicles within the SSR (Figures 2.5A and 2.5B; arrows and insets). In summary, at the postsynaptic region, Evi is present in association with SSR membranes and with novel postsynaptic vesicles.

Evi was also associated with the pre- and postsynaptic membrane (Figure 2.5F, arrows) and sometimes the signal was observed at the synaptic bouton cleft (Figure 2.5H, arrow and inset). Within the presynaptic bouton, Evi was observed in large multimembrane structures (Figure 2.5G, arrowhead). Thus, Evi is present in multiple structures at synapses, including pre-and postsynaptic vesicular structures, the SSR, and synaptic membranes.

To determine if these vesicles were endocytosed from the muscle surface, we next conducted an internalization assay. These experiments were facilitated by the finding that the Evi-Nex antibody can bind to surface Evi *in vivo* (Figure S2.3A). For these studies, unfixed and unpermeabilized body wall muscles were incubated with the Evi- Nex antibodies in the cold, washed, and brought to room temperature for 30 min prior to fixation. Then, samples were permeabilized and incubated with the gold-conjugated secondary antibody, followed by preparation for electron microscopy (EM). Interestingly we found that the Evi label was found at SSR membranes as well as inside the large SSR vesicles (Figure 2.5C, arrows and insets), suggesting that at least a subset of these postsynaptic vesicles are derived from the endocytosis of postsynaptic surface Evi.

To verify that Evi was transferred from presynaptic boutons to the postsynaptic SSR at the ultrastructural level, GFP-tagged Evi was expressed in motorneurons using the C380-Gal4 driver, and the NMJ was examined by immunoelectron microscopy using an anti-GFP antibody. We found that the GFP label was found not only within synaptic boutons (Figure 2.5D, arrowhead) but also throughout the postsynaptic SSR membrane (Figure 2.5D). We also expressed Evi-GFP in the motorneurons of *evi* mutants and immunolabeled Evi with the Evi-Cin antibody using the postembedding technique. Again, we found the label in the presynaptic compartment (Figure 2.5I, arrowhead), at the synaptic bouton cleft (Figure 2.5J, arrowhead), as well as in the postsynaptic SSR region (Figures 2.5I and 2.5K, arrows). Thus, Evi is transferred transsynaptically as expected from the observations at the light level.

Postsynaptic Evi Is Required for the Trafficking of DFz2 through the DFz2-Interacting Protein dGRIP

Given that presynaptic Evi alone is not sufficient for normal NMJ development, we predicted that Evi was also endogenously expressed in muscle. To test this prediction we carried out real-time PCR experiments from body wall muscle mRNA. We found that there were significant levels of Evi-mRNA in muscles and that these levels were substantially decreased upon expressing Evi-RNAi (Figure S2.5). What is the cell-autonomous role of Evi in the postsynaptic target cell? To address this issue we examined postsynaptic Wg signaling while downregulating Evi selectively in the muscle using Evi-RNAi. Previous studies suggested that Wg is secreted by presynaptic boutons (Packard et al., 2002) and unraveled a novel postsynaptic Wg signal transduction pathway in the postsynaptic muscles, the frizzled nuclear import (FNI) pathway (Speese and Budnik, 2007), which is also shared by other WNT receptors (Lyu et al., 2008). In this pathway, the Wg receptor, DFz2, is internalized from the postsynaptic muscle membrane and back-transported from the synapse to the nucleus through a mechanism that requires an interaction between the PDZ-binding C-terminal tail of DFz2 and the PDZ4-5 domain of the 7-PDZ protein dGRIP (Ataman et al., 2006a). The entire cytoplasmic domain of DFz2 (DFz2-C) is then cleaved and imported into the nucleus (Mathew et al., 2005).

In muscles expressing Evi-RNAi we found that DFz2 was localized normally at the postsynaptic region of the NMJ. However, the postsynaptic levels of DFz2 were substantially increased (Figures 2.6A, 2.6B, and 2.6E). In contrast,

no such increase in DFz2 levels was observed in the presynaptic cell upon expression of Evi-RNAi in motorneurons (normalized presynaptic DFz2 intensity in wild-type is 1.0 ± 0.07 versus 0.93 ± 0.07 in Evi-RNAi-pre). The same phenotype has been previously observed when the transport of DFz2 from the synapse to the nucleus is prevented by interfering with dGRIP function in muscles (Ataman et al., 2006a). Interestingly, a similar accumulation of Wg at the postsynaptic region was observed upon downregulating Evi in muscle (Figures 2.6C–2.6E), consistent with the notion that Wg is trafficked with its receptor (Gagliardi et al., 2008). To determine if the increase in DFz2 at synapses of Evi-RNAi-post larvae was due to a defect in the internalization and/or trafficking of DFz2, we carried out DFz2 internalization assays. In these experiments we used an anti-DFz2-N antibody that binds to the extracellular domain of the receptor in vivo, allowing us to follow the fate of internalized DFz2. Dissected third instar body wall muscles were incubated with the DFz2-N antibody at 4°C in vivo, and after washing the excess antibody, samples were brought to room temperature and fixed at 5 and 60 min after the antibody-binding step. To determine the fraction of DFz2 that remained at the surface, samples were then incubated with Alexa 647-conjugated secondary antibody in the absence of detergent permeabilization as previously reported (Ataman et al., 2006a); (Mathew et al., 2005). To determine the amount of internalized DFz2, the above procedure was followed by permeabilization and incubation with a FITC-conjugated secondary antibody.

As in previous studies (Ataman et al., 2006a); (Mathew et al., 2005), in

wild-type samples, surface DFz2 was internalized and observed near synaptic boutons at 5 min after the antibody-binding step (Figures 2.6G2 and 2.6F). However, at 60 min after the antibody-binding step, internalized DFz2 was significantly reduced at the NMJ as a result of its trafficking away from the synapse (Figures 2.6H2 and 2.6F; (Ataman et al., 2006a); (Mathew et al., 2005)). In contrast, upon expressing Evi-RNAi in muscles, no decrease in internalized synaptic DFz2 was observed at 60 min (Figures 2.6I2, 2.6J2, and 2.6F). No significant changes were observed in surface DFz2 in both genotypes (Figures 2.6G1–2.6J1 and 2.6F), suggesting that only a small pool of the DFz2-antibody complexes become internalized. Thus, similar to alterations in dGRIP, a decrease in Evi function in muscles appears to interfere with the trafficking of DFz2 away from the synapse. This conclusion was further supported by examination of the levels of DFz2-C imported into the muscle nuclei. Previous studies show that the C-terminal region of DFz2 is cleaved and imported into the nucleus, where it is observed in the form of discrete immunofluorescent puncta (Figure 6K; (Mathew et al., 2005)). In *evi* mutants and upon expressing Evi-RNAi in muscles alone, nuclear DFz2-C puncta were almost completely abolished (Figures 2.6K–2.6M), in agreement with the model that in the absence of Evi function, DFz2 is not properly transported to the muscle nucleus. Furthermore, a complete rescue of the DFz2-C nuclear spots to wild-type levels was observed in the *evi* mutant by expressing the Evi transgene in the muscle alone. In contrast, expressing Evi in motorneurons provided only a partial rescue of the nuclear DFz2-C foci (Figure 2.6M). Therefore, we conclude that muscle Evi is involved in

the trafficking of DFz2 to the nucleus.

Given the substantial similarities between the phenotypes observed upon knocking down *evi* and *dgrip* in postsynaptic DFz2 trafficking as well as in the synaptic morphology and NMJ growth (Ataman et al., 2006a), we next examined whether interfering with Evi function could be disrupting the postsynaptic function of dGRIP. For these studies we examined the localization of dGRIP in larvae expressing Evi-RNAi in muscles. In wild-type, dGRIP is present in small trafficking vesicles highly concentrated at postsynaptic sites (Figure 2.7A, arrows; (Ataman et al., 2006a)), as well as in Golgi bodies in juxtaposition to the *cis*-Golgi marker Lavalamp (Lva; Figure 2.7A, arrowheads; (Ataman et al., 2006a)). Notably, we found that upon knocking down Evi specifically in muscles, dGRIP was substantially reduced from postsynaptic sites as well as from Golgi bodies in muscle (Figures 2.7B and 2.7C). In addition, dGRIP was localized throughout the muscle submembrane region in a diffuse manner (Figures 2.7B and 2.7C). Thus, Evi controls dGRIP localization at the postsynaptic muscle region, and in the absence of Evi function dGRIP is not normally localized to the Golgi and synapses, likely disrupting postsynaptic DFz2 trafficking. A prediction of this model is that overexpressing dGRIP in muscles should overcome some of the defects arising from the lack of Evi in muscles. To test this model we overexpressed dGRIP in muscles while downregulating Evi in these cells. We found that the DFz2 accumulation at the postsynaptic region of Evi-RNAi-post was completely rescued, and indeed the postsynaptic levels of DFz2 became significantly lower than wild-type (Figure 2.7D). In addition, both the number of

synaptic boutons and nuclear DFz2-C spots were partially rescued by overexpressing dGRIP in *evi* mutants (Figures 2.7E and 2.7F).

An additional prediction is that a population of Evi vesicles should traffic with dGRIP vesicles. To determine if this was the case we performed time-lapse imaging of muscles expressing both Evi-GFP and dGRIP-mRFP. We found that in many instances Evi and dGRIP vesicles colocalized and followed the same trajectory. These results demonstrate that Evi, in addition to its important role in the Wg-secreting cell, has a critical function in Wg-target cells, as it mediates the transport of the downstream Wg signaling component, dGRIP.

DISCUSSION

Here we show that the multipass transmembrane protein Evi has a critical role in *trans*-synaptic WNT-1/Wg transport through vesicular structures. To our knowledge, this is the first report to identify *trans*-synaptic communication through a vesicular structure. Further, our studies identify a mechanism by which secreted factors can be transmitted from cell to cell. We propose that presynaptic Evi is required for trafficking Wg from the cell body to the presynaptic terminals, and across the synaptic cleft, to present Wg to postsynaptic DFz2 receptors (Figure 2.7G). On the other hand, postsynaptic Evi is required to transport dGRIP to postsynaptic sites. At the postsynaptic region dGRIP interacts with postsynaptic DFz2 receptors and participates in the trafficking of DFz2 to the nucleus, where its C-terminal tail is cleaved and imported to the nucleus (Figure 2.7G). Previous studies had implicated Evi only in the secretion of WNTs in

WNT-expressing cells (e.g., (Banziger et al., 2006)). However, endogenous Evi was also found in WNT-target cells (Port et al., 2008), where it plays an as yet unidentified role. Our studies here identify an unprecedented role for Evi in Wg-receiving cells in trafficking the Wg receptor DFz2 through the regulation of the synaptic targeting of the DFz2-interacting protein dGRIP, which was previously shown to function in transporting DFz2 receptors from the postsynaptic membrane to the muscle nucleus (Ataman et al., 2006a). These studies unravel new processes and cellular mechanisms by which Evi functions as an essential component of synaptic WNT signaling.

Trans-Synaptic Signaling in the Nervous System: Role of WNTs

Intercellular communication in the brain is primarily accomplished through the exocytosis of neurotransmitter-laden vesicles or by direct current conduction through gap junctions. Pre- and postsynaptic partners also release factors important for cell survival, synapse development, synapse maintenance, and synaptic plasticity (reviewed in (Lu and Figurov, 1997); (Marques, 2005)). Among these are neurotrophins such as *b*one-*d*erived *n*eurotrophic *f*actor (BDNF) and *n*erve *g*rowth *f*actor (NGF), members of the *b*one *m*orphogenetic *p*rotein (BMP) family, and WNTs. These molecules are released from pre- or postsynaptic terminals and they function in retrograde or anterograde manners to influence synaptic growth, function, and plasticity. At the *Drosophila* larval NMJ, continuous coordination of synaptic growth in relationship to muscle size requires the release of a retrograde signal of the BMP family that acts on BMP receptors in the

presynaptic cell (Marques, 2005). This correlated synaptic growth is also controlled by the release of Wg, which is thought to act on DFz2 receptors in both the pre- and postsynaptic cells where it initiates alternative transduction pathways (Ataman et al., 2008); (Franco et al., 2004); (Miech et al., 2008).

A major gap in our understanding of how WNTs function is the mechanism by which they reach their destination once released. Despite the presence of charged amino acid residues in the primary sequence of WNTs, WNTs are hydrophobic molecules tightly bound to cell membranes due to the addition of palmitate moieties during maturation (Willert et al., 2003); (Zhai et al., 2004). This hydrophobic nature of WNTs argues against the simple model of passive diffusion in the extracellular milieu. The studies presented here suggest that one mechanism for this transport is the association of Wg with Evi-containing vesicles, which are released from presynaptic boutons and become localized to postsynaptic sites. This model is supported by several lines of evidence. (1) Downregulating Evi in the presynaptic motorneurons (Evi-RNAi-pre) not only led to a reduction in Evi immunoreactivity inside presynaptic terminals but also substantially reduced the label at the postsynaptic region. (2) Expressing Evi-GFP in motorneurons (Evi-GFP-pre) led to the localization of the GFP label in the postsynaptic junctional region in the form of puncta that colocalized with both the Evi-Cin and Evi-Nex antibodies and that showed substantial colocalization with secreted Wg at the postsynapse. (3) Evi-GFP could be transferred from transfected to untransfected S2 cells, and S2 cell-culture medium contained full-length Evi protein, suggesting that Evi was also secreted in cultured cells. In

addition, the secreted and transferred Evi vesicles contained Wg. This *trans*-synaptic transfer of a synaptogenic signal through specialized vesicles containing a dedicated membrane protein is a novel signaling mechanism in the nervous system that might be used for a number of secreted signaling factors.

The release of endosomal vesicles, called exosomes, has been reported in a variety of tissues, including cultured neurons (Faure et al., 2006); (Fevrier and Raposo, 2004); (van Niel et al., 2006). These exosomes are released by the fusion of multivesicular bodies (MVBs) with the plasma membrane and are thought to be involved both in the removal of cellular debris as well as in intercellular communication. For example, in the immune system integrin- and MHC-containing exosomes are used for antigen presentation, and they are able to prime T lymphocytes in vivo (van Niel et al., 2006). In cultured cortical neurons, the release of exosomes containing the cell adhesion molecule L1, the GPI-anchored prion protein, and the GluR2/3 subunit of glutamate receptors has been reported in a process that is regulated by membrane depolarization (Faure et al., 2006). Our finding that exosome-like vesicles containing a synaptogenic factor are released at synapses provides a previously unidentified mechanism for *trans*-synaptic communication.

The mechanism by which Evi-containing vesicles are released from the presynaptic cell is not known, but a few potential possibilities are depicted in Figure 3O. For example Evi might be transported within the presynaptic cell in MVBs that fuse with the plasma membrane thus releasing the Evi vesicle. In turn, after presentation of Wg to DFz2 receptors, the vesicle might fuse with the

postsynaptic membrane. Interestingly, we found that Evi in presynaptic terminals was present in multimembrane compartments. Similarly, in Wg-secreting wing disc epithelial cells, Evi (Franch-Marro et al., 2008) and Wg (van den Heuvel et al., 1989) have been shown to be localized within MVBs. We also found that Evi label was found in association with postsynaptic SSR membranes and in the form of approximately 200 nm vesicles in the SSR. Our internalization assays suggest that these vesicles are endocytosed from the postsynaptic membrane.

Cell-Autonomous Role of Evi in Wg-Target Muscles

Besides its involvement in transporting the Wg signal across the synapse, we also found that Evi had a cell-autonomous function in the postsynaptic target cell, as revealed by specifically downregulating Evi in muscle. In this case both Wg and DFz2 accumulated at the postsynaptic region. In addition, DFz2 did not traffic normally from the NMJ and the nuclear import of DFz2-C was largely abolished. These findings suggest that Evi, beyond the regulation of WNT secretion, organizes further downstream signaling events in the Wg-target cell.

The phenotypes observed upon downregulating Evi in muscle cells were highly reminiscent of those observed upon loss of dGRIP function. Further, decreasing Evi levels led to the virtual elimination of synaptic and Golgi dGRIP. The evidence relating Evi to dGRIP function is further supported by the findings that Evi and dGRIP are often observed trafficking in the same vesicles, and that overexpressing dGRIP in either *evi* mutants or Evi-RNAi-post elicited partial rescue of phenotypes resulting from *evi* loss of function. Thus, Evi appears to be

required for the trafficking of dGRIP to synaptic sites where dGRIP binds DFz2 receptors and functions to traffic them toward the nucleus. The elimination of dGRIP from the Golgi complex might arise from a defect in its recycling to the Golgi due to its abnormal targeting to synapses. In the absence of postsynaptic dGRIP, DFz2 is not trafficked toward the nucleus leading to its accumulation at postsynaptic sites. Interestingly, Evi has been demonstrated to be involved in trafficking Wg from the Golgi to the plasma membrane in Wg-secreting cells (Belenkaya et al., 2008); (Franch-Marro et al., 2008); (Pan et al., 2008); (Port et al., 2008); (Yang et al., 2008). Our studies showing that Evi is required for the trafficking of dGRIP to postsynaptic sites suggest that Evi might have a role not solely in transporting WNTs, but also in trafficking components associated with WNT pathways.

Although this study identifies a pre- and postsynaptic role for Evi, it is clear that the roles are not completely independent. For example, we found that restoring Evi levels only in the motorneurons of *evi* mutants was sufficient for a complete rescue of the ghost bouton phenotype and resulted in a partial rescue in the number of nuclear DFz2C spots. These results were surprising given that in the absence of postsynaptic Evi, dGRIP does not traffic normally and thus interferes with postsynaptic WNT signaling. A potential explanation is that the transferred presynaptic Evi can partially compensate for the lack of Evi in the postsynaptic cell.

In conclusion, our studies identify a mechanism by which the WNT-1/Wg signal is transmitted across the synapse, through the use of an Evi vesicle, and

find an additional cell-autonomous role of Evi in WNT-receiving cells, the synaptic recruitment of dGRIP, which functions in transporting the signal to the muscle nucleus.

MATERIALS and METHODS

Fly Strains

Flies were reared in standard *Drosophila* media at 25°C unless otherwise stated. (See Supplemental Materials and Methods for fly strains.) RNAi crosses and controls were performed at 29°C. The wg^{ts} flies were tested at the restrictive temperature (25°C).

Cytochemistry

Third instar larvae were dissected in Ca^{++}-free saline and fixed in either 4% paraformaldehyde or non-alcoholic Bouin's fixative (see Supplemental Materials and Methods for antibodies and Hoechst conditions).

Image Quantification

Confocal images were acquired using a Zeiss Pascal Confocal Microscope. Preparations from different genotypes were processed simultaneously and imaged using identical confocal acquisition parameters. Fluorescence signal intensity was quantified by volumetric measurements of confocal stacks using Volocity 4.0 Software (see Supplemental Materials and Methods). Measurements were taken from muscles 6 and 7, abdominal segment 3. A Student's t test was

performed for pair-wise comparisons between each genotype and controls. Error bars in the histograms represent mean ± standard error of the mean (SEM), where *** = $p < 0.0001$; ** = $p < 0.001$; * = $p < 0.05$.

Schneider-2 Cell Cultures

Schneider-2 (S2) cells were transfected as described in Supplemental Materials and Methods. For Evi-GFP transfer experiments, pAc-Evi-EGFP (Bartscherer et al., 2006) transfected S2 cells were washed 24 hr after transfection and mixed with pAc-mCherry transfected S2 cells. For cotransfection experiments we used pAc-Wg (Bartscherer et al., 2006), pAc-Evi-EGFP, pAcrCD2- RFP, and pAc-DFz2-myc (Mathew et al., 2005). Cells were then grown for 24–48 hr and processed for immunocytochemistry.

Live Imaging

Live imaging of transfected S2 cells and body wall muscles was performed using an Improvision Spinning Disk confocal microscope as described in Supplemental Materials and Methods.

Western Blots

Western blots were performed as in (Mendoza-Topaz et al., 2008). For examination of Evi in S2 cells and the culture medium, transfected cells were washed with fresh medium 24 hr after transfection, and 24 to 48 hr later cells and medium were harvested for immunoblotting (Supplemental Materials and

Methods).

Immunoelectron Microscopy

For the pre-embedding technique, third instar body wall muscles were fixed and incubated with anti-Evi-Nex (1:100) or anti-GFP (1:300) followed by anti-rabbit IgG-1.4 nm nanogold (1:50; Nanoprobes) and intensification using HQ silver reagents (Nanoprobes). The EM Internalization assay was performed as above, except that 1.4 nm nanogold secondary antibody was used after permeabilization. For the post-embedding technique, samples were fixed and then embedded in LR White resin followed by antibody staining on grids with secondaries conjugated to 18 nm gold (1:75; Jackson). Transmission electron microscopy analysis was performed as described by (Torroja et al., 1999).

SUPPLEMENTAL MATERIALS and METHODS

Fly Strains

The following fly strains were used for these studies: wild type (Canton-S), *evi*^{2} (Bartscherer et al., 2006) (referred to as *evi* in the text), *wg*^{ts} (*wg* ^{IL114}; (Nusslein-Volhard et al., 1985)), UAS-myr-mRFP (Bloomington Stock Center), UAS-Evi- EGFP (Bartscherer et al., 2006), UAS-Evi-RNAi (stock 5215; Vienna Drosophila RNAi Center www.vdrc.at/), UAS-dGRIP-mRFP (Ataman et al., 2006a), UASLacZ- NLS and the Gal4 drivers C380, BG487 and C57 (Budnik et al., 1996), Elav-Gal4 (Luo et al., 1994), and Wg-Gal4 (gift of Dr. S. Cohen).

Immunocytochemistry and cytochemical staining.

The following primary antibodies were used: anti-Wg (1:300 (Packard et al., 2002)), anti-DLGPDZ (1:20,000 (Koh et al., 1999)), anti-Evi-Nex (1:100; see below), anti-Evi-Cin (1:100; see below), anti-DFz2-N (1:600 (Packard et al., 2002)), anti-DFz2-C (1:100 (Mathew et al., 2005)), anti-GFP (1:200; Molecular Probes), anti-dGRIP (1: 300 (Ataman et al., 2006a)), anti-Wg monoclonal (1:2, clone 4D4; Developmental Studies Hybridoma Bank (DSHB)), anti-elav (1:50; clone 9E8A10; DSHB), anti-myc (1:200; Roche), mouse anti-GFP (1:200; Molecular Probes), Rabbit anti-GFP (1:300; MBL International), anti-β-gal (1:1000; Organon Teknika Corporation), Texas red (TxR) conjugated anti-HRP (1:200; Sigma), FITC conjugated anti-HRP (1:800; Sigma). FITC-, TxR-, and Alexa 647-conjugated secondary antibodies (Jackson Immunoreasearch) were used at 1:200. Rhodamine conjugated Phalloidin (Molecular Probes) was used at 1:200. Hoechst nuclear stain (33342, Invitrogen) was used at 10 µg/ml for 15 minutes at room temperature.

Quantification of immunoreactivity levels and morphometric analysis

Images were acquired using a Zeiss (Oberkochem, Germany) Pascal Confocal Microscope with a 63X (1.4 numerical aperture) objective. Preparations from different genotypes were processed simultaneously and imaged using identical confocal acquisition parameters for comparison. Fluorescence signal intensity was quantified by volumetric measurements of confocal stacks using Volocity 4.0

Software (Improvision, Waltham, MA). For measurement of pre- and postsynaptic intensity, single boutons were selected and analyzed as three- dimensional volumes in Volocity. The labeled region around the boutons was segmented by intensity thresholding based on the difference in the intensities at the NMJ vs background intensity. Fluorescence intensity represents the sum of the intensities of each of the voxels that fell above the threshold value. Presynaptic intensity was measured by calculating the volume occupied by the label of interest that overlapped with the volume occupied by the anti-HRP label (presynaptic bouton volume) and measuring the total intensity within that volume. To obtain postsynaptic intensity, the volume occupied by the anti-HRP label was subtracted from the total volume of the labeled region resulting in the postsynaptic volume. The total intensity of the label within the postsynaptic volume was computed to obtain the postsynaptic intensity. Both pre and postsynaptic intensities were expressed as $V_{post\text{-}\,int}$ / V_{bouton} and normalized to wild type controls dissected and processed in the same experimental session. For determination of the number of type I boutons and ghost boutons, body wall muscle preparations were double stained with anti-HRP and anti-DLG. Measurements were taken from muscles 6 and 7, abdominal segment 3. For measurements of Wg accumulation in the brains of wild type and *evi* mutant larvae, regions of the brain that included either the motorneuron cell bodies or the neuropil were selected from both genotypes and mean intensity of Wg in that region were measured. A Student's t test was performed for pair-wise comparisons between each genotype and its simultaneously processed wild type

control samples.

Schneider-2 (S2) cell cultures

Drosophila Schneider (S2) cells were cultured in SFX (Hyclone) medium containing 10%FBS, penicillin (100 U/µl) and streptomycin (100 µg/µl) (SFX-SPS). 3x2ml-wells/sample of 60-80% confluent S2 cells were transfected with 1.0 µg DNA using Cellfectin and Serum Free Medium (Invitrogen). For Evi- GFP transfer experiments, pAc-Evi-EGFP (Bartscherer et al., 2006) transfected S2 cells were washed 24 hours after transfection and mixed with pAc-mCherry transfected S2 cells. For co-transfection experiments, pAc-Wg (Bartscherer et al., 2006) was used along with pAc-Evi-EGFP. In addition pAc-rCD2-RFP and pAc-DFz2-myc (Mathew et al., 2005) constructs were used for transfections. Cells were then grown for 24-48 hours and processed for immunocytochemistry.

Live Imaging

Live imaging of cells was performed on transfected S2 cells grown on 22mm coverslips, and then mounted over cell culture medium, and sealed in place with dental wax. These slides were then imaged using an Improvision Spinning Disk confocal microscope using a 40X Zeiss 1.2 NA objective. Z-stacks were taken once every 5 seconds. Live imaging of larval muscles was performed basically as in (Ataman et al., 2008). Briefly, larvae were dissected under 0.1mM $CaCl_2$ HL-3 saline, covered with a coverslip and imaged under the Improvision Spinning Disk confocal microscope. Due to two color live imaging, Z-stacks were taken once

every 15 seconds.

Western blots

Larval brains were dissected in ice cold Ca^{++}-free saline and homogenized at 4°C in RIPA buffer containing protease inhibitors as previously described (Mendoza-Topaz et al., 2008). Proteins were separated on an 8% SDS PAGE gels, transferred onto nitrocellulose membranes and sequentially immunoblotted with anti-Wg (1:3000) and anti-tubulin (1:5000). For examination of Evi in S2 cells and the culture medium, the culture medium of S2 cells transfected with pAc-Evi-EGFP was changed 24 hours after transfection. Cells were then harvested the next day and spun down at 4,000rpm to collect the cellular pellet and the supernatant. The supernatant was subsequently centrifuged at 12,000rpm. Cell lysates and supernatants were separated on 8% SDS PAGE gels and immunoblotted as above with anti-GFP (1:5000; Abcam) and anti-Lamin C (1:300; LC28.26, Developmental Studies Hybridoma Bank) antibodies. Signal was detected using chemiluminescence reagents (Amersham).

Extraction and Isolation of RNA and cDNA synthesis

Larvae were homogenized in trizol reagent using a pellet pestle (Kimble-Kontes, Vineland, NJ). Total RNA was treated with DNAse and eluted with the RNeasy Micro Kit (Qiagen, CA). RNA was quantified by UV spectrophotometry using a NanoDrop 2000c spectrophotometer (Thermo scientific). cDNA synthesis was performed using a SuperScript III cDNA synthesis kit from 1 µg of eluted total

RNA (Invitrogen, CA). Expression of Evi mRNA was analyzed by Real time PCR with Taqman Gene expression assays, house keeping: GapDH [assay ID: Dm01841185_m1 gpdh], Target: Evi [assay ID:Dm 01802231_g1 wls] using the ABI 7000 SDS software, Applied Biosystems and analyzed via the delta-delta Ct method. Absence of DNA contamination in total RNA was confirmed by realtime qRT-PCR using -RT as a control.

Generation of Evi antibodies

Affinity purified antibodies anti-Evi-Nex and anti-Evi-Cin, were raised in rabbits using the peptides TIDMRLAYRNKGDPDN and SHKQHPTMHHSDETTQSN as immunogens (Biosource).

Internalization assay

The internalization assay was performed as in (Mathew et al., 2003). Wandering third instar larvae were dissected in 0.1 mM Ca^{++} HL-3 saline and incubated in saline containing DFz2-N antibody for 2 hr at 4°C. Samples were then washed and shifted to room temperature for 5 or 60 min, fixed, and labeled with Alexa 647-conjugated secondary antibody under nonpermeabilized conditions to label surface DFz2. To label internalized DFz2, samples were permeabilized and labeled with a FITC-conjugated secondary antibody.

Immunoelectron microscopy

For the pre-embedding technique, third instar body wall muscles were dissected in 0.1 mM $CaCl_2$ HL-3 saline and fixed using 0.1% Glutaraldehyde in Trump's

fixative with 2mM $MgCl_2$ for 1 hour at room temperature. The samples were then washed and incubated with anti-Evi-Nex (1:100) or anti-GFP (1:300) antibody for 1 hour at room temperature. The secondary antibody was anti-rabbit IgG-1.4 nmnanogold (1:50; Nanoprobes, NY). The samples were then washed, rinsed with deionized water and the signal intensified by using silver enhancement using HQ silver reagents (Nanoprobes, NY) in the dark for 4 minutes. Samples were then post-fixed for 1 hour at 4°C. Boutons from muscles 6 and 7 at segments A3 were serially sectioned and photographed at 19,500X and 66,000X using a TEM. For the internalization assay, samples were dissected as above and incubated in saline containing anti-Evi-Nex for 1 hr at 4°C. Samples were then washed and shifted to room temperature for 0 or 60 min and fixed in Trump's fixative containing 0.1% glutaraldehyde and 2 mM MgCl2 for 1 hr at room temperature. After washing, samples were incubated with 1.4 nm nanogold conjugated antirabbit secondary (1:50; Nanoprobes, NY) prior to processing for TEM as above. For the post-embedding technique, samples were fixed in Trump's fixative containing 0.1% glutaraldehyde and 2mM MgCl2 for 2.5 hours, and then embedded in LR White resin. Thin sections were captured on nickel grids, treated with glycine to quench free aldehyde groups, blocked, and incubated with anti-Evi-Cin (1:100), and anti-rabbit IgG antibody conjugated to 18nm gold (1:75; Jackson). Samples were then stained and visualized by TEM.

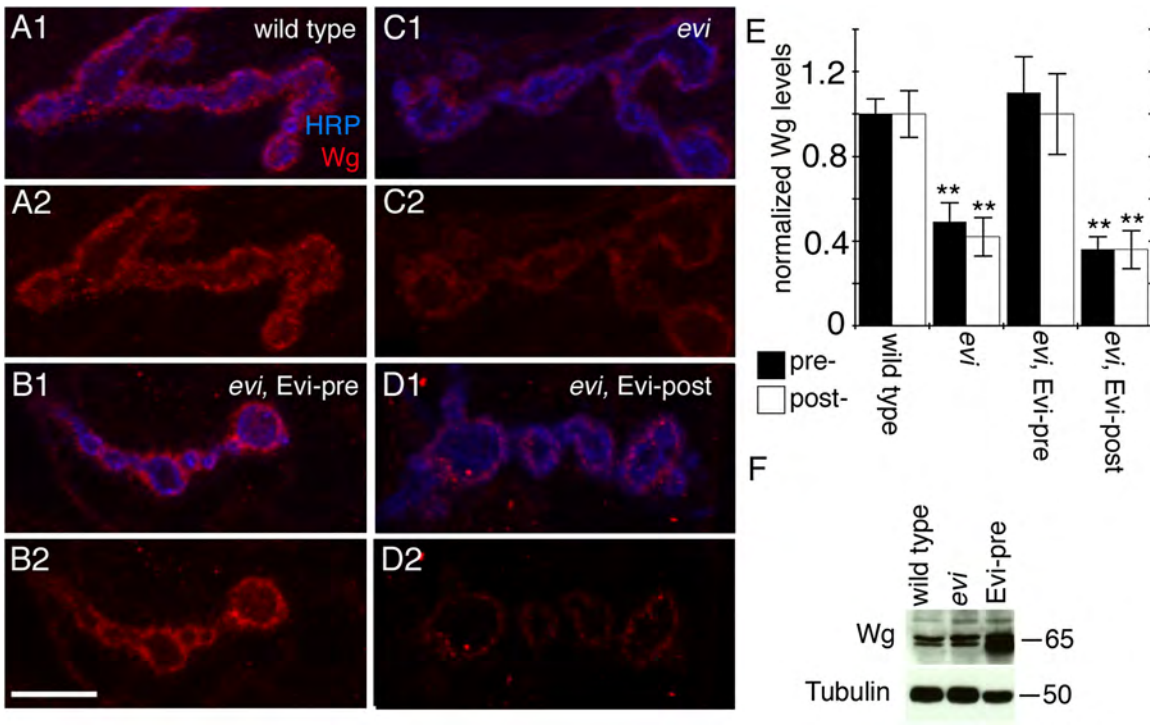

Figure 2.1. Wg Localization at the Neuromuscular Junction Is Regulated by Presynaptic Evi

(**A-D**) Single confocal slices of 3rd instar larval NMJs at muscles 6 or 7, labeled with anti-HRP (blue) and anti-Wg (red) in (**A**) Wild type, (**B**) an *evi* mutant expressing transgenic Evi in motorneurons to determine if it rescues the Wg decrease (*evi,* Evi-pre), (**C**) an *evi* mutant, and (**D**) an *evi* mutant expressing transgenic Evi in muscles to determine if it rescues the Wg decrease (*evi,* Evi-post). Note that Wg levels were decreased at NMJs of *evi* mutants, and this phenotype could be rescued by expression of Evi in motorneurons but not in muscles. (**E**) Normalized Wg levels inside synaptic boutons (black bars; pre-), and at the postsynaptic region (white bars; post-) in the indicated genotypes (see methods for details on the volumetric quantification). Number of samples is 33 for wild type, 11 for *evi* mutants, 13 for *evi*, Evi-pre, and 11 for *evi*, Evi-post. Bars in

the histogram represent mean±SEM. ***= p<0.0001; **= p<0.001. (**F**) Western blot of larval brain extracts showing that Wg levels do not change in *evi* mutants, but they are enhanced when Evi is expressed in the presynaptic motorneurons. Numbers at the right of the blot represent molecular weigh in KDa. Calibration bar is 7 μm.

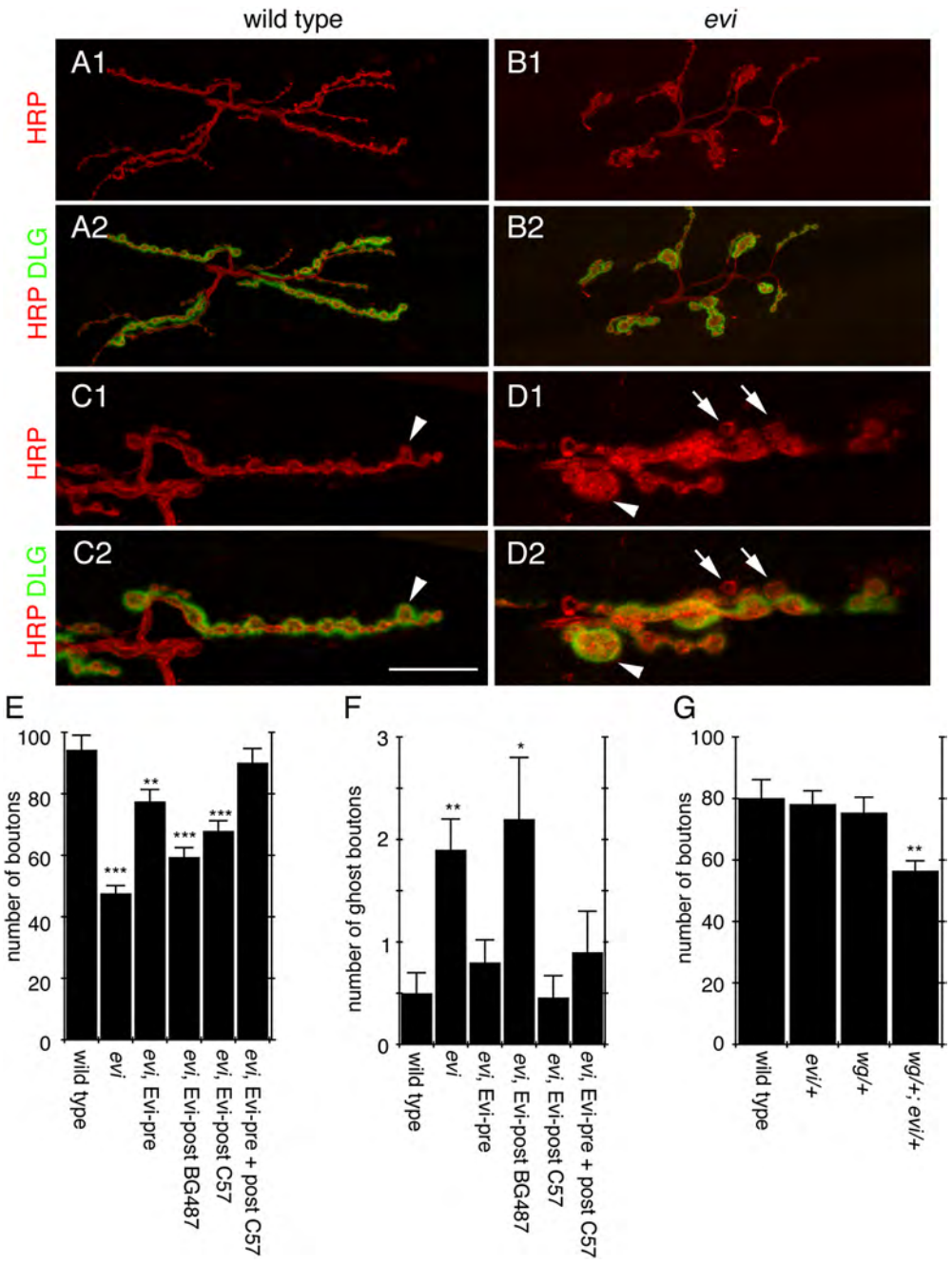

Figure 2.2. Mutations in *evi* mimic abnormal synaptic phenotypes observed in *wg* mutants

(**A-D**) Confocal images of 3rd instar larval NMJs at muscles 6 and 7, labeled with anti-HRP (red) and anti-DLG (green) in (**A**, **C**) wild type, and (**B**, **D**) an *evi* mutant. (**A**, **B**) are low magnification projections of an entire NMJ at muscles 6

and 7, while (**C**, **D**) are high magnification single confocal slices of NMJ branches. In *evi* mutants the number of synaptic boutons is drastically reduced, and boutons have an abnormal shape (arrowheads in C, D). These mutants also have an abnormally high number of undifferentiated boutons (ghost boutons; arrows in D). (**E**-**G**) Quantification of the number of (**E**, **G**) boutons and (**F**) ghost boutons at the 3rd instar larval stage at muscles 6 and 7, abdominal segment A3 in the indicated genotypes. Number of samples in E and F is 26 for wild type; 12 for *evi* mutants, 14 for *evi*, Evi-pre; 13 for *evi*, Evi-post-BG487; 15 for evi, Evi-post-C57; and 13 for *evi*, Evi-pre + post-C57. Number of samples in G is 13 in wild type, 11 in wg^{ts}/+, 14 in *evi/*+, and 10 in *wg/+;evi/*+. Bars in the histograms represent mean±SEM. ***= p<0.0001; **= p<0.001; *=p<0.05. Calibration bar is 30 μm for A, B and 13 μm for C, D.

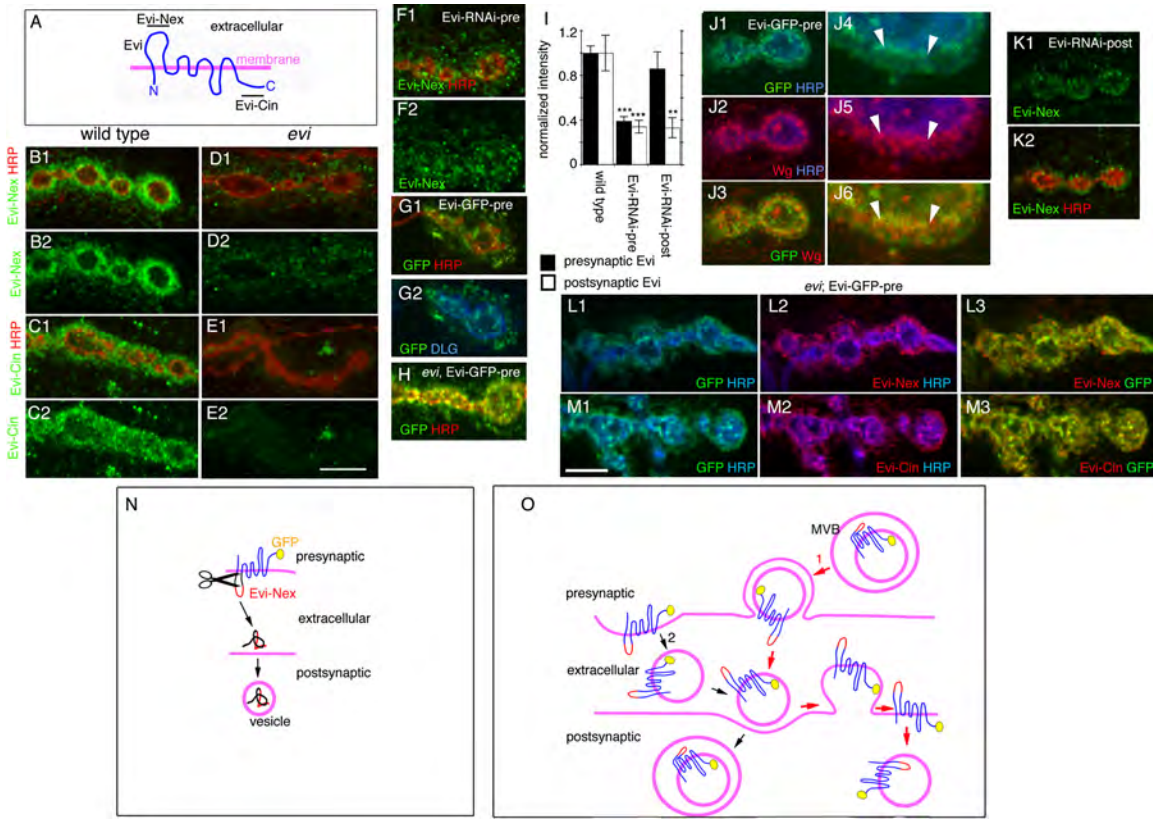

Figure 2.3. Evi Is Localized Pre- and Postsynaptically at the Neuromuscular Junction, and It Is Transported *Trans*-Synaptically as an Intact Protein

(A) Diagram showing the predicted structure of Evi and the protein regions (underlined) used for generation of the Evi-Nex and Evi-Cin antibodies. (**B-E)** Single confocal slices of NMJs at muscles 6 or 7 double stained with anti-HRP (red) and antibodies to (green) (**B**, **D**) Evi-Nex and (**C, E**) Evi-Cin, in (**B, C**) wild type, (**D, E**) *evi* mutant. Both the Evi-Nex and Evi-Cin antibodies label the NMJ, and this immunoreactivity is severely decreased in *evi* mutants.

(F) Confocal slices stained with Evi-Nex (green) and HRP (red) in **(F)** Evi-RNAi-pre, (**G, H**) Single confocal slices of NMJs at muscles 6 or 7 of **(G)** Evi-GFP-pre triple stained with anti-GFP (green), anti-HRP (red) and anti-Dlg (blue) or **(H)** *evi*;

Evi-GFP-Pre stained with anti-GFP (green),anti-HRP (red). **(I)** Quantification of normalized pre- (black bars) and postsynaptic (white bars) Evi levels in the indicated genotypes. Number of samples is 17 for wild type, 10 for Evi-RNAi-pre, and 12 for Evi-RNAi-post. (**J**) Single confocal slices of a bouton at **(J1-J3)** low magnification and **(J4-J6)** high magnification in Evi-GFP-pre stained with anti-GFP (green), anti-Wg (red) and anti-HRP (blue) showing that secreted Evi-GFP colocalizes with secreted Wg at the postsynaptic region. **(L, M)** Confocal images of NMJs from *evi*; Evi-GFP-Pre triple stained with GFP (green), anti-HRP (blue) and antibodies to red **(L2, L3)** Evi-Nex or **(M2, M3**) Evi-Cin. Note that postsynaptic GFP is colocalized with both anti-Evi-Nex and anti-Evi-Cin suggesting that Evi is transferred trans-synaptically as an intact vesicle (see text for details). (**N, O**) Models on the potential mode of Evi trans-synaptic transfer. Note that Evi is fused to GFP at the C-terminal tail, and that the Evi-Nex antibody binds to the first extracellular loop (red) of Evi. In **(N**) an extracellular region of Evi is cleaved and transported to the postsynaptic compartment. In **(O)** Evi is transferred as an intact protein through the use of vesicular compartments. 1 (red arrows) and 2 (black arrows) represent potential vesicular pathways. In 1, an Evi-containing vesicle is released from the presynaptic membrane through a multivesicular body (MVB), which either fuses with the postsynaptic membrane or is taken up as an intact vesicle in an MVB. In 2, a presynaptic Evi vesicle is released from the presynaptic membrane and either fuses with the postsynaptic membrane or is taken up as an intact vesicle in an MVB. Bars in the histograms

represent mean±SEM. ***= p<0.0001; **= p<0.001. Calibration bar is 2 μm for panels J1-J3 and 6 μm for the rest of the panels.

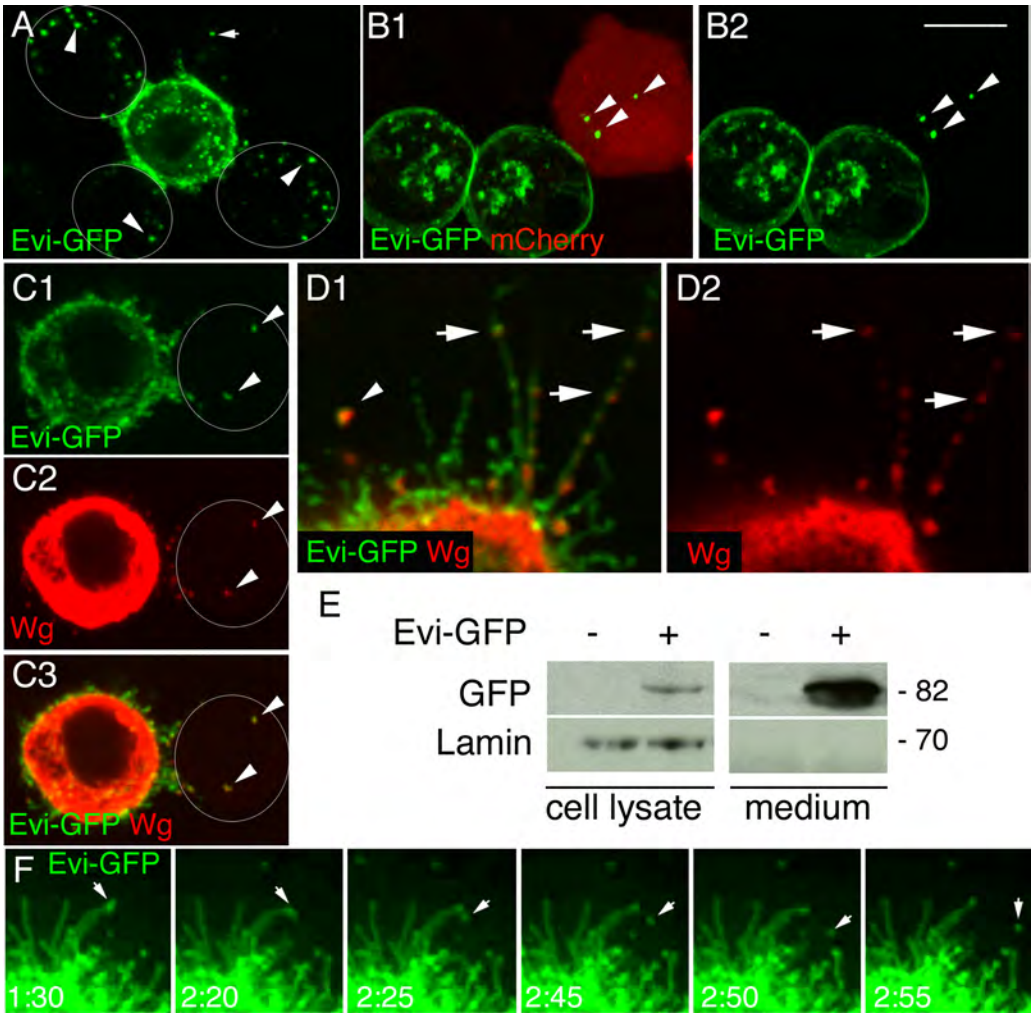

Figure 2.4. Evi Is Transferred from Cell to Cell and to the Medium

(**A, B**) Single confocal slice through a mixture of S2 cells (**A**) either untransfected (outlined by white circles) or transfected with Evi-GFP (green) and (**B**) either transfected with mCherry (red) or Evi-GFP (green). Note that in either case, Evi-GFP puncta are observed in the Evi-negative cells (arrowheads) and in the media (arrow). **(C)** Evi-GFP and Wg are transferred together into an untransfected cell (arrowheads) **(D)** Wg localizes with Evi into punctuate structures within filopodia (arrows), as well as in the medium (arrowhead) (**E**) Western blot of lysates and media from Evi-GFP transfected (+) S2 cells. Note

the presence of GFP signal in the growth medium from transfected cells, indicating the secretion of Evi to the medium. (**F**) time-lapse imaging of an S2 cell transfected with Evi-GFP and showing the shedding of an Evi-GFP vesicle to the medium (arrows). Calibration bar is 3μm for panel 4D and 8 μm for the rest of the panels. Time points in 4F are (in minutes).

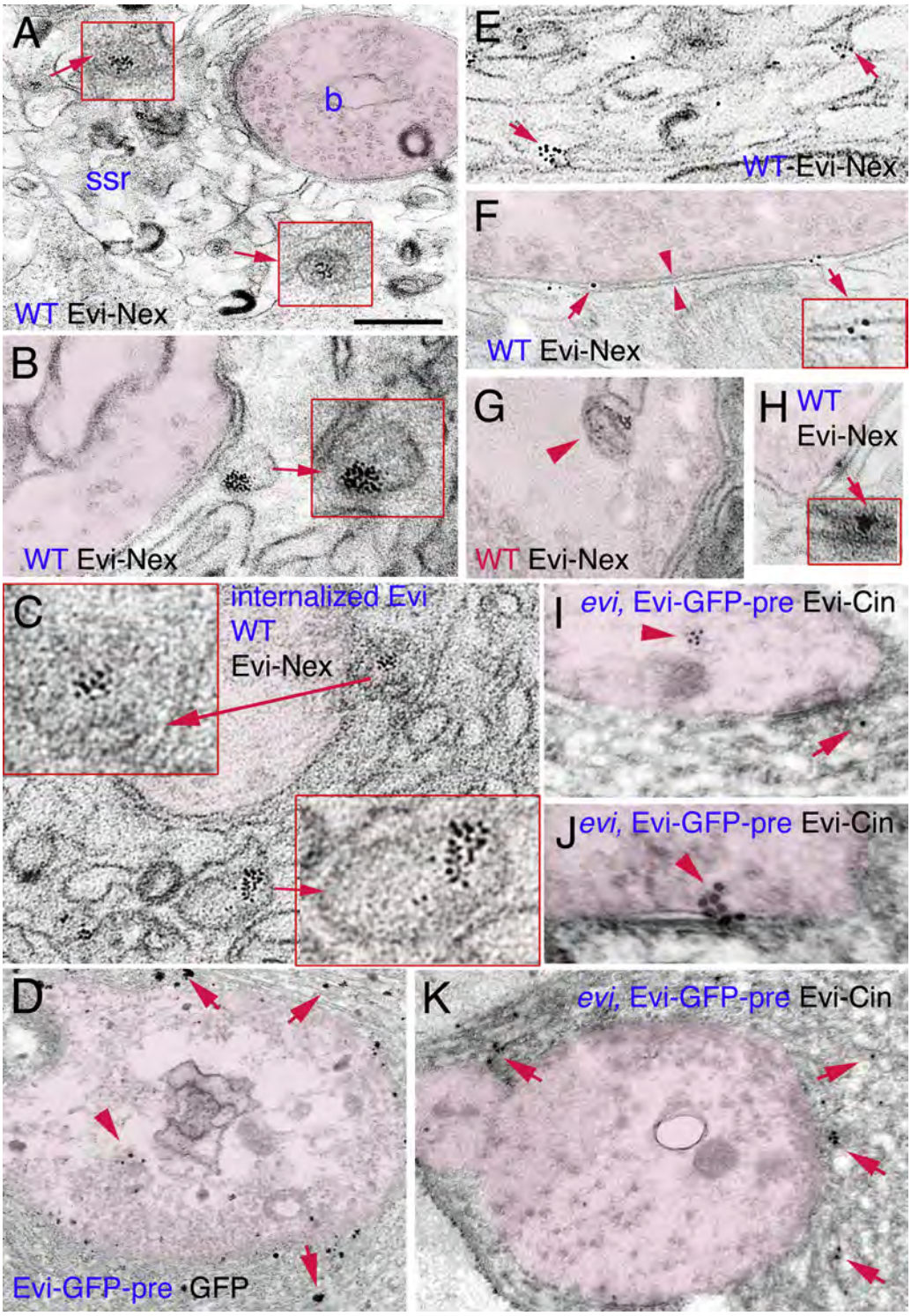

Figure 2.5. Evi Is Localized to Pre- and Postsynaptic Vesicular Structures as well as Pre- and Post-Perisynaptic Membranes

(**A-K**) Electron micrographs of synaptic bouton regions in preparations labeled with antibodies to Evi-Nex or GFP, followed by 1.4 nm gold-conjugated secondary and silver intensification, or antibodies to Evi-Cin labeled with 18 nm gold-conjugated secondary. In these micrographs the presynaptic compartment has been overlayed in pink. Insets are high magnification views of the structures indicated by the arrows. In (**A**, **B**, **D-H**) samples were fixed and permeabilized followed by primary and secondary antibody incubation. In (**C**) samples were processed for an internalization assay (see text for details). **(I-K)** Samples were stained post-embedding with anti-Evi-Cin. (**A, B**) Immunoreactive vesicles found at the SSR region. (**C**) Internalized Evi is found in postsynaptic SSR vesicles. (**D, K**) Localization of label at SSR membranes. (**E-H**) Evi label at the perisynaptic region of pre- and postsynaptic membranes. Arrowheads in **(F)** mark the active zone. (**I**) Evi localization at a presynaptic multimembrane body. **(J)** Evi-immunoreactive gold particles at the presynaptic region and the synaptic cleft. Calibration bar is 0.6μm in A, C, D, K; 0.3μm in B, E-H; 0.2μm in the insets of A; 0.15μm in the inset of B, and 0.1 μm in the inset of C.

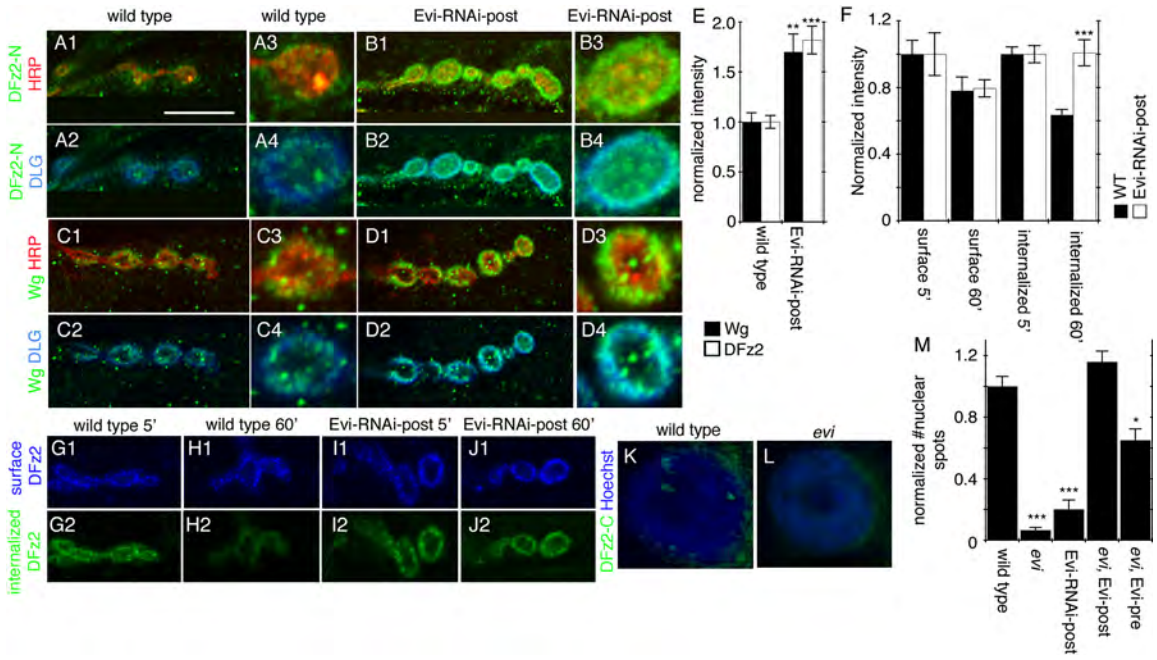

Figure 2.6. Evi Downregulation in Muscle Results in Postsynaptic Wg and DFz2 Accumulation and Alterations in the Frizzled Nuclear Import Wg Pathway

(**A-D**) Single confocal slices through NMJs at muscles 6 or 7 triple stained with antibodies to HRP (red), DLG (blue) and (**A, B**) DFz2 (green) or (**C, D**) Wg (green) in **(A, C)** wild type and **(B, D**) Evi-RNAi-Post. Note that both Wg and DFz2 accumulate at the postsynaptic region of NMJs expressing Evi-RNAi-postsynaptically. (**E**) Quantification of Wg (black bars) and DFz2 (white bars) immunoreactivity levels at the postsynaptic region of the indicated genotypes. Number of samples is 10 for wild type, and 10 for Evi-RNAi-post. (**F**) Intensity of surface and internalized DFz2 at 5 and 60 min after the antibody-binding step in wild type (black bars) and Evi-RNAi-post (white bars). Number of samples is 13 and 10 for wild type at 5 and 60 min; 11 and 10 for *evi* mutants at 5 and 60 min. (**G-J**) Single confocal slices of branches form NMJs subjected to the

internalization assay, showing (**G1-J1**) surface DFz2 (blue) and (**G2-J2**) internalized DFz2 (green) (**G, I**) at 5 min and (**H, J**) 60 min after the antibody binding step, in (**G, H**) wild type, and (**I, J**) Evi-RNAi-post. Note that in Evi-RNAi-post internalized DFz2 remains at high levels at the NMJ at 60 min. (**K, L**) Confocal slices of muscle nuclei in preparations stained with anti-DFz2-C (green) and Hoechst (blue) in (**K**) wild type and (**L**) *evi* mutants showing the drastic decrease in intranuclear DFz2-C in the mutants. (**M**) Normalized number of DFz2-C nuclear spots in the indicated genotypes. Number of nuclei quantified is 159 for wild type, 154 for *evi* mutants, 115 for Evi-RNAi-post, 163 for *evi*, Evi-GFP-post, and 92 for *evi*, Evi-GFP-pre. Bars in the histograms represent mean±SEM. **= $p<0.001$; *=$p<0.05$ Calibration bar is 10 μm for panels A-H1-2, I-L; 5 μm for panels A-D3-4.

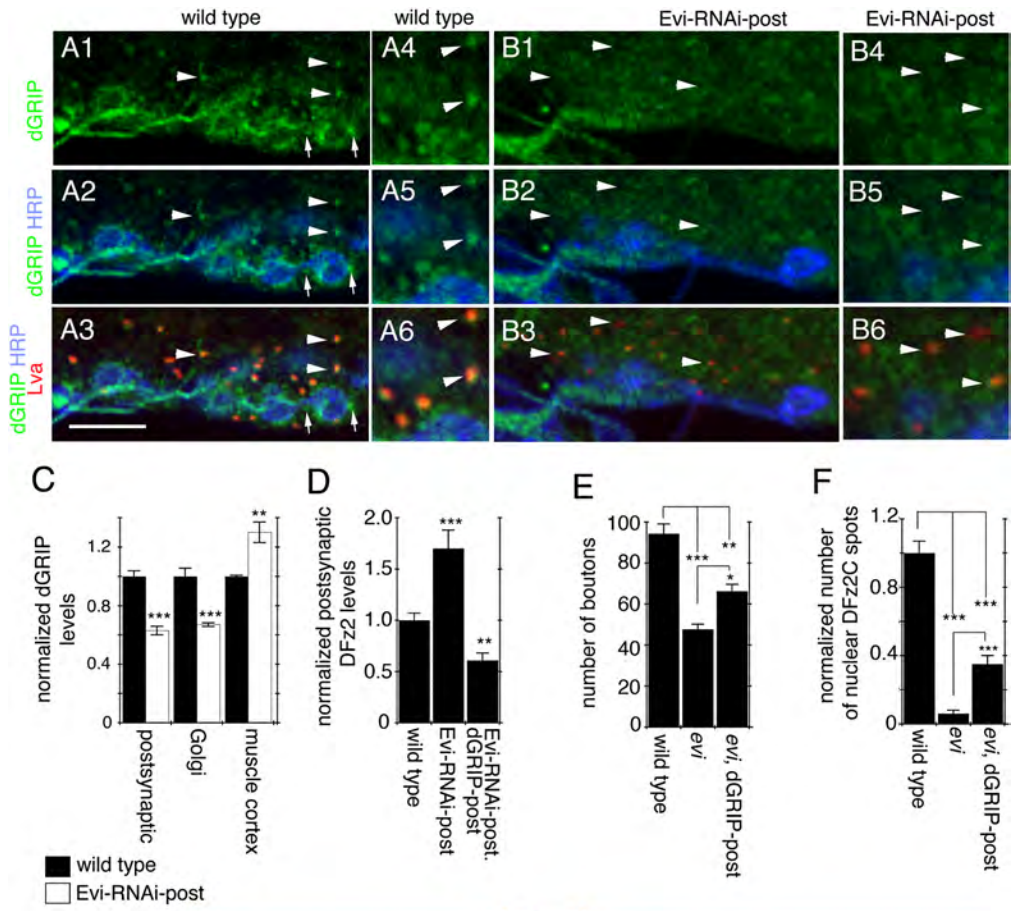
wild type
wild type
Evi-RNAi-post
Evi-RNAi-post
A1
A4
B1
B4
dGRIP
A2
A5
B2
B5
dGRIP HRP
A3
A6
B3
B6
dGRIP HRP Lva
C
normalized dGRIP levels
postsynaptic
Golgi
muscle cortex
wild type
Evi-RNAi-post
D
normalized postsynaptic DF2 levels
wild type
Evi-RNAi-post
Evi-RNAi-post. dGRIP-post
E
number of boutons
wild type
evi
evi, dGRIP-post
F
normalized number of nuclear DF2C spots
wild type
evi
evi, dGRIP-post

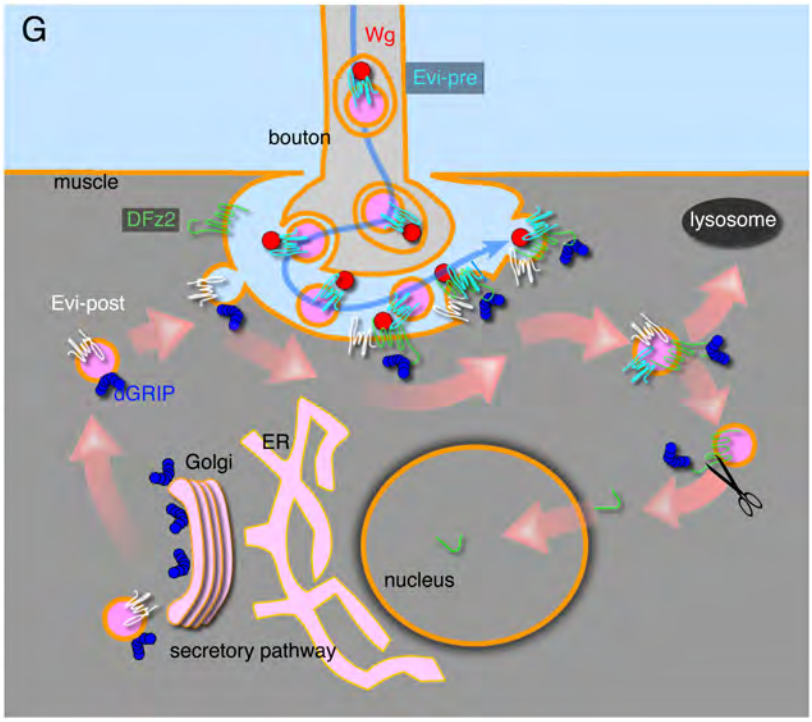
G
Wg
Evi-pre
bouton
muscle
DFz2
lysosome
Evi-post
dGRIP
ER
Golgi
nucleus
secretory pathway

Figure 2.7. Downregulating Evi in Postsynaptic Muscles Alters the Localization of dGRIP and Proposed Function of Evi in the Pre- and Postsynaptic Compartment

(**A, B**) Single confocal slices through NMJs at muscles 6 or 7 in preparations triple labeled with antibodies to HRP (blue), dGRIP (green) and Lavalamp (Lva; red) in (**A**) wild type, and (**B**) Evi-RNAi-post. Arrows in A point to synaptic dGRIP. Arrowheads in A and B point to dGRIP positive and dGRIP negative Golgi bodies (marked with lava lamp) respectively. Note the decrease in synaptic and Golgi immunoreactivity and the diffuse appearance of dGRIP in the muscle cortex. (**C**) Quantification of dGRIP levels at the postsynaptic junctional region, Golgi bodies, and muscle cortex, in wild type (black bars) and Evi-RNAi-post (white bars), showing that dGRIP is significantly reduced from postsynaptic sites and Golgi, but increased at the muscle cortex in Evi-RNAi-post. Number of samples is 10 for wild type and 10 for Evi-RNAi-post. **(D)** Quantification of postsynaptic DFz2 levels in wild type, Evi-RNAi-post and Evi-RNAi-post, dGRIP-post. Number of samples is 10 for wild type, 10 for Evi-RNAi-Post and 16 for Evi-RNAi-post, dGRIP-Post **(E)** Quantification of bouton number in wild type, *evi* mutants, and *evi* mutants expressing dGRIP-post. Number of samples is 26 for wild type,12 for *evi* mutants, and 8 for *evi* mutants expressing dGRIP-post. **(F)** Quantification of DFz2C spots in wild type, *evi* mutants, and *evi* mutants expressing dGRIP-post. Number of samples is 205 for wild type, 154 for *evi* mutants, and 136 for *evi* mutants expressing dGRIP-post. (**G**) Proposed model for Evi function in the pre- and postsynaptic compartment (see text for details). Bars in the histograms

represent mean±SEM. ***= p<0.0001; **= p<0.001; *=p<0.05. Calibration bar is 6 μm for A-B1-3, and 3 μm for A-B4-6.

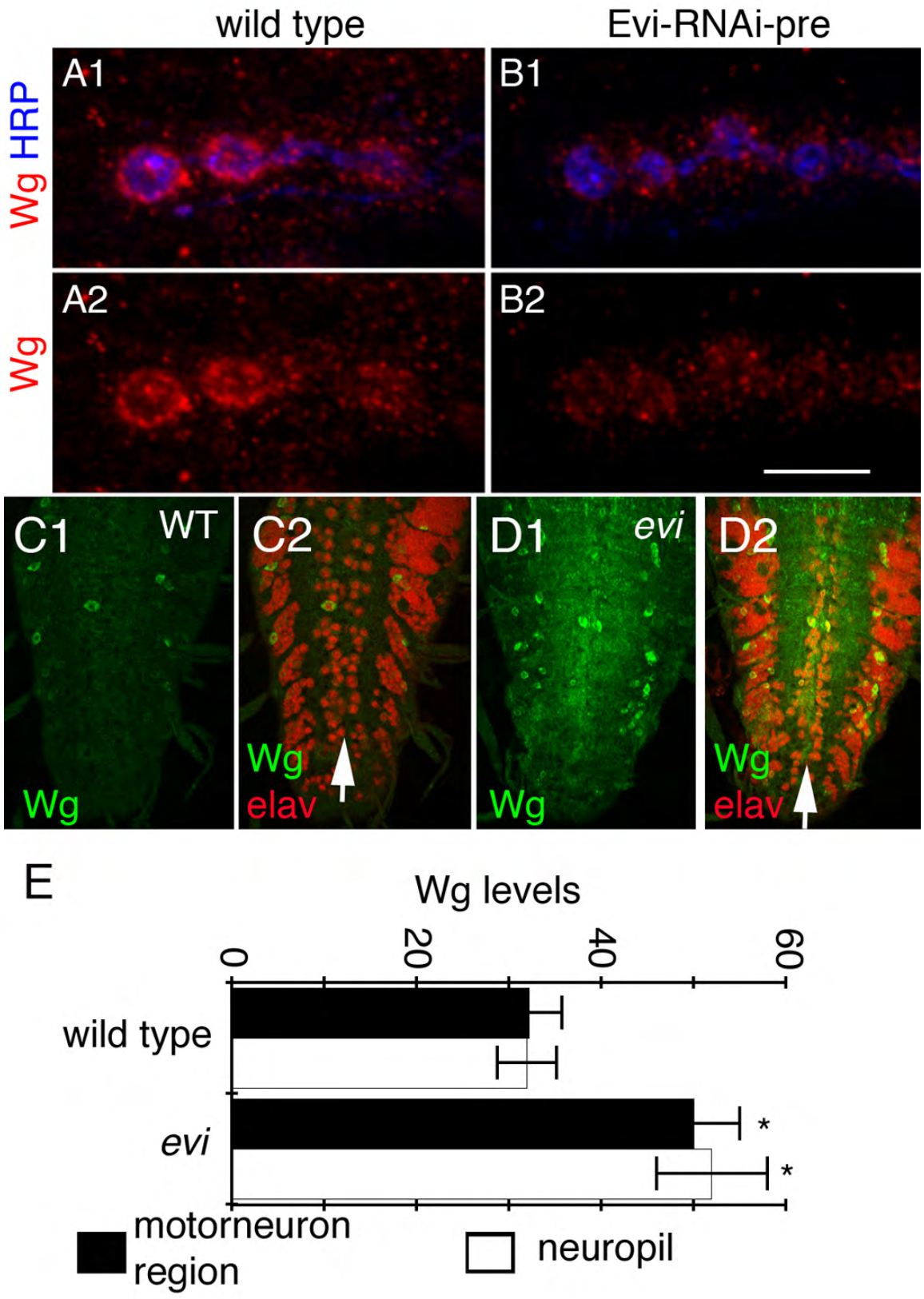

Supplementary Figure 1
Korkut et al.

Suppl. Figure 2.1. Reduction of postsynaptic Wg by expressing Evi-RNAi in neurons and accumulation of Wg in the ventral ganglion of evi mutants. (A, B) Single confocal slices through muscles 6 or 7 in preparations double labeled with antibodies against HRP (blue) and Wg (red) in **(A)** wild type, and **(B)** in larvae expressing Evi-RNAi in neurons. **(C, D)** Single confocal slices through the ventral ganglion of **(C)** wild type and **(D)** an *evi* mutant stained with Wg (green) and Elav (red). **(E)** Quantification of Wg levels either in the neuropil or the motor neuron region of the indicated genotypes. Number of samples is 8 for wild type and 10 for the *evi* mutant. Calibration bar is 7µm for panels 1A, B and 90µm for 1C, D.

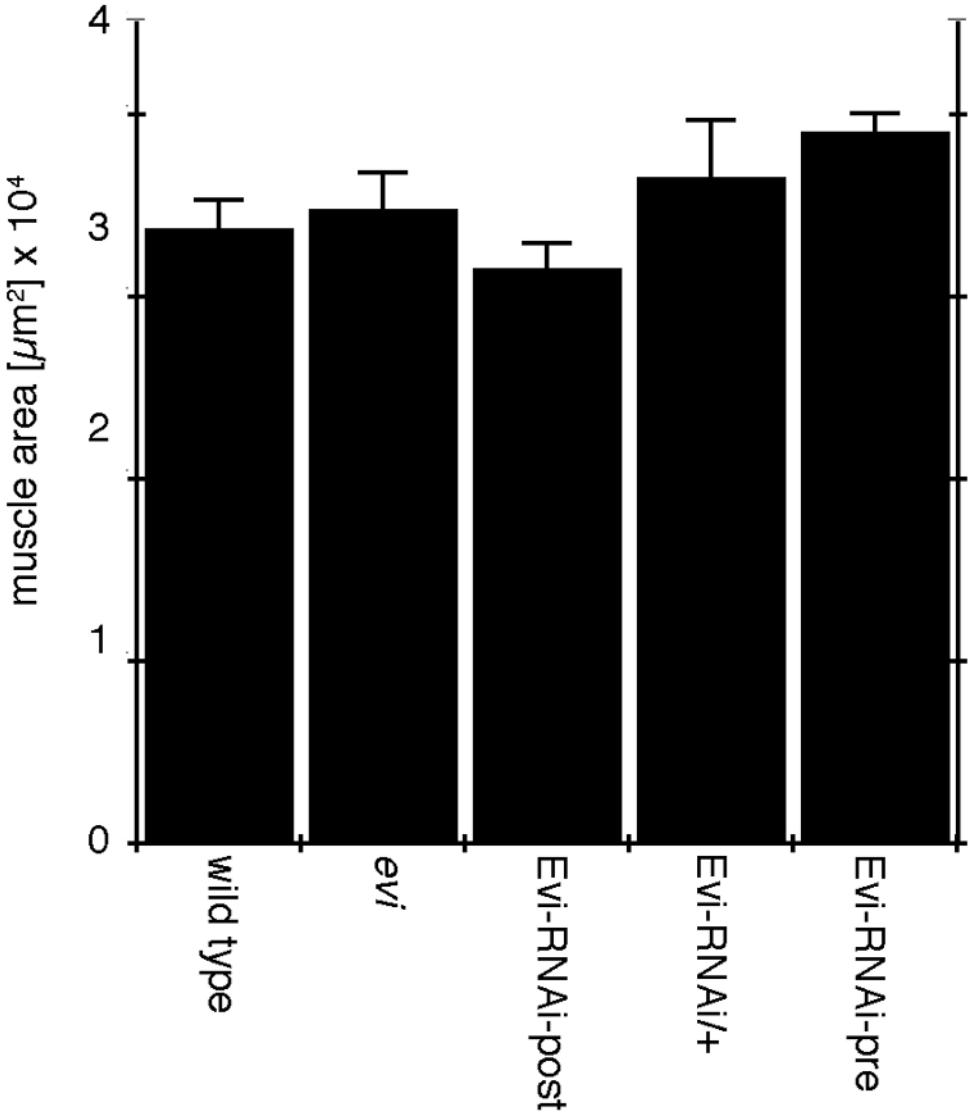

Suppl. Figure 2.2. Muscle surface area in different genotypes used in this study.

Number of samples is 20 for wild type, 13 for *evi* mutants, 6 for Evi-RNAi-post, 11 for Evi-RNAi-pre, 6 for Evi-RNAi/+.

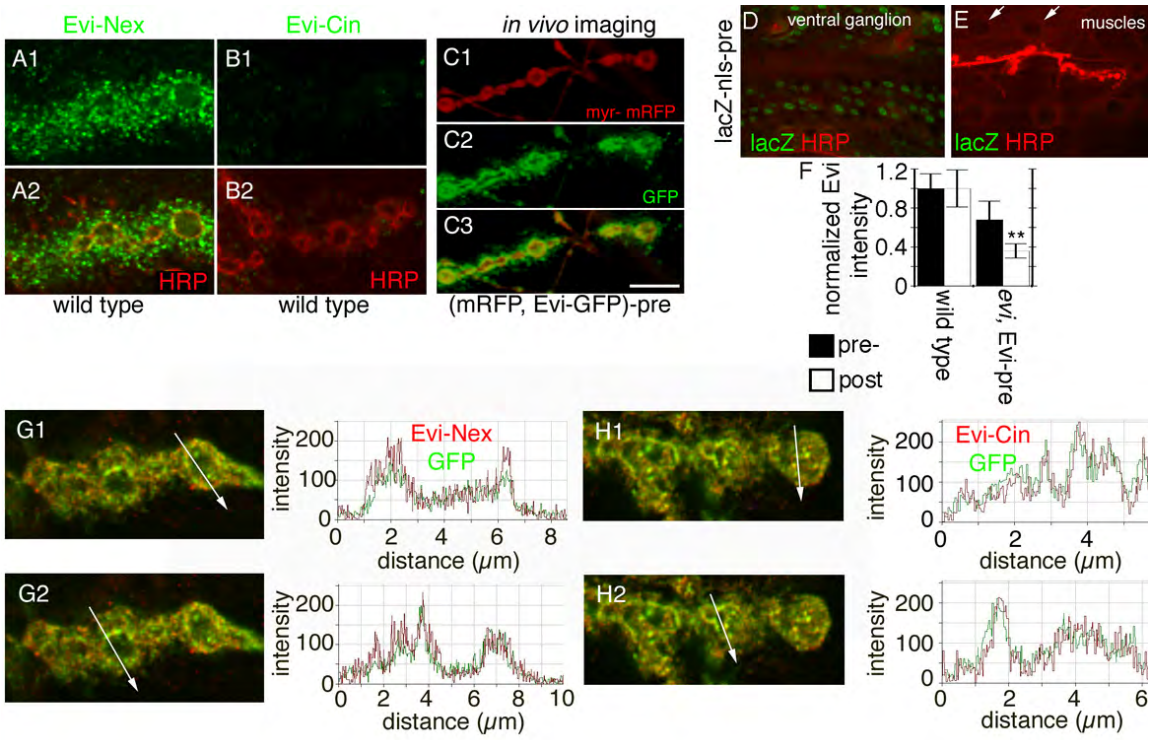

Suppl. Figure 2.3. Localization of the Evi antibody epitopes to extra- and intracellular sites, and in vivo shedding of Evi-containing vesicles. (A,B) Single confocal slices of unpermeabilized NMJs at muscles 6 or 7 double stained with antibodies against HRP (red) and **(A)** Evi-Nex (green) or **(B)** Evi-Cin (green). Note that only the Evi-Nex antibody stains the NMJ in unpermeabilized samples, consistent with the idea that the Evi-Nex epitope is localized extracellularly and the Evi-Cin epitope likely intracellularly. **(C)** Single confocal slice of an NMJ imaged live, in a larva expressing myr-mRFP (red) in motorneurons to label the presynaptic compartment and Evi-GFP (green) in motorneurons to show that presynaptic Evi-GFP vesicles are shed to the postsynaptic compartment. **(D,E)** Confocal image of a larva expressing LacZ-NLS with the Gal4 driver C380 showing **(D)** the ventral ganglion —note the clear nuclear localization, and **(E)** the NMJ —note the lack of signal in muscle nuclei (arrows). **(F)** Volumetric

quantification of Evi signal in either wild type or presynaptic rescue of *evi* mutants. **(G-H)** Confocal slices and colocalization measurements between presynaptically expressed Evi-GFP and **(G)** anti-Evi-Nex or **(H)** anti-Evi-Cin. Calibration bar is 5 µm for A-B and G-H, 7µm for C and 160µm for D and 13µm for E.

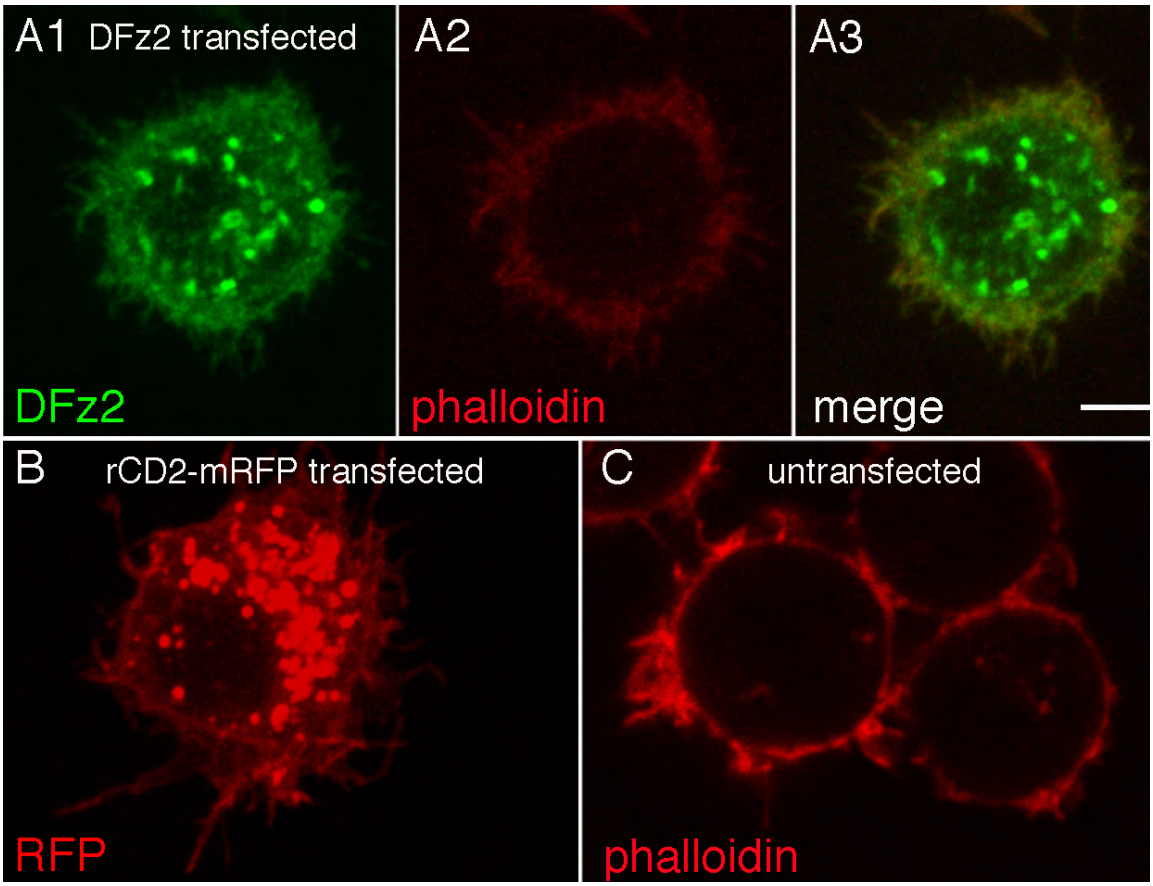

Suppl. Figure 2.4. S2 cells do not transfer DFz2 or rCD2-mRFP to the medium. (A-C) Confocal images of S2 cells transfected with **(A)** DFz2, **(B)** rCD2-mRFP, and **(C)** untransfected. Note that the transfected cells are not transferring transmembrane proteins, as previously observed with Evi-GFP. Also, the formation of filopodia is independent of transfection as they are observed in untransfected cells as well. Calibration bar is 5µm.

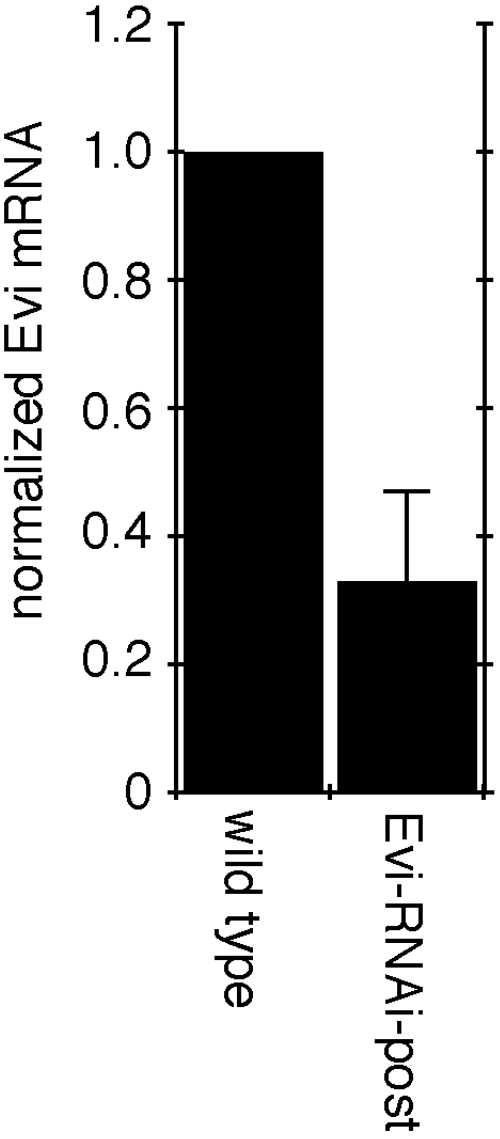

Suppl Fig 2.5. Realtime PCR analysis of Evi mRNA levels in body wall muscles.

Normalized Evi mRNA levels in wild type and Evi-RNAi-post.

CHAPTER 3

REGULATION OF POSTSYNAPTIC RETROGRADE SIGNALING BY PRESYNAPTIC EXOSOME RELEASE

The following work is under peer review for publication in *Neuron* (Korkut, C. Li, Y., Brewer, C., Koles, K., Ashley, J., Yoshihara, M., and Budnik, V. (2012). Regulation of postsynaptic retrograde signaling by presynaptic exosome release).

ABSTRACT

Retrograde signals from postsynaptic targets are critical during development and plasticity of synaptic connections. These signals serve to adjust the activity of presynaptic cells according to postsynaptic cell outputs and to maintain synaptic function within a dynamic range. Despite their importance, the mechanisms that trigger the release of retrograde signals and the role of presynaptic cells in this signaling event are unknown. Here we show that a retrograde signal mediated by Synaptotagmin 4 (Syt4) is transmitted to the postsynaptic cell through anterograde delivery of Syt4 via exosomes. Thus, by transferring an essential component of retrograde signaling through exosomes, presynaptic cells enable retrograde signaling.

INTRODUCTION

The *Drosophila* neuromuscular junction (NMJ) has proven to be a powerful model system to investigate mechanisms underlying retrograde signaling (Keshishian and Kim, 2004). Spaced stimulation of *Drosophila* embryonic and larval NMJs results in potentiation of spontaneous (quantal) release (Ataman et al., 2008; Yoshihara et al., 2005), through a retrograde signaling mechanism requiring postsynaptic function of the vesicle protein, Synaptotagmin-4 (Syt4) (Barber et al., 2009; Yoshihara et al., 2005).

Synaptotagmins are a family of membrane trafficking proteins composed of an N-terminal transmembrane domain, a linker sequence, and two C-terminal C2 domains (Littleton et al., 1999; Vician et al., 1995). The most abundant

isoform in the nervous system, Synaptotagmin 1, is associated with synaptic vesicles and has been proposed to function as a Ca^{++} sensor for neurotransmitter release (Brose et al., 1992). Among the multiple Synaptotagmin family members, Syt4 occupies an interesting, yet poorly understood position. Its expression is regulated by electrical activity (Babity et al., 1997; Vician et al., 1995), it is present in vesicles containing regulators of synaptic plasticity and growth, such as BDNF (Dean et al., 2009), it regulates learning and memory (Ferguson et al., 2001), and in humans the *syt4* gene is localized to a chromosome 18 locus linked to schizophrenia and bipolar disorder (Ferguson et al., 2001).

At the fly NMJ, spaced stimulation not only results in potentiation of spontaneous neurotransmitter release (Ataman et al., 2008; Yoshihara et al., 2005), but also in structural changes at presynaptic arbors, the rapid formation of ghost boutons, nascent boutons which have still not developed postsynaptic specializations or recruited postsynaptic proteins (Ataman et al., 2008). However, whether this activity-dependent bouton formation also requires Syt4-dependent retrograde signaling was unknown.

Here we demonstrate that retrograde Syt4 function in postsynaptic muscle is required for activity-dependent synaptic growth and that this function depends on exosomal release of Syt4 by presynaptic terminals. Although Syt4 protein is present both in presynaptic terminals and postsynaptic muscles, trapping or downregulating endogenous Syt4 in presynaptic motorneurons eliminates its localization in postsynaptic muscle cells, suggesting that postsynaptic Syt4 is

derived from presynaptic cells. Consistent with this, *syt4* transcript is detected in motorneurons but not in muscle cells. We provide compelling evidence that Syt4 is present within presynaptic exosome vesicles, which are transferred to postsynaptic cells. This exosomal transfer of Syt4 is required both for activity-dependent synaptic growth and potentiation of miniature neurotransmitter release. Thus, our data suggest a presynaptic control of postsynaptic retrograde signaling through the exosomal transfer of an essential retrograde signaling component. To our knowledge, this is the first demonstration of exosomal transfer of a transmembrane regulator of vesicle release and the involvement of exosomes in retrograde signaling.

RESULTS and DISCUSSION

Postsynaptic depolarization is required for rapid activity-dependent synaptic growth

To determine if similar to the potentiation of miniature release (Barber et al., 2009; Yoshihara et al., 2005) the rapid formation of ghost boutons in response to spaced stimulation required retrograde signaling, we used an optogenetic approach to inhibit responses in the postsynaptic muscle cell. Specifically, while preparations bathed in normal Ca^{++} saline (1.5 mM) were being stimulated, they were simultaneously hyperpolarized by expressing the light-gated Cl^- channel, Halorhodopsin (NpHR) (Zhang et al., 2007a), specifically in muscles using the C57-Gal4 driver (Budnik et al., 1996). Illuminating resting preparations by expressing NpHR in muscle resulted in rapid and robust

hyperpolarization of the muscle membrane potential (Fig. 3.1A). This hyperpolarization was sufficient to induce a ~50% decrease in the amplitude of evoked excitatory junctional potentials (EJPs; Fig. 3.1B, C) and over a 10-fold increase in evoked EJP failures (Fig. 3.1D). Spaced stimulation of wild type NMJs (lacking NpHR) in the presence or absence of light elicited a 3-4-fold increase in the number of ghost boutons (Fig. 3.1E), which were labeled by the presynaptic membrane marker, anti-HRP (Jan and Jan, 1982), but lacked postsynaptic Discs-Large (DLG) immunoreactivity (Fig. 3.1F, G). Similarly, spaced stimulation of NMJs expressing NpHR in muscles in the absence of light, resulted in a significant increase in the number of ghost boutons (Fig. 3.1E). In contrast, activation of light-induced NpHR gating in larval muscles, completely blocked this effect (Fig. 3.1E). Thus, postsynaptic depolarization is required for the formation of presynaptic ghost boutons in response to spaced stimulation, establishing that ghost bouton formation requires a retrograde signal.

Syt4 is required either pre- or postsynaptically for activity-induced ghost bouton formation and mEJP potentiation

To determine if Syt4 was required for the retrograde signal involved in activity-dependent ghost bouton formation, we conducted the above experiments in *syt4* null mutants over a deficiency of the *syt4* locus. Consistent with a requirement for Syt4 in mediating the formation of activity-dependent ghost boutons, *syt4* mutants prevented the formation of such boutons upon spaced stimulation (Fig. 3.1E). If Syt4 was part of a retrograde signaling mechanism that

regulates nascent bouton formation, then expressing Syt4 in postsynaptic muscles in a *syt4* mutant background should rescue the block in ghost bouton formation upon spaced stimulation. This prediction was tested by expressing a wild type Syt4 transgene in either muscles or neurons using the cell-specific Gal4 drivers, Mhc (Myosin heavy chain)-Gal4 (for muscles) and elav-Gal4 (for neurons). Surprisingly, expressing Syt4 in either muscles or neurons completely rescued the ability of NMJs to respond to spaced stimulation by forming ghost boutons (Fig. 3.1E).

Previous studies at the larval NMJ suggested that the potentiation of miniature EJP (mEJP) frequency upon spaced stimulation was due to a Syt4-mediated retrograde signal, based on the observation that postsynaptic expression of Syt4 in a *syt4* null mutant background, could rescue the lack of mEJP frequency potentiation upon stimulation (Barber et al., 2009). However, the ability of presynaptically expressed Syt4 to rescue this *syt4* mutant phenotype was not tested in those studies. Given that *syt4* mutants were unable to form ghost boutons upon spaced stimulation and this phenotype could be rescued either by pre- or postsynaptic Syt4 expression, we determined if mEJP frequency potentiation could be rescued by expressing Syt4 in neurons of *syt4* mutants. Recording from body wall muscles after spaced stimulation (Ataman et al., 2008) demonstrated over a 2-fold increase in mEJP frequency in wild-type larvae (Fig. 3.1H). This response was significantly reduced but not eliminated in *syt4* mutants (Fig. 3.1H). Nevertheless, expressing Syt4 in the neurons of *syt4* mutants completely rescued this phenotype (Fig. 3.1H). Thus, Syt4 is required

either pre- or postsynaptically for activity-dependent ghost bouton formation and mEJP frequency potentiation at the larval NMJ, raising questions about the retrograde role of Syt4 in controlling the above presynaptic phenotypes.

Syt4 is transferred *trans*-synaptically from presynaptic boutons to postsynaptic muscle compartments

To further ascertain the site of Syt4 function, we first determined its localization at the NMJ. As previously reported (Adolfsen et al., 2004), antibodies to Syt4 revealed a localization both in pre- and postsynaptic compartments of the NMJ, as determined by double labeling with anti-HRP antibodies a neuronal membrane marker that is used to determine the boundary between pre-synaptic boutons and postsynaptic muscles (Fig. 3.2A). The Syt4 immunoreactive signal was specific, as it was virtually eliminated in *syt4* null mutants (Fig. 3.2B). Notably, expressing a Syt4 transgene exclusively in the neurons of *syt4* null mutants, rescued both the presynaptic and postsynaptic localization of Syt4 (Fig. 3.2C). As the neuronal Gal4 driver does not express any Gal4 in muscles, this observation raises the possibility that presynaptic Syt4 might be transferred to the postsynaptic region, and that postsynaptic Syt4 might at least be partly derived from presynaptic boutons. Consistent with this observation, expressing a C-terminally Myc-tagged Syt4 (Syt4-C-Myc) transgene in motor neurons of wild type animals using the OK6-Gal4 driver (Aberle et al., 2002) mimicked the endogenous localization of Syt4 in both presynaptic boutons and the postsynaptic muscle region (Fig. 3.2D). The same postsynaptic localization of

Syt4-C-Myc was observed when expressing the transgene using either the neuronal Gal4 drivers elav-Gal4 (Lin et al., 1994) or C380-Gal4 (Budnik et al., 1996) (Suppl Fig. 3.1). Like the wild type, untagged transgene, Syt4-C-Myc completely rescued the mutant *syt4* mutant phenotype upon spaced stimulation (Fig. 3.2G), suggesting that the tagged transgene is functional. These observations suggest that endogenous Syt4 might be transferred from synaptic boutons to muscles.

The hypothesis that at least a fraction of postsynaptic Syt4 protein is derived from presynaptic boutons was tested by downregulating endogenous presynaptic Syt4 by expressing Syt4-RNAi in neurons. In agreement with the above model, downregulating presynaptic Syt4 resulted in near elimination of the Syt4 signal, not only in presynaptic boutons, but also from the postsynaptic muscle region (Fig. 3.2E, H). Thus, the transfer of Syt4-C-Myc from neurons to muscles is not just the result of overexpressing the transgene in neurons, but likely an endogenous process. Further, although Syt4-RNAi was highly efficient in decreasing the Syt4 signal from motorneurons and muscles when expressed in motorneurons, expressing Syt4-RNAi in muscles, using the strong C57-Gal4 driver, did not decrease Syt4 levels either in the pre- or postsynaptic compartment (Fig. 3.2F, H). These results support the idea that at least an important fraction, if not all postsynaptic Syt4 is derived from presynaptic neurons.

Given that downregulating Syt4 in neurons but not in muscles decreased postsynaptic Syt4 signal (Fig. 3.2H), we determined which of the above cell types

contained *syt4* transcripts. Reverse transcription (RT)-PCR using equal amounts of total RNA derived from either the nervous system or body wall muscles, revealed the presence of a strong *syt4* band in the nervous system (Fig. 3.2I). However, virtually no *syt4* transcript was in the muscles of wild type controls or larvae expressing Syt4-RNAi in muscles (Fig. 3.2I). This is again consistent with the possibility that muscle Syt4 might be exclusively derived from the transfer of neuronal Syt4 by synaptic boutons.

Syt4 and Evi exist in a complex and are transferred together from pre- to postsynaptic cells

Syt4 is a transmembrane protein (Adolfsen et al., 2004; Sudhof and Rizo, 1996), and thus its transfer from pre- to postsynaptic cells is not possible through classical vesicle exocytosis. However, we have previously observed the intercellular transfer of a transmembrane protein through exosome-like vesicles at the NMJ (Koles et al., 2012; Korkut et al., 2009), a process also observed in the immune system (Raposo et al., 1996a; Thery et al., 2009). In particular, the release and extracellular trafficking of hydrophobic WNT-1 molecules at the NMJ appears to be mediated by WNT binding to a multipass transmembrane protein, Evi/Wls, which is released to the extracellular space in the form of exosome-like vesicles (Koles et al., 2012; Korkut et al., 2009). Exosomes are vesicles generated by the inward budding of endosomal limiting membrane into multivesicular bodies (MVBs). MVBs can either fuse with lysosomes to dispose of

obsolete cellular material or with the plasma membrane to release vesicle-associated signaling components (Simons and Raposo, 2009).

The similar transfer of transmembrane Evi and Syt4 across cells raised the possibility that both molecules could shuttle together in the same exosome-like vesicle. To address this possibility, we first determined if Evi and Syt4 colocalized at the NMJ. Neuronally expressed Evi-GFP exactly colocalizes with endogenous Evi at the NMJ (Fig. 3.3A). Given that antibodies to Syt4 and Evi were raised in the same species, we therefore expressed Evi-GFP in motorneurons and examined the colocalization of the GFP label with endogenous Syt4. Although colocalization of GFP and Syt4 signal was not complete, many of the postsynaptic GFP positive puncta also contained endogenous Syt4 signal (Fig. 3.3B; arrows), suggesting that some of the Evi vesicles contain Syt4. Further, when both transgenic Syt4-C-Myc and Evi-GFP were overexpressed in neurons, both proteins became trapped inside synaptic boutons, where they colocalized with the endosomal marker, hepatocyte growth factor (HGF)1-regulated tyrosine kinase substrate (Hrs) (Komada et al., 1997) (Fig. 3.3C, D). Most importantly, labeling the NMJs of animals overexpressing both Syt4 and Evi, using Syt4 antibodies, which should label both endogenous and transgenically expressed Syt4, revealed that the entire Syt4 protein pool accumulated in Hrs positive endosomes, and that no detectable Syt4 signal was observed at the postsynaptic region (Fig. 3.3E). Taken together, the fact that *syt4* transcript is virtually absent in muscles, the ability of Syt4-RNAi expressed in neurons to eliminate Syt4 protein in muscles, and the observation that trapping

Syt4 within presynaptic endosomes completely eliminates postsynaptic Syt4 immunoreactivity, provide compelling evidence that Syt4 protein is synthesized in neurons and not in muscles of larvae. It also suggests a mechanism similar to the trans-synaptic trafficking of Evi, through the release of exosomes (Koles et al., 2012; Korkut et al., 2009).

The colocalization of Evi and Syt4 in a subset of postsynaptic puncta, as well as their similar transfer across cells, suggested that the proteins might exist within a protein complex. To test this, we first coexpressed Sy4-C-Myc and Evi-GFP in the neurons of larvae to immunoprecipitate Syt4-Myc from body wall muscle and CNS extracts using anti-Myc antibodies. We found that Myc antibodies specifically immunoprecipitated Evi-GFP *in vivo* (Fig. 3.3F). We were also able to co-immunoprecipitate Evi-GFP and endogenous Syt4 from body wall muscle and CNS extracts of larvae expressing Evi-GFP in neurons, by using a chicken anti-Syt4 antibody (Fig. 3.3G). Because the IgY heavy chain of the chicken antibody runs at approximately the same molecular mass as Syt4, masking the Syt4 band (Fig. 3.3G, asterisk), we also immunoprecipitated Syt4-C-Myc in larvae expressing Syt-C-Myc in neurons using the chicken Syt4 antibody, which allowed us to probe the blot with a mouse secondary antibody against anti-Myc, demonstrating that the Syt4 antibody immunoprecipitated tagged Syt4 (Fig. 3.3I). Finally, we were also able to immunoprecipitate untagged Syt4 and Evi-GFP when expressed in S2 cells (Fig. 3.3H). Thus, Syt4 and Evi colocalize, are present in the same complex, and both proteins are transferred from presynaptic boutons to postsynaptic muscles, likely in the same exosome.

The *trans*-cellular transfer of Syt4 is through exosomes

Specific transfer of Evi-exosomes from cell to cell has been demonstrated in non-neuronal S2 cells (Koles et al., 2012; Korkut et al., 2009). To determine if similar transfer of Syt4 could be observed across S2 cells, S2 cells were separately transfected with either Sy4-C-V5 or mCherry. Then, Syt4-C-V5 and mCherry S2 cells were co-incubated in the same culture dish. We observed that Syt4-C-V5 puncta, likely exosomes, were transferred to mCherry S2 cells (Fig. 3.4A, B), consistent with our observations at the NMJ. Similarly, when S2 cells were co-transfected with Evi-GFP and untagged Syt4, exosomes were observed to be transferred to untransfected cells (Fig. 3.4C). The transferred exosomes contained Evi-GFP, and a subset of these also contained Syt4 (Fig. 3.4C).

To corroborate that exosomes contained Syt4, we generated a stable S2 cell line expressing Syt4-C-HA. Then, exosomes from this cell line were purified by differential centrifugation and immunolabeled with antibodies to HA, followed by nanogold conjugated secondary antibody and silver intensification for examination at the electron microscopy (EM) level. We found that a population of exosomes contained Syt4 (Fig. 3.4E; see Suppl Fig. 3.2 for control).

In conclusion, we show that Syt4 protein functions in postsynaptic muscles to mediate activity-dependent presynaptic growth and potentiation of miniaturerelease. However, to mediate this function Syt4 needs to be transferred from presynaptic terminals to postsynaptic muscle sites. We present evidence that, most likely, the entire pool of postsynaptic Syt4 is derived from presynaptic cells. We also show that like the WNT binding protein, Evi, Syt4 is packaged in

exosomes, which provides a mechanism for the unusual transfer of transmembrane proteins across cells. Taken together, our studies support a novel mechanism for the presynaptic control of a retrograde signal, through the presynaptic release of exosomes containing Syt4.

MATERIALS and METHODS

Fly Strains

Flies were reared at 25°C except for RNAi knockdown experiments, where the fly crosses were kept at 29°C. The following fly strains were used: wild type (Canton-S); *syt4*^{BA1} (Adolfsen et al., 2004); *rn*^{16} (deficiency of the Syt4 locus) (Agnel M, 1989); UAS-Syt4-RNAi (transformant ID 33317; Vienna Drosophila RNAi Center); UAS-Evi-EGFP (Bartscherer et al., 2006); UAS-Syt4-C-Myc (see below); UAS-eNpHR3.0-EYFP (see below) and the Gal4 drivers C155 (Lin and Goodman, 1994), C380, C57 (Budnik et al., 1996), OK6 (Aberle et al., 2002).

Immunocytochemistry

Third instar larval body wall muscles were dissected in ice cold Ca^{++} free saline (Jan and Jan, 1976b) and fixed using either 4% Paraformaldehyde or nonalcoholic Bouin's fixative (Budnik et al., 2006). The following primary antibodies were used: anti-Syt4 (1:1000, (Adolfsen et al., 2004)); anti-c-Myc (1:500, Roche); anti-GFP (1:200, Molecular Probes); anti-DLG_{PDZ} (1:20,000, (Koh et al., 1999)); anti-Evi-Cin (1:100, (Korkut et al., 2009)); anti-FL-Hrs (1:1000, (Lloyd TE, 2002)); anti-V5 (1:500, Invitrogen); anti-HRP-DyLight488 (1:400) and anti-HRP-Cy5 (1:200, Jackson ImmunoResearch); anti-HRP-DyLight594 (1:400, Jackson ImmunoResearch); anti-HRP-TxRed (1:200, Sigma). The following fluorescent secondary antibodies from Jackson ImmunoResearch were used: anti-rabbit-DyLight594 (1:400), antirabbit- FITC (1:200); anti-rabbit-

TxRed (1:200); anti-mouse-FITC (1:200); antimouse- TxRed (1:200); anti-guineapig-TxRed (1:200). We also used anti-mouse- Alexa647 (1:200, Molecular Probes).

Image Acquisition, Fluorescence Intensity Quantification and Morphometric Analysis

Confocal images were acquired using a Zeiss LSM5 Pascal confocal microscope with a Zeiss 63X Plan-Apochromat (1.4 numerical aperture) DIC oil immersion objective at 3X digital zoom. Fluorescence signal intensity was quantified by volumetric measurements of confocal stacks using Volocity 5 Software (Improvision) as described in (Korkut et al., 2009). Briefly, control and experimental samples were imaged at identical settings and the presynaptic intensity was measured by normalizing total intensity inside the presynaptic volume to the volume of the presynaptic terminals. Similarly, the postsynaptic intensity was measured by subtracting the presynaptic volume from the total and measuring the intensity in this subtracted region, followed by normalizing it to the presynaptic volume. For ghost bouton quantification, body wall muscle preparations were double stained with anti-HRP and anti-DLG, to identify HRP positive boutons devoid of DLG label. Measurements were taken from muscles 6 and 7, abdominal segment 3.

Statistical analysis

Unpaired two-tailed Student’s t-tests were run for comparisons of experiments

where a single experimental sample was processed in parallel with a wild type control. In cases where multiple experimental groups were compared to a single control, a one-way ANOVA was performed, with Dunnet post-hoc test. Error bars in all graphs represent ±SEM.

Spaced Stimulation

Spaced K^+ stimulation was performed as described previously (Ataman et al., 2008). Briefly, third instar larvae were dissected in ice-cold normal HL3 saline containing 0.1mM Ca^{++}, with the nervous system remaining intact. Osmotically balanced high K^+ (90mM K^+) HL3 containing 1.5mM Ca^{++} was applied to the larval samples as 3X2 min, 4 min and 6 min pulses separated by 15 min incubation in normal HL3 saline. Control larvae were dissected and incubated the same way except with normal HL3 instead of high K^+ HL3. After the last incubation, the larvae were fixed with 4% paraformaldehyde fixative for 15 min followed by immunostaining with selected antibodies. For Halorhodopsin experiments, larvae expressing NpHR in muscle and control larvae were fed with 100µM all trans-retinal (Sigma) and treated as described above with the exception of illuminating at 540-580 nm (Zeiss HBO 100 mercury lamp focused through a 10X Plan-Neofluor objective, and a Zeiss 3 BP565/30 Filter) on the larvae during the high K^+ HL3 stimulations. As a control experiment, NpHR expressing larvae underwent spaced K^+ stimulation in complete darkness.

Electrophysiology

Spaced stimulation and sham stimulation was performed as above, and then samples were prepared for electrophysiology as in (Ashley et al., 2005). Briefly, larvae were bathed in 0.5mM Ca^{++} HL3 saline (Stewart et al., 1994), and impaled with a 15-20MΩ electrode (filled with 3M potassium chloride). Only samples with resting potentials between -60 and -63 mV were used for quantification. The signal was collected through an Axoclamp2B (Molecular Devices) and digitally recorded with Pulse software (HEKA instruments). Miniature EJP events were analyzed using Minianalysis software (Synaptosoft). All data was quantitated using Origin software (Originlab), or KaleidaGraph (Synergy).

Recording from samples expressing NpHR was performed as follows. Samples were dissected in 0.3mM Ca^{++} HL3 saline, and then perfused with 0.5mM Ca^{++} HL3 saline, and impaled with a 15-20MΩ electrode as above. Evoked responses were triggered by 1msec suprathreshold stimulations (<5 V) of the segmental nerve, which was drawn into a 10µm suction electrode. After 2 minutes of evoked responses, the fluorescent shutter on the microscope was opened, exposing the preparation to 560nm light. The sample was continually recorded throughout the 2-minute exposure to the 560nm light pulse. Evoked signals were then analyzed using Minianalysis. As there were several pulses per animal that elicited no response, the number of failed responses per animal was divided by the total number of stimulations per animal and multiplied by 100 to give the percentage of failures.

S2 Cell Culture

Drosophila Schneider (S2) cells were cultured at 25 °C in SFX insect medium (HyClone) containing 10% FBS (HyClone), penicillin (50 U/ml) and streptomycin (50 µg/ml) (Sigma). Cells were maintained in Nunclon ^{TM} Δ Surface T-flasks (Thermo Scientific). For immunocytochemistry or coimmunoprecipitation4 experiments, cells were plated on 6-well Nunclon plates (Thermo Scientific) and when cells reached 60-80% confluency, they were transfected with 0.5 µg DNA using Effectene transfection kit (Qiagen). The following plasmids were used: pAc-Evi-EGFP (Bartscherer et al., 2006), pAc-Gal4, pUAST-Syt4 (Barber et al., 2009); pUAST-Syt4-C-Myc (see below); pAc-Syt4-V5 (see below); pAc-mCherry (Korkut et al., 2009). Cells were grown for 24- 48 hours and then processed for either immunocytochemistry or coimmunoprecipitation experiments. For exosome isolation and subsequent immunoelectron microscopy experiments, the following stable S2 cell lines with copper incucible promoters were used: Evi-EGFP (in pMK33 vector) (Koles et al., 2012), Syt4-C-HA (in pMT-puro vector) (see below). The Evi-EGFP stable cell line was maintained under 0.5 mg/ml hygromycin (Invitrogen) selection and the Syt4-C-HA stable cell line was maintained under 0.005 mg/ml puromycin (Invitrogen) selection.

Exosome Preparation

Exosomes were prepared as in (Lässer et al., 2012) with slight modifications. Shaking cultures of stable S2 cell line of pMT-puro-Syt4-C-HA were induced for 24 hours with 0.7 mM Cu_2SO4 before exosome isolation. Cells (3-4X106) were

pelleted by centrifugation at 600 g for 10 min. The supernatant was then cleared of larger debris by centrifugation at 16,500 g for 20 min. The supernatant was passed through a 0.22 µm filter and exosomes were pelleted at 120,000 g for 75 min. The resulting exosome pellet was resuspended in minimal volume of 100 mM Tris pH 7.4 and kept at -80 °C until further use or fixed overnight in 2% paraformaldehyde for subsequent immunoelectron microscopy.

Immunoelectron Microscopy of Exosomes

Exosomes were fixed in 2% paraformaldehyde at 4 °C overnight and 5µl was spotted onto formvar coated Nickel grids (200 mesh). Exosomes were allowed to adhere to the grids for 20 min at room temperature. Next, grids were rinsed in 2X 3 min washes of 0.1M Tris pH 7.4 and free aldehyde groups were quenched by 4X 3 min incubations in 50 mM glycine (in 0.1M Tris pH 7.4). The grids were subsequently blocked in 0.1M Tris pH 7.4 containing 5% BSA (w/v) with 0.05% (w/v) saponin for 10 min. Prior to antibody incubation step the grids were rinsed once briefly in 0.1M Tris pH 7.4 containing 0.5% BSA (w/v). Rat anti-HA (1:400, Roche) was used in blocking buffer (0.1M Tris pH 7.4 containing 5% BSA (w/v) and 0.2% (w/v) acetylated BSA-c (Aurion)) for both permeabilized and nonpermeabilized exosomes. After 1 hr of incubation at room temperature, grids were washed for 6X 3 min in wash buffer (0.1M Tris pH 7.4 containing 0.1% BSA (w/v) and 0.2% (w/v) acetylated BSA-c). After washing, the grids were blocked for 6X 3 min in blocking buffer (0.1M Tris pH 7.4 containing 0.5% BSA (w/v) and 0.2% (w/v) acetylated BSA-c). Secondary nanogold (1.4 nm) conjugated goat

anti-rat (1:60, Nanoprobes) in blocking buffer (0.1M Tris pH 7.4 containing 0.5% BSA (w/v) and 0.2% (w/v) acetylated BSA-c) for 1 hr. Grids were then rinsed for 8X 2 min in 0.1M Tris pH7.4 and the antibody complexes were crosslinked with 1% glutaraldehyde (in 0.1M Tris pH 7.4) for 1 min. The grids were washed for additional 8X 2 min in water and the nanogold particles were silver enhanced for 8-10 min using the HQ Silver (Nanoprobes) silver enhancement kit. The grids were washed for 8X 2 min in water and negatively stained as described in (Koles et al., 2012).

Immunoprecipitation and Western Blotting

For Syt4-C-myc and Evi-EGFP co-immunoprecipitation, 20 third instar larvae for each genotype were dissected in ice cold Ca^{++} free saline and body wall muscles together with the nervous system were homogenized in lysis buffer (20mM HEPES, 100mM KCl, 0.05% TritonX-100, 5% Glycerol, 2.5mM EDTA, 1mM Dithiothreitol, with protease inhibitors). Lysates were then precleared with Protein G beads (GE life sciences) and then incubated with 2 µg anti-c-myc (Roche) together with Protein G beads for 2 hrs at 4°C. After incubation, the beads were washed with ice cold PBS with 0.05% Triton X-100 and boiled with 2X SDS loading buffer for 5 minutes at 95°C and then separated by 8% SDSPAGE gel. Subsequently, they were transferred to a nitrocellulose membrane (Bio-Rad). The blot was probed with the following antibodies: rabbit anti-GFP (1:5000, Abcam Ab290, preabsorbed with S2 cell powder); mouse anti-c-myc (1:5000, Roche); anti-rabbit-HRP light chain (1:2000, Jackson

ImmunoResearch); anti-mouse-HRP (1:5000, Sigma). For endogenous Syt4 and Evi-EGFP co-immunoprecipitation, 50 third instar larvae for each genotype were dissected, such that only body wall muscles and the nervous system remained, and homogenized in lysis buffer as stated above. The lysates were precleared with Protein G beads and then incubated with ~5 µg chicken anti-Syt4^{leghorn} antibody (see below) overnight at 4°C. Then, samples were incubated with 4 µg anti-chicken antibody (Abcam, Ab8922) for 2 hrs and then with Protein G beads for an additional 1hr at 4°C. The samples were then washed with PBS with 0.05% Triton x-100, boiled with 2X loading buffer for 5 minutes at 95°C and then separated by 8% SDS-PAGE gel. Subsequently, they were transferred to a nitrocellulose membrane (Bio-Rad). The blot was probed with the following antibodies: anti-GFP (1:5000, Abcam Ab290, preabsorbed with S2 cell powder); chicken anti-Syt4^{egghead} (1:2000, preabsorbed with S2 cell powder); anti-chicken-HRP (1:10000, Jackson ImmunoResearch); anti-rabbit-HRP light chain (1:2000, Jackson ImmunoResearch). For co-immunoprecipitation of S2 cell extracts, S2 cells were transfected with pUAST-Syt4-C-myc or pUAST-Syt4, together with pAc-Evi-EGFP and pAc-Gal4, harvested and lysed as above. The IP were performed either with anti-c-myc (Roche) or chicken anti-Syt4^{leghorn} antibody as stated above.

RT-PCR

Total RNA was extracted by homogenizing dissected larval body wall muscles (without CNS) or larval brains in Trizol (Invitrogen) at 4 °C using a BBX24B Bullet

Blender Blue homogenizer (Next Advance Inc.) and then treating with DNase and eluting with the RNeasy Micro Kit (Qiagen). RNA concentrations were measured using a NanoDrop 2000c Spectrophotometer (Thermo scientific). cDNA was synthesized using a SuperScript III Kit (Invitrogen) from 500 ng of total RNA, primed with random hexamers. Reverse transcription reactions were then diluted to 1:12.5 and were amplified by PCR (35 cycles) with the following *syt4* primers. Forward: ATCCCAGATGCCAGCGTCAT; reverse: AATCGGGGAGGTGGACTGGT. Both of these primers were designed to hybridize with exon junctions, to avoid false signals from genomic DNA. For the GAPDH control experiment, the reverse transcription reactions were diluted to 1:50 and were amplified using the forward ACTCGACTCACGGTCGTTTC and reverse GCCGAGATGATGACCTTCTT primers.

Generation of Syt4 Antibodies

Anti-Syt4 polyclonal antibodies were raised by New England peptide by immunizing chickens with the peptides: KYSEEGDGPAQHAEQC and SKEIQPRSLKIRAC. Affinity purification of IgY isolates against KYSEEGDGPAQHAEQC sequence resulted in the anti-Syt4^{leghorn} and SKEIQPRSLKIRAC sequence resulted in anti-Syt4^{egghead}.

Molecular Biology

To generate pUAST-Syt4-C-Myc, Syt4 cDNA was PCR amplified from pUAST-Syt4 (Barber et al., 2009) using a forward primer containing an EcoRI site and a

reverse primer containing a NotI site. The PCR product was then ligated into a pUAST-5Myc plasmid, which was constructed by PCR amplifying 5 tandem Myc tags (1xMyc repeat = TCTGAGCAGAAGCTGATCTCCGAGGAGGACCTGAACGGA/ SEQKLISEEDLNG) with primers containing 5' KpnI and a 3' stop codon followed by an XbaI site. This 5Myc-stop PCR fragment was ligated into the KpnI-XbaI sites of pUAST yielding pUAST-5Myc-stop. To construct the pAc-Syt4-C-V5, Syt4 cDNA was PCR amplified from pUAST-Syt4 (Barber et al., 2009) using a forward primer containing an EcoRI site and a reverse primer containing an XhoI site. The PCR product was then ligated into a pAc5.1/V5-His plasmid (Invitrogen) to obtain a Cterminally V5 tagged Syt4. Syt4-HA was PCR amplified from pUAST-attB-Syt4- C-HA (see below) using a forward primer with an EcoRV site and a reverse primer with a NotI site. The PCR product was then ligated into pMT-puro plasmid (Addgene, ID: 17923). To make the original pUAST-attB-Syt4-HA, Syt4 cDNA was PCR amplified from pUAST-Syt4 (Barber et al., 2009) using a forward primer containing a NotI site and a reverse primer containing an AgeI site. The PCR product was then ligated into the pUAST-attB plasmid (from Dr. Konrad Basler). Subsequently, a synthetic oligonucleotide coding for three tandem HA tags- YPYDVPDYASGYPYDVPDYAGSYPYDVPDYAS (GS are linker amino acids) was ligated into the AgeI site of pUAST-attB-Syt4. To clone UAS-eNpHR3.0- EYFP, the pLenti-CaMKIIa-eNpHR3.0-EYFP vector (Zhang et al., 2010) was obtained from Dr. Carl Deisseroth, and the eNPHR3.0-EYFP was PCR amplified using the following primers: F-eNpHR3.0

(ATAATAGAATTCaacATGACAGAGACCCTGCCTCC) and R-EYFP (ATAATATCTAGATCATTACACCTCGTTCTCGT). The resultant PCR product was cloned into pWalium10 (GU931386) (TRIP Facility, Harvard) using EcoRI and XbaI restriction enzymes. UAS-eNpHR3.0-EYFP flies were prepared by targeting the construct to the attP2 site on the third chromosome (Genetivision).

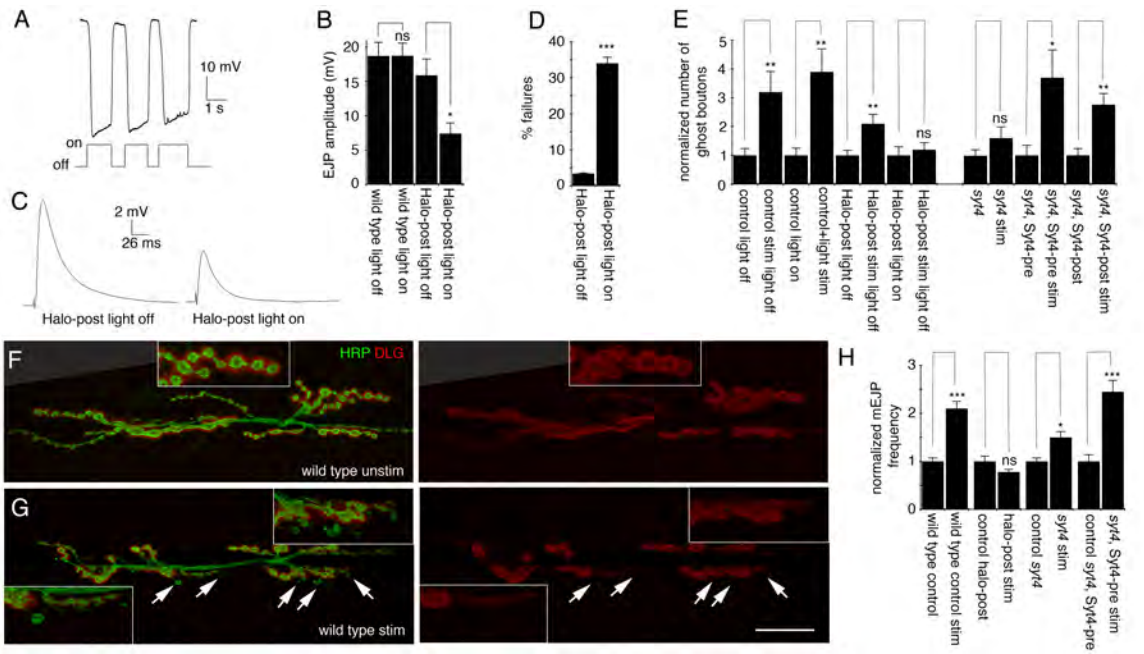

Figure 3.1. Retrograde control of synaptic growth and miniature release: role of Syt4.

(A) Rapid hyperpolarization of muscle membrane potential (upper trace) upon 560 nm illumination as shown in the bottom trace, in a 3rd instar larva expressing NpHR in muscle.

(B) Quantification of nerve-evoked EJP amplitude in wild type and postsynaptic NpHR-expressing larvae, showing that NpHR gating inhibits evoked potentials. N (from left to right) = 5, 5, 7, 7.

(C) Representative nerve-evoked EJP traces in control and upon activating NpHR in muscles.

(D) Percentage of undetected EJP (failures) in control and upon activating NpHR in muscles, showing that NpHR activation induces a 10-fold increase in failures. N (from left to right) =5, 7.

(E) Number of ghost boutons normalized to unstimulated controls induced after spaced stimulation of controls, animals expressing NpHR in muscles, and *syt4* mutants, showing that NpHR activation in muscles or a mutation in *syt4* suppresses activity-dependent nascent bouton formation and that the mutant phenotype can be rescued by expressing a wild type Syt4 transgene in either neurons or muscles. N (from left to right)= 14, 15, 11, 12, 27, 20, 16, 15, 28, 25, 15, 15, 15, 13.

(F, G) Representative NMJs from 3rd instar larval muscles 6 and 7 (A3) labeled with antibodies to HRP and DLG in unstimulated wild type **(F)** and **(G)** after spaced stimulation, showing the induction of nascent boutons (arrows) after stimulation. Insets are high magnification views of NMJ branches. Calibration bar is 25 μm for F, G and 13 μm for the insets.

(H) Quantification of mEJP frequency normalized to unstimulated controls. N (from left to right) = 27, 30, 24, 26, 21, 23, 21, 21.

***=p<0.001; **=p<0.01; *=p<0.05. Bars in plots represent mean±SEM.

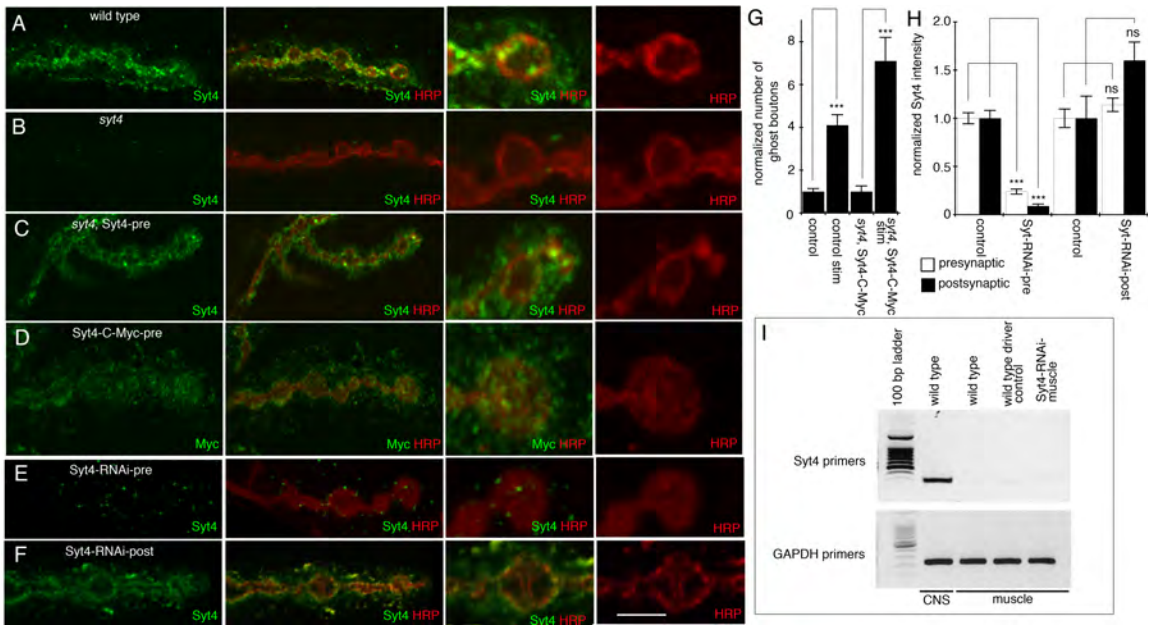

Figure 3.2. Syt4 is transferred from presynaptic boutons to postsynaptic muscle compartments.

(A-F) Confocal micrographs of 3rd instar larval NMJ branches at muscles 6 or 7 (A3) shown at low (left two columns) or high (right two columns) magnification labeled with antibodies to HRP and (**A-C, E, F**) anti-Syt4 or (**D**) anti-Myc. (**A**) wild type control showing the presence of endogenous Syt4 both inside synaptic boutons and at the postsynaptic muscle region;

(**B**) *syt4* null mutant, showing virtual absence of Syt4 immunoreactivity; (**C**) *syt4* null mutant expressing a wild type Syt4 transgene in neurons, showing the presence of transgenic Syt4 in both synaptic boutons and the postsynaptic muscle region, suggesting that Syt4 is transferred from the pre- to the postsynaptic compartment;

(**D**) a larva expressing Syt4-C-Myc in neurons, showing that Syt4-C-Myc is transferred to the postsynaptic region;

(**E**) a larva expressing Syt4-RNAi in neurons, showing that both pre- and postsynaptic Syt4 are virtually eliminated, and suggesting that endogenous postsynaptic Syt4 protein is derived from presynaptic boutons; (**F**) a larva expressing Syt4-RNAi in muscles shows no change in Syt4 levels. Calibration bar is 6 μm for A-F left two columns and 2.5 μm for A-F right two columns.

(G) Normalized number of ghost boutons in unstimulated and stimulated wild type controls, as well as in unstimulated and stimulated *syt4* mutants expressing the Syt4-C-Myc transgene in neurons, showing that this transgene can rescue the mutant phenotype.

(**H**) Quantification of Syt4 immunoreactivity levels normalized to control levels, showing that presynaptic Syt4 downregulation severely decreases Syt4 in both presynaptic boutons and postsynaptic muscles. In contrast, expressing Syt4-RNAi in muscle does not significantly alter Syt4 protein levels in either site.

(**I**) RT-PCR from larval CNS and muscles, showing that Syt4 mRNA can be detected in neurons but not in muscles with GAPDH mRNA levels shown as controls.

***=$p<0.0001$. Bars in plots represent mean±SEM.

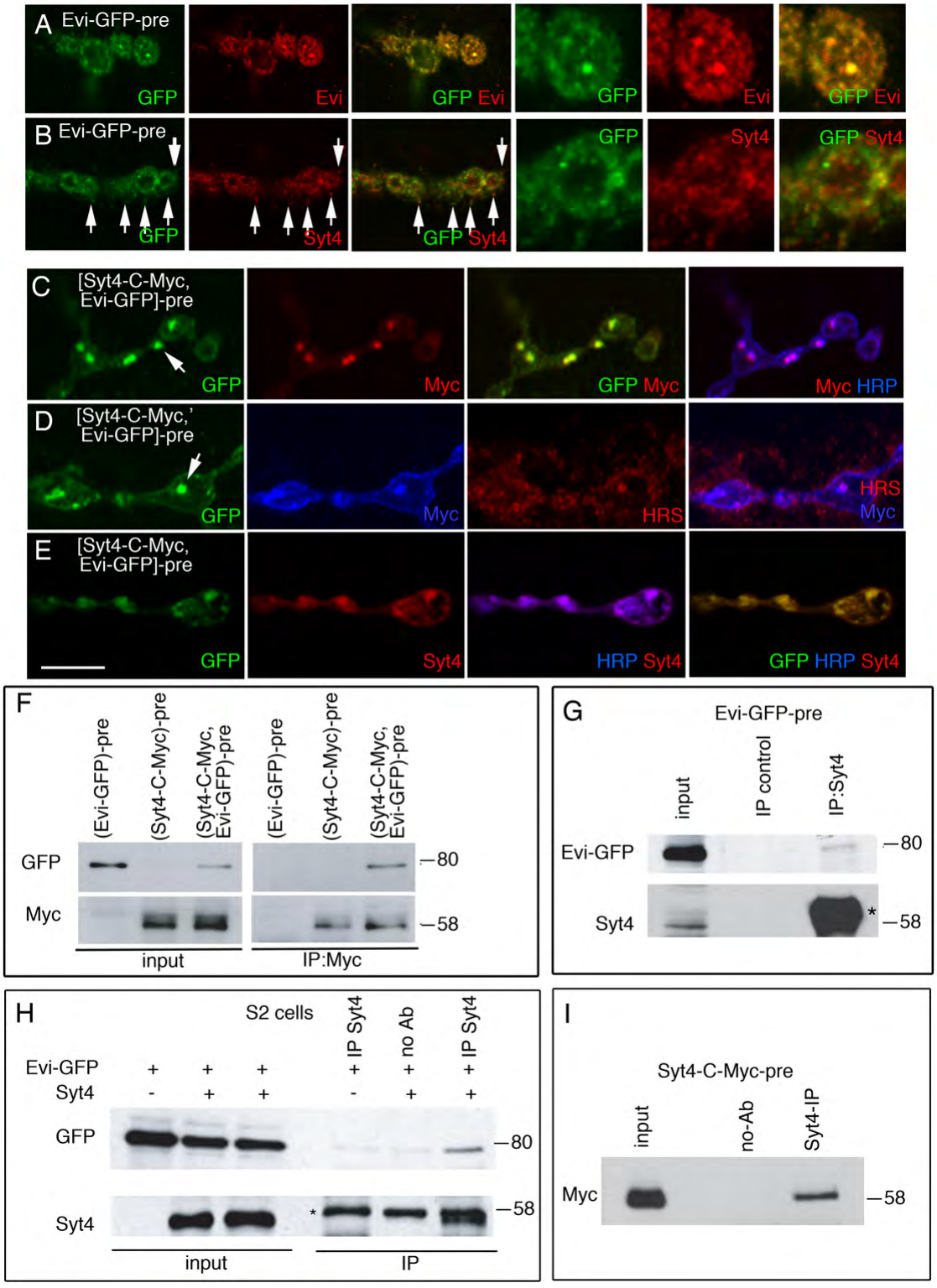

Figure 3.3. Syt4 and Evi colocalize in compartments at the NMJ and exist in a protein complex *in vivo*.

(A-E) Confocal images of 3rd instar larval NMJs at muscles 6 or 7 in larvae expressing (**A, B**) Evi-GFP in neurons and (**C-E**) both Evi-GFP and Syt4-C-Myc in neurons, labeled with antibodies to

(**A**) GFP and Evi, showing that transgenic Evi-GFP exactly colocalizes with endogenous Evi;

(**B**) GFP and Syt4, showing that Evi and Syt4 partially colocalize in synaptic compartments, particularly in postsynaptic puncta (arrows);

(**C**) GFP, Myc and HRP, showing that when both Evi and Syt4 are overexpressed, they become trapped within an internal compartment in synaptic boutons, and that neither of the proteins is transferred to the postsynaptic region;

(**D**) GFP, Myc and the endosomal marker, HRS, showing that Evi and Syt4 become trapped within a bouton endosome when co-overexpressed; (**E**) GFP, Syt4 (labeling both endogenous and transgenic Syt4), and HRP, showing that trapping Syt4 in presynaptic endosomes eliminates endogenous Syt4 signal in postsynaptic muscles, providing additional evidence that endogenous postsynaptic Syt4 is derived from synaptic boutons.

(**F**) Co-immunoprecipitation of Evi-GFP by Myc antibodies in body wall muscle extracts obtained from larvae expressing both Evi-GFP and Syt4-C-Myc in neurons, showing that Evi and Syt4 exist in a protein complex. (**G**) Co-immunoprecipitation of endogenous Syt4 and neuronally expressed Evi-GFP from body wall muscle extracts by using a Syt4 antibody raised in chicken. Note that the Syt4 band is partially occluded by chicken IgY (asterisk).

(H) Co-immunoprecipitation of Evi-GFP and untagged Syt4 by Syt4 antibody in S2 cells cotransfected with Evi-GFP and untagged Syt4. Asterisk marks chicken IgY heavy chain.

(I) Immunoprecipitation of Syt4-C-Myc by chicken Syt4 antibody in body wall muscle and CNS extract from larvae expressing Syt4-C-Myc in neurons, demonstrated by probing the blot with anti-Myc antibody. Numbers at the right of the blots correspond to molecular weight in kDa.

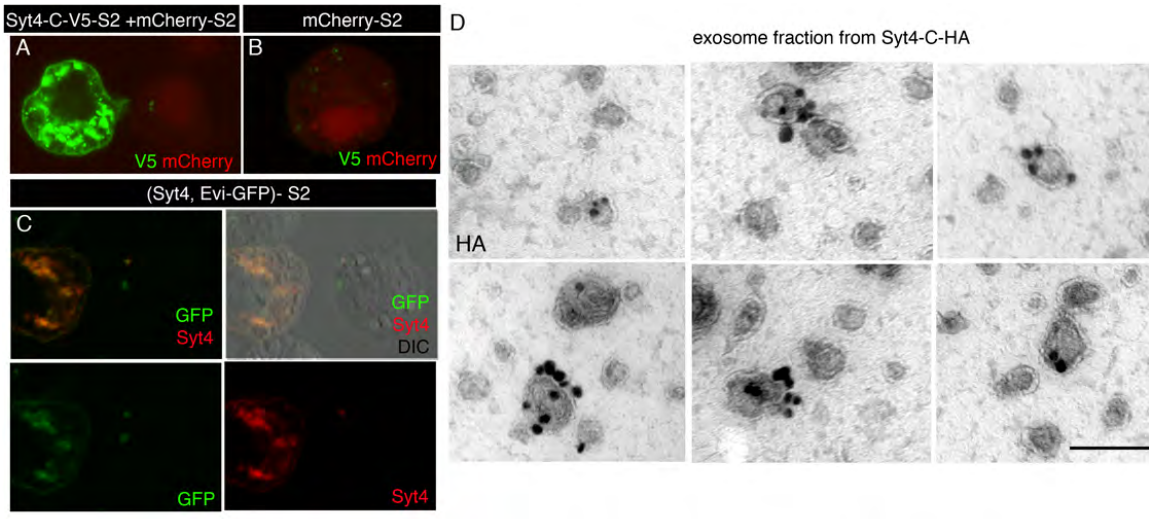

Figure 3.4. *Trans*-cellular transfer of Syt4 in S2 cells and localization of Syt4 in purified S2 cell exosomes.

(A-C) Confocal images of S2 cells labeled with (**A, B**) V5 antibodies and mCherry fluorescence in co-cultures of Syt4-C-V5 S2- and mCherry S2 cells. In (**A**) both a Syt4-C-V5 transfected and a mCherry transfected cell are observed. Note that V5 positive puncta are observed inside the mCherry cell, suggesting that Syt4-C-V5 is transferred transcellularly. In (**B**) a mCherry cell from the co-culture in (A) is shown, demonstrating the presence of transferred Syt4-C-V5 puncta. (**C**) Shows the transfer of Evi-GFP and or Syt4 containing exosomes to an untransfected cell from S2 cells co-expressing Evi-GFP and untagged Syt4.

(D) Electron micrographs of the purified exosome fraction from the culture medium of Syt4-C-HA transfected S2 cells, labeled with primary antibody to HA, followed by nanogold-conjugated secondary antibody and silver intensification. Calibration bar is 12 μm for A-C and 170 nm for D.

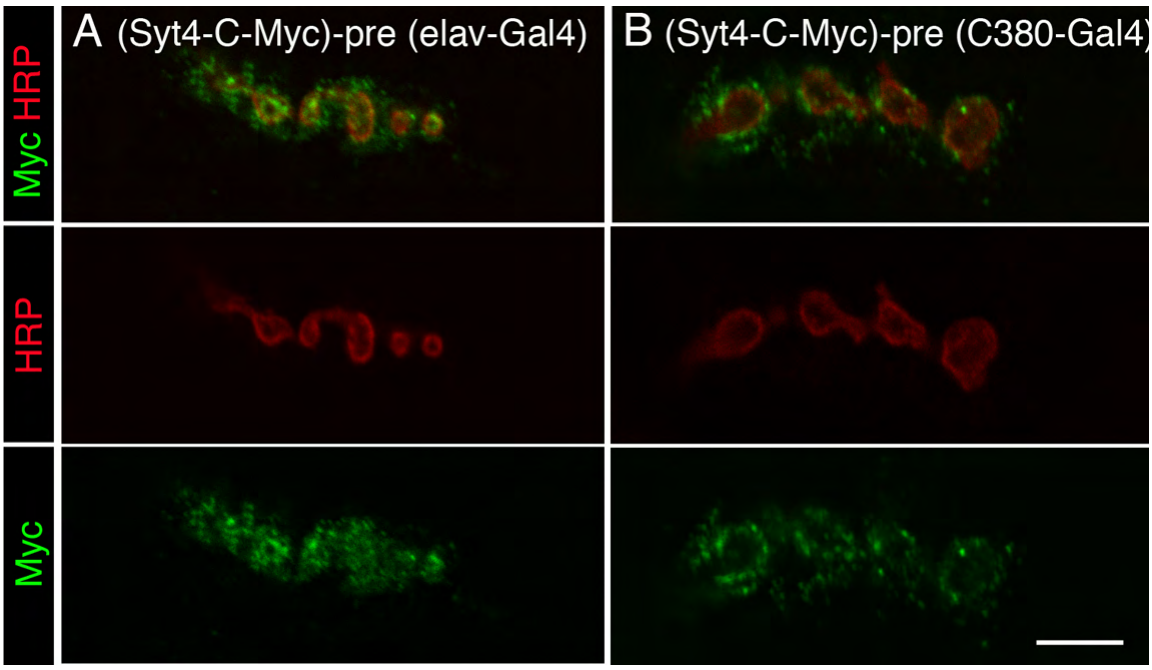

Suppl. Figure 3.1. Syt4-C-Myc transfer from synaptic boutons using different neuronal Gal4 drivers.

Neuromuscular junctions double labeled with anti-Myc and anti-HRP antibodies in larvae expressing Syt4-C-Myc with (**A**) the pan-neuronal driver, Elav-Gal4, and (**B**) the motorneuron driver C380-Gal4. Calibration bar is 5 µm.

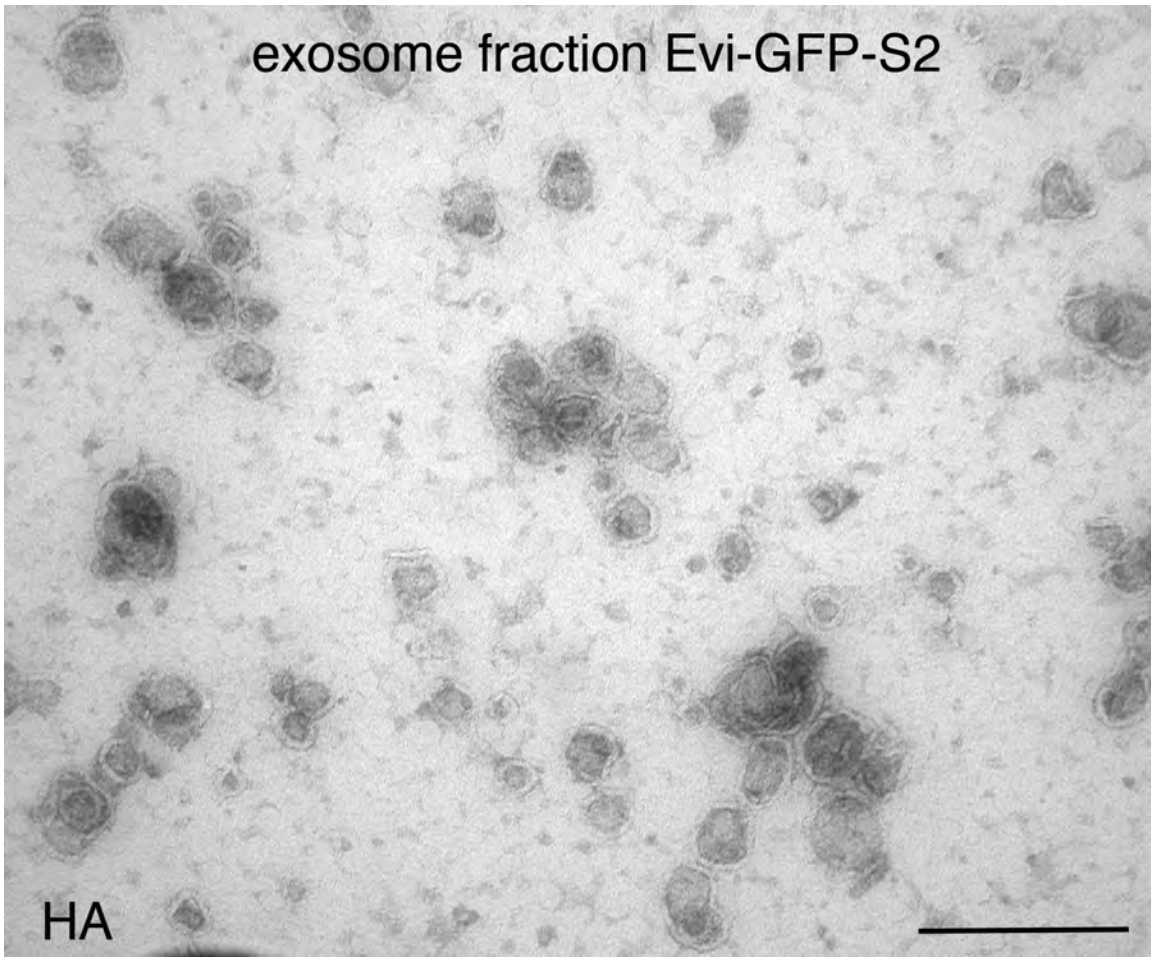

Suppl. Figure 3.2. Control for the exosome immunoelectron microscopy. Micrograph of purified exosomes from Evi-GFP-S2 cell medium labeled with anti-HA primary antibody and a nanogold-conjugated secondary followed by silver intensification. Note the absence of signal in the entire field. Calibration bar is 250 nm.

CHAPTER 4

DISCUSSION

Nervous system function relies on proper communication between pre- and postsynaptic cells. The primary means of intercellular communication in the nervous system is accomplished via the exocytosis of neurotransmitter vesicles or by electrical current flow through gap junctions. In addition, secreted signaling factors are crucial for normal synapse development, synapse maintenance and synaptic plasticity (Lu and Figurov, 1997; Marques, 2005). The coordinated development and functioning of the pre- and postsynapse require bi-directional signaling mechanisms. Signaling molecules act in an anterograde, retrograde or autocrine fashion to coordinate proper matching of pre- and postsynaptic function. At the *Drosophila* larval neuromuscular junction, WNT-1/Wingless is released from the motor neuron terminals in an activity-dependent manner and is critical for normal differentiation of both the pre- and postsynapse (Ataman et al., 2008; Packard et al., 2002). While the intracellular signal transduction pathways activated by WNT signals are well studied, the tightly regulated secretion and extracellular transport of highly hydrophobic WNT signals, until now, were not fully understood, not only at synapses but also during pattern formation in the embryo and in metamorphosing organisms (Hausmann et al., 2007). In the second chapter of my thesis, we identified a cellular mechanism by which Wingless (Wg) is secreted from presynaptic terminals and transported extracellularly in order to reach its receptor, DFrizzled-2 (DFz2), on the postsynaptic muscle cell membrane. Our study shows that the multipass transmembrane protein Evi/Wls/Srt, a WNT binding partner, is required for the secretion of Wg from motor neuron terminals and its navigation in the

extracellular space (Korkut et al., 2009). In this process, Evi functions to traffic Wg, intracellularly, from motor neuron cell bodies to presynaptic terminals, and extracellularly across the synapse, via exosomes, for presentation to its receptor on postsynaptic muscle membranes. This is a novel mechanism for *trans*-synaptic transfer of signals through exosomes. To my knowledge, this is the first instance in which exosomal communication across cells has been demonstrated in an intact living organism, and in particular during the *trans*-cellular transmission of a WNT signal. Additionally, we identified a function for Evi in the Wg-responsive postsynaptic muscle cell, where it is involved in the proper targeting of DFz2 receptors to the postsynaptic cell membrane through its interaction with the PDZ protein DGRIP. While previous studies had demonstrated that Evi is expressed in both the Wg-secreting and Wg-receiving cells (Port et al., 2008), the role of Evi in the signal-receiving cell had not been addressed.

In the third chapter of my thesis, I demonstrated that presynaptic cells can actually control the release of postsynaptic retrograde signals through the delivery of Synaptotagmin-4 (Syt4) (Korkut et al., 2012), a crucial component of the retrograde signaling machinery (Yoshihara et al., 2005), to postsynaptic muscle cells via presynaptic exosome release. We demonstrated that activity-dependent synaptic growth and potentiation of spontaneous neurotransmitter release require retrograde signaling depending on Syt4. We also showed that postsynaptic Syt4 protein is not likely generated in the postsynaptic muscle cell, but it is actually derived from presynaptic motor neuron terminals; presynaptic

terminals release Syt4-containing exosomes and muscle cells uptake these exosomes. We propose a mechanism by which the presynaptic cell regulates postsynaptic retrograde signaling through exosome release, thereby coordinating communication between the pre- and postsynaptic cell.

A Model for the Extracellular Movement of Hydrophobic WNT Signals

While the production, secretion and extracellular transport of WNT proteins are thought to be tightly regulated processes, little is known about the molecular and cellular mechanisms involved. The discovery that WNT proteins are lipid modified through acylation by palmitoyl and palmitoleoyl groups, most likely by the acyltransferase Porcupine in the endoplasmic reticulum, revealed that WNTs are in fact highly hydrophobic molecules that are probably membrane-associated (Kadowaki et al., 1996; Takada et al., 2006; Willert et al., 2003; Zhai et al., 2004). In contrast to prior belief, the hydrophobic nature of WNTs argues against a simple model of passive diffusion in the extracellular milieu. Porcupine had been the only known component in the WNT secretory pathway until Evi/Wls/Srt was identified simultaneously by three independent groups as a protein dedicated for WNT secretion (Banziger et al., 2006; Bartscherer et al., 2006; Goodman et al., 2006). The evolutionarily conserved multipass transmembrane protein Evi was shown to be required for trafficking WNTs from the *trans*-golgi network (TGN) to the plasma membrane of secreting cells for their release (Belenkaya et al., 2008; Franch-Marro et al., 2008; Pan et al., 2008; Port et al., 2008; Yang et al., 2008). Given that WNT secretion and its extracellular

transport are crucial, yet unclear processes, our findings described in Chapter 2 are highly significant. We propose a mechanism by which hydrophobic Wg can still travel in the extracellular space in association with membranous structures through its binding to Evi. This mechanism allows Wg to easily spread in the extracellular space upon its release.

Is the larval NMJ a good system to study extracellular WNT spread? At the NMJ, presynaptic boutons are surrounded by the subsynaptic reticulum (SSR), a specialized structure formed by a folded and multilayered extension of the postsynaptic muscle membrane. Although at the active zones, the sites of neurotransmitter release, the pre- and postsynaptic membranes are only separated by a 20 nm cleft and directly apposed to each other, the same is not true for the periactive bouton region of the membrane. Further, postsynaptic DFz2 receptors are located deep into SSR cisternae, and thus far away from the sites of Wg release. Our immuno-electron miscroscopy (immuno-EM) analysis of Evi localization shows that Evi is excluded from active zones (Korkut et al., 2009), and Evi-containing-vesicles are seen within SSR cisternae (Koles et al., 2012). Thus, Wg is required to travel a relatively long distance to bind to DFz2. Given this topology, it is likely that problems faced by the spread of Wg in the embryo are similar to those encountered at the NMJ.

We suggest that the membranous structures to which Wg and Evi are localized and transported extracellularly are most likely vesicles. This is the most parsimonious explanation to our observations that Wg is associated with a transmembrane protein, Evi, outside the secreting cells; that Evi is released most

likely as an intact protein; and that Evi is required for Wg secretion to the extracellular space. In the study described in Chapter 2, we proposed two potential models by which extracellular vesicles could be released from presynaptic terminals: (1) out-budding and scission of the plasma membrane to form an extracellular vesicle, or (2) fusion of a multivesicular body (MVB) with the plasma membrane, resulting in the release of exosome-like vesicles to the extracellular space. MVBs are formed by the inward budding of an endosomal limiting membrane to form intraluminal vesicles, which are released to the extracellular space upon fusion of the outer membrane of MVBs with the plasma membrane (Thery et al., 2009). The extracellular vesicles thus formed have been referred to as exosomes (Thery, 2011), and they serve both as intercellular signaling structures or for the disposal of obsolete cellular material (Record et al., 2011); and see below). The most likely nature of the Evi/Wg vesicles was unraveled in studies described below (Koles et al., 2012).

Evi-Vesicles are Exosomes

Various types of membrane vesicles have been shown to be released by cells into the extracellular environment. These extracellular vesicles have distinct structural and biochemical features (Thery et al., 2009). Both healthy and dying/apoptotic cells generate membrane-bound vesicles that are released to the extracellular milieu. However, vesicles from healthy and dying cells have different properties. For example, apoptotic vesicles are much larger and heterogenous in size; highly electron dense and they contain distinct proteins such as histones

(Thery et al., 2001). Even if released by healthy cells, extracellular vesicles differ in their size, shape, sedimentation coefficient, density on a sucrose gradient, protein and lipid composition, intracellular origin, and most importantly, their function. While some vesicles, such as microvesicles and ectosomes, originate from the plasma membrane of secreting cells, exosomes originate from endosomal MVBs. Among extracellular vesicles, exosomes are by far the best characterized, mostly due to their crucial function in antigen presentation during immune responses by T-cells (Thery et al., 2009). However, most, if not all cell types including cultured neurons secrete exosomes. Indeed, exosomes are found in all fluids so far examined, including milk, tears, seminal fluid, and blood (Simpson et al., 2008). The ability of exosomes to signal cellular processes is attracting considerable attention from the clinical perspective, as they could serve as important vectors to interfere with disease (Simpson et al., 2009).

In Chapter 2 of this thesis we demonstrated that Evi localizes to large multi-membrane structures inside presynaptic boutons. Similarly, Evi and Wg were found at MVBs in Wg-secreting cells of the *Drosophila* wing imaginal disc (Franch-Marro et al., 2008; Pfeiffer et al., 2002). Recently, I contributed to a study by the Budnik lab, where we further investigated the nature of Evi vesicles (Koles et al., 2012). Using electron microscopy, this study demonstrated that most synaptic boutons contain MVBs and that some MVBs are closely associated with the presynaptic cell membrane. Some MVBs appeared to be fusing with the presynaptic plasma membrane and releasing vesicular structures (Koles et al., 2012). Further, immuno-EM experiments showed that Evi is

localized within these MVBs and that Evi-labeled vesicles originating from presynaptic boutons could be found at the postsynaptic SSR.

Our studies also demonstrated that Evi is released to the culture medium and transferred to neighboring cells in *Drosophila* Schneider-2 (S2) cells (Korkut et al., 2009). In our recent study, Evi was found in S2 cell MVBs by using immuno-EM (Koles et al., 2012). The finding that Evi localizes to MVB both at the NMJ and in S2 cells and that Evi is secreted to the extracellular space in both systems, suggested that S2 cells constituted a good system to biochemically isolate exosomes and to determine if these secreted vesicles contained Evi. Exosomes were isolated from the supernatant of Evi-expressing S2 cells using an established protocol that involves differential centrifugation and density separation on a sucrose gradient (Koles et al., 2012; Thery et al., 2006). In these studies, Evi was found to be enriched over 100-fold in the exosome fraction compared to the cell lysate. Similarly, Wg was also enriched in this fraction. Typical protein markers of exosomes include tetraspanins, Alix and Tsg101. Therefore, as a positive control, *Drosophila* Alix and a tetraspanin family member Late Bloomer (Lbm) were also examined and demonstrated to be enriched in the exosome fraction compared with the cell lysate (Koles et al., 2012). Electron microscopy analysis of the purified exosome preparation also confirmed that they were in fact exosomes, as the unique shape and size matched exactly with the reported ‘’saucer-like’’ cup-shaped morphology of exosomes. Immuno-EM of the isolated exosome fraction, using an antibody against the extracellular domain of Evi, demonstrated that Evi was present in exosomes. All together, these findings

strongly suggest that Wg and Evi are released to the extracellular space on exosomes.

A role for exosomes in neuronal communication is just beginning to be recognized. In 2006, cultured cortical neurons were demonstrated to secrete exosomes to the culture media (Faure et al., 2006). Subsequent studies reported that exosome secretion was modulated by calcium influx and glutamatergic synaptic activity in cultured neurons, suggesting an exosome function in synaptic physiology (Lachenal et al., 2011). However, the function of exosomes *in vivo* had remained unclear. Our studies demonstrated that larval NMJs are likely to release exosomes for the presentation of hydrophobic Wg to postsynaptic DFz2 receptors (Koles et al., 2012; Korkut et al., 2009).

In 2008, a study from the Budnik lab showed that Wg is secreted from motor neuron terminals in an activity-dependent manner and that Wg signaling functions downstream of synaptic activity to induce structural and functional changes at the NMJ, in particular, the formation of new synaptic boutons (Ataman et al., 2008). Taken these findings into account, exosome release *in vivo* at the NMJ is likely to be modulated by synaptic activity. To investigate whether the release of exosomes from motor neuron terminals are regulated by synaptic activity, one could, for example, examine the level of exosome secretion before and after stimulation paradigms such as in (Ataman et al., 2008). Furthermore, to determine whether presynaptic exosome release is required for activity-dependent synapse formation, one could specifically disrupt the secretion of exosomes from the presynaptic terminals without affecting the classical

secretory pathway (see next section) and examine the NMJs to see whether new synapses form upon spaced stimulation.

Mechanisms for Evi-exosome Release at the NMJ

The mechanism for Evi-exosome release has been recently investigated using a dsRNA assay in cultured S2 cells (Koles et al., 2012). In this approach, the supernatant of dsRNA-treated Evi-expressing-S2 cells was applied to untransfected cells, searching for genes that when downregulated resulted in the absence of Evi-exosomes within untreated cells. Evi was then tested for its reduction in the culture medium from S2 cells treated with dsRNA against the candidate genes by Western blot. Then, the corresponding RNAi was expressed in the neurons of larvae simultaneously expressing Evi-GFP in motorneurons to determine if Evi-GFP transfer to the postsynaptic region of the NMJ was inhibited *in vivo* (Koles et al., 2012). The downregulation of several genes including the small GTPase Rab11 and Syntaxin1A (Syx1A) resulted in a significant reduction in the release of Evi exosomes from S2 cells without interrupting the classical secretory pathway. These results were confirmed i*n vivo* as motor neuron-specific interference of either Rab11 or Syx1A showed a significant reduction in Evi and Wg transfer to the postsynaptic cell. This study also demonstrated that the Rab11 effector and Syx1A-binding protein, Myosin 5 (Myo5), was required for Evi exosome release at the NMJ (Koles et al., 2012).

Rab family of proteins is composed of numerous members that regulate various steps of intracellular vesicle trafficking processes in a highly specific

manner (Zhang et al., 2007b). There are three Rab proteins, Rab11, Rab 27 and Rab35 that had been previously implicated in exosome release. Rab11 had been demonstrated to be involved in exosome secretion through docking and fusion of MVBs with the plasma membrane of a K562 myelogenous leukemia cell line (Savina et al., 2005). On the other hand, in HeLa cells, Rab27, but not Rab11, and in oligodendroglial cells, Rab35, played a role in exosome release (Hsu et al., 2010; Ostrowski et al., 2010). At the larval NMJ, downregulating Rab11, but not Rab27 or Rab35, prevented exosome release *in vivo* (Koles et al., 2012). These findings suggest that different cell types may employ distinct Rab proteins for exosome secretion. Also, it would be worthwhile to study *in vivo* functions of Rab27 and Rab35 in exosome release, as the above studies used only cultured cells.

Membrane fusion events depend on the formation of a SNARE complex that consists of a vesicle-associated, v-SNARE, and a target membrane-associated t-SNARE. Syntaxin 1A, a t-SNARE, has been known to be involved in synaptic vesicle exocytosis at the active zone (Schulze et al., 1995). Although Syx1A and Rab3 function in synaptic vesicle fusion, Syx1A and Rab11 are required for exosome release at the NMJ, consistent with the idea that Rabs function to target different types of vesicles to distinct membrane regions (Hutagalung and Novick, 2011). Interestingly, mass spectrometry analysis from exosomes derived from Drosophila S2 cells demonstrated the presence of Syx1A in exosomes (Koppen et al., 2011). It would be interesting to identify a v-SNARE anchored to the limiting membrane of MVBs that interacts with Syx1A.

The unconventional Myosin, Myo5, is a Syx1A binding protein and functions in anterograde transport of cargo to the cell periphery. Myo5 is also a Rab11 effector and disrupting its function in motor neurons results in a reduction in Evi-exosome release at the NMJ. Due to its role in the transport of vesicles along actin filaments, it is possible that Myo5 is involved in trafficking of MVBs to the presynaptic cell membrane at the NMJ. Moreover, it can be speculated that Myo5 could mediate the tethering of MVBs to the plasma membrane through its interaction with Syx1A. While the study by (Koles et al., 2012) focused on the role of only three proteins Rab11, Syx1A and Myo5 in exosome release, it is likely that numerous other candidate proteins exist. Liquid chromatography-tandem mass spectrometry of exosomes from S2 cells identified various classes of proteins such as cytoskeletal proteins, scaffolding proteins, G-proteins, vesicle trafficking and fusion proteins including a v-SNARE, Synaptobrevin. Studying candidate proteins from the mass spectrometry analysis *in vivo* can potentially provide insight in the mechanisms of exosome release and function.

Another emerging mechanism of exosome formation and trafficking is through the ESCRT complex (Endosomal Sorting Complex Required for Transport) and an adaptor protein, Alix. Exosomes are generated by inward budding of MBV limiting membrane. The four protein complexes composing the ESCRT are required for the sequential sorting of cargo proteins to MVBs and lysosomes. Subsequently, Alix mediates the inward budding of the MVB limiting membrane (Matsuo et al., 2004). While knocking down the ESCRT-0 complex component, Hrs (Hepatocyte Growth Factor-Regulated Tyrosine Kinase

Substrate), results in a significant reduction in exosome release from dendritic cells (Tamai et al., 2010), ESCRT- and Alix-independent exosome biogenesis mechanisms have also been identified (Fang et al., 2007; Trajkovic et al., 2008). Unpublished results from the Budnik lab suggest that Evi-exosome release is likely an ESCRT- and Alix-independent process as down regulation of some of these components (Hrs, Vps28, and Vps4) and Alix did not interfere with Evi-exosome secretion from S2 cells. These findings demonstrate that there are a variety of exosome populations and biogenesis mechanisms in different cell types.

The sorting of proteins into intraluminal vesicles of the MVB is thought to be a highly regulated, yet unclear process. There is some evidence that the ESCRT machinery that is localized on the limiting membrane of MVBs recognizes ubiquitinated proteins and sorts them into the vesicles (Record et al., 2011). The sorting of proteins for degradation by lysosomes is generally accomplished through ubiquitination of their cytoplasmic domains and subsequent recognition by the ESCRT. However, some proteins such as the transferring receptor (TfR) are sorted into intraluminal MVBs vesicles independent of ubiquitination (Marsh and van Meer, 2008). Moreover, a recent study demonstrated that targeting MHC II proteins to exosomes is completely independent of ubiquitination (Buschow et al., 2009). It has been suggested that the MVB sorting mechanism involving ubiquitination leads to lysosomal degradation, while the unbiquitination-independent pathway results in plasma membrane targeting of MVBs (Buschow et al., 2009). Although there is still much

to be uncovered, the mechanisms underlying distinct fates of MVBs are beginning to emerge. A recent study demonstrated that the sorting of proteins into exosome-generating MVBs depends on raft-based microdomains that contain high concentration of sphingolipid ceramide (Trajkovic et al., 2008). Moreover, an independent study showed that the sorting of MHC II into exosomes, rather than to lysosomes, correlated with its integration into detergent-resistant membranes of the MVB (Buschow et al., 2009). Therefore, it can be speculated that the targeting of proteins to exosomes depends on their incorporation into selected lipids within the MVB membrane.

Fate of Exosomes in Target Cells

Upon contact with their target cell membranes, exosomes have three possible routes: (1) direct fusion with the plasma membrane of the recipient cell, (2) endocytosis of the intact exosome and subsequent degradation by the recipient cell and (3) endocytosis of the intact exosome followed by fusion with the endosomal membrane of the recipient cell. While, the first and third routes allow the contents of the exosome vesicles to be exposed or delivered to the cytoplasm of the target cell, the second route does not expose the recipient cell to exosome contents. The physiological significance is that the first and third routes allow for the modulation of recipient cell function by delivering biologically active molecules such as signal transduction proteins and genetic material. The fate of exosomes in the recipient cell appears to depend on the cell type and phagocytic capabilities of the target cell (Record et al., 2011). Since miRNAs

have been found to be delivered by exosomes and to regulate gene expression in recipient cells, it is believed that exosomes have the ability to release their contents into the target cells (Valadi et al., 2007), supporting the use of route 1 and 3 in their transfer to the target cells. At the *Drosophila* NMJ, Wg is localized to the outer surface of exosomes, as the Wg binding domain in Evi projects to this side. Therefore, Wg becomes available for binding to its receptor, DFz2, on the target muscle membrane. However, the fate of exosomes after Wg interacts with postsynaptic DFz2 is not known. Nevertheless, we have shown that presynatically driven Evi is found inside the target muscle cell by immuno-EM, suggesting that the exosome is internalized. However, whether the sole function of all Evi-exosomes is to present Wg to DFz2 receptors, to carry additional signals to the postsynaptic cell, or to be targeted for degradation is not known.

In Chapter 3, we have demonstrated that the retrograde signaling component, Syt4, is delivered to the postsynaptic cell from the presynaptic terminals in exosomes. Syt4 has an N-terminal transmembrane domain, a linker sequence, and two C-terminal C2 domains (Sudhof, 2002). The functional C2 domains of Syt4 are located inside the exosomes. Therefore, for Syt4 to function in the muscle cells upon its delivery, the lumen of Syt4 exosomes should be exposed to the muscle cytoplasm. One way to determine if this is the case, would be to take advantage of the GRASP system (Feinberg et al., 2008), where GFP protein is split into two complementary fragments, spGFP1-10 and spGFP11. These individual fragments have high affinity for each other and are non-fluorescent unless they are reconstituted. Using the Gal4 and LexA systems,

Syt4 tagged with spGFP11 on its C-terminus could be expressed in the motor neurons while the other GFP fragment spGFP1-10 could be expressed in the cytoplasm of the muscle cell simultaneously. If the functional C-terminus of Syt4 were exposed to the cytoplasm of the target muscle cell, we would expect the two fragments of GFP to be reconstituted and fluoresce. A drawback of this approach is the possibility that the two complementary fragments of GFP are not brought close enough proximity to reconstitute. In addition, fluorescence from the reconstituted GFP signal may be weak to detect over autofluorescence. These limitations could be overcome using an approach that involves amplification in the exosome-receiving muscle cell. A Syt4-Gal4 fusion protein could be constructed so that if Gal4 is exposed to the muscle cytoplasm upon its transfer from the motor neuron terminals in exosomes, Gal4 gets cleaved and translocated into the nucleus where it induces reporter gene expression under UAS control. To achieve this, a specific cleavage site such as TEV (Tobacco Etch Virus) protease site, could be inserted between Syt4 and Gal4. This fusion construct could be expressed in motor neurons while the target muscle cell expresses the TEV protease that recognizes the specific cleavage site (Harder et al., 2008). Reporter gene expression in the muscle cells mean the lumen of Syt4-exosomes is exposed to the cytoplasm of the target muscle cells.

Presynaptic Exosomes Regulate Postsynaptic Retrograde Signaling through Syt4

Syt4 has been shown to play a postsynaptic role in retrograde signaling to regulate synaptic plasticity at the *Drosophila* NMJ. *syt4* null mutants failed to exhibit an increased spontaneous release (miniature frequency) upon high frequency stimulation. This defect was rescued by expressing a wild type Syt4 transgene in the postsynaptic muscle cell (Barber et al., 2009; Yoshihara et al., 2005). In addition to Syt4, postsynaptic Ca^{++} was demonstrated to be required for enhanced miniature release upon high frequency stimulation (Yoshihara et al., 2005). In chapter 3, we used a spaced stimulation paradigm that was also shown to increase spontaneous release at the larval NMJ (Ataman et al., 2008). In addition, the spaced stimulation paradigm induces structural changes such as rapid formation of ghost boutons, nascent boutons which have still not developed postsynaptic specializations or recruited postsynaptic proteins (Ataman et al., 2008). Our results identified a role for Syt4 in activity-dependent structural and functional changes at larval NMJ synapses. Interestingly, we show that expressing a full length Syt4 in presynaptic motorneurons is sufficient to rescue *syt4* null defects in ghost bouton formation upon spaced stimulation. We have also demonstrated that activity-dependent changes in synapses depend on retrograde signaling from the postsynaptic muscle cell. The findings that *syt4* transcript is virtually absent in muscles, the ability of Syt4-RNAi expressed in neurons to eliminate Syt4 protein in muscles, the observation that trapping Syt4 within presynaptic endosomes completely eliminates postsynaptic Syt4

immunoreactivity, and the localization of Syt4 on exosomes originating from the presynapse suggest a model where the postsynaptic Syt4 functions in retrograde signaling however it originally comes from the presynaptic motor neuron terminals. Because we have separate evidences that both Syt4 and retrograde signaling is involved on activity-dependent changes at synapses, it would be important to connect these two pieces of evidence and show that Syt4-dependent retrograde signaling plays a role in structural and functional changes at synapses upon activity. To achieve this, one can block postsynaptic depolarization in *syt4* null animals expressing a full length Syt4 transgene in the presynaptic cell and observe ghost bouton formation and potentiation of spontaneous release. The disruption in activity-dependent changes at synapses would be consistent with the model that presynaptic Syt4 transfers to the postsynaptic cell to function in a retrograde manner.

In conclusion, the studies in this dissertation have uncovered crucial cellular and molecular mechanisms relevant to synapse development and plasticity. The identification of a novel communication mechanism through exosome vesicles using *Drosophila* NMJ as a model system has advanced our understanding of nervous system communication. Since fundamental synaptic mechanisms are conserved between the fly NMJ synapses and mammalian excitatory synapses, it is likely that the mechanisms explained in this thesis are also essential for mammalian synapse function.

REFERENCES

Aberle, H., Haghighi, A.P., Fetter, R.D., McCabe, B.D., Magalhaes, T.R., and Goodman, C.S. (2002). wishful thinking Encodes a BMP Type II Receptor that Regulates Synaptic Growth in Drosophila. Neuron *33*, 545-558.

Adolfsen, B., Saraswati, S., Yoshihara, M., and Littleton, J.T. (2004). Synaptotagmins are trafficked to distinct subcellular domains including the postsynaptic compartment. J Cell Biol *166*, 249-260.

Agnel M, K.S., Vola C, Griffin-Shea R. (1989). Two transcripts from the rotund region of Drosophila show similar positional specificities in imaginal disc tissues. Genes Dev *3*, 85-95.

Alberini, C.M., Ghirardi, M., Huang, Y.Y., Nguyen, P.V., and Kandel, E.R. (1995). A molecular switch for the consolidation of long-term memory: cAMP-inducible gene expression. Ann N Y Acad Sci *758*, 261-286.

Anderson, M.S., Halpern, M.E., and Keshishian, H. (1988). Identification of the neuropeptide transmitter proctolin in Drosophila larvae: characterization of muscle fiber-specific neuromuscular endings. J Neurosci *8*, 242-255.

Ashley, J., Packard, M., Ataman, B., and Budnik, V. (2005). Fasciclin II signals new synapse formation through amyloid precursor protein and the scaffolding protein dX11/Mint. J Neurosci *25*, 5943-5955.

Ataman, B., Ashley, J., Gorczyca, D., Gorczyca, M., Mathew, D., Wichmann, C., Sigrist, S.J., and Budnik, V. (2006a). Nuclear trafficking of Drosophila Frizzled-2 during synapse development requires the PDZ protein dGRIP. Proc Natl Acad Sci U S A *103*, 7841-7846.

Ataman, B., Ashley, J., Gorczyca, M., Ramachandran, P., Fouquet, W., Sigrist, S.J., and Budnik, V. (2008). Rapid activity-dependent modifications in synaptic structure and function require bidirectional wnt signaling. Neuron *57*, 705-718.

Ataman, B., Budnik, V., and Thomas, U. (2006b). Scaffolding proteins at the Drosophila neuromuscular junction. Int Rev Neurobiol *75*, 181-216.

Atwood, H.L., Govind, C.K., and Wu, C.F. (1993). Differential ultrastructure of synaptic terminals on ventral longitudinal abdominal muscles in Drosophila larvae. J Neurobiol *24*, 1008-1024.

Babity, J.M., Armstrong, J.N., Plumier, J.C., Currie, R.W., and Robertson, H.A. (1997). A novel seizure-induced synaptotagmin gene identified by differential display. Proc Natl Acad Sci U S A *94*, 2638-2641.

Baeg, G.H., Lin, X., Khare, N., Baumgartner, S., and Perrimon, N. (2001). Heparan sulfate proteoglycans are critical for the organization of the extracellular distribution of Wingless. Development *128*, 87-94.

Banziger, C., Soldini, D., Schutt, C., Zipperlen, P., Hausmann, G., and Basler, K. (2006). Wntless, a conserved membrane protein dedicated to the secretion of Wnt proteins from signaling cells. Cell *125*, 509-522.

Barber, C.F., Jorquera, R.A., Melom, J.E., and Littleton, J.T. (2009). Postsynaptic regulation of synaptic plasticity by synaptotagmin 4 requires both C2 domains. J Cell Biol *187*, 295-310.

Barco, A., Bailey, C.H., and Kandel, E.R. (2006). Common molecular mechanisms in explicit and implicit memory. J Neurochem *97*, 1520-1533.

Baron, M., Aslam, H., Flasza, M., Fostier, M., Higgs, J.E., Mazaleyrat, S.L., and Wilkin, M.B. (2002). Multiple levels of Notch signal regulation (review). Mol Membr Biol *19*, 27-38.

Bartscherer, K., Pelte, N., Ingelfinger, D., and Boutros, M. (2006). Secretion of Wnt ligands requires Evi, a conserved transmembrane protein. Cell *125*, 523-533.

Belenkaya, T.Y., Wu, Y., Tang, X., Zhou, B., Cheng, L., Sharma, Y.V., Yan, D., Selva, E.M., and Lin, X. (2008). The retromer complex influences Wnt secretion by recycling wntless from endosomes to the trans-Golgi network. Dev Cell *14*, 120-131.

Berlucchi, G., and Buchtel, H.A. (2009). Neuronal plasticity: historical roots and evolution of meaning. Exp Brain Res *192*, 307-319.

Bliss, T.V., and Lomo, T. (1973). Long-lasting potentiation of synaptic transmission in the dentate area of the anaesthetized rabbit following stimulation of the perforant path. J Physiol *232*, 331-356.

Bourne, H.R., and Nicoll, R. (1993). Molecular machines integrate coincident synaptic signals. . Cell *72*, 65-75.

Brand, A.H., and Perrimon, N. (1993). Targeted gene expression as a means of altering cell fates and generating dominant phenotypes. Development *118*, 401-415.

Brose, N., Petrenko, A.G., Südhof, T.C., and Jahn, R. (1992). Synaptotagmin: a calcium sensor on the synaptic vesicle surface. Science *256*, 1021-1025.

Brown, R.E., and Milner, P.M. (2003). The legacy of Donald O. Hebb: more than the Hebb synapse. Nat Rev Neurosci *4*, 1013-1019.

Budnik, V., Gorczyca, M., and Prokop, A. (2006). Selected methods for the anatomical study of Drosophila embryonic and larval neuromuscular junctions. Int Rev Neurobiol *75*, 323-365.

Budnik, V., Koh, Y.H., Guan, B., Hartmann, B., Hough, C., Woods, D., and Gorczyca, M. (1996). Regulation of synapse structure and function by the Drosophila tumor suppressor gene dlg. Neuron *17*, 627-640.

Budnik, V., Zhong, Y., and Wu, C.F. (1990). Morphological plasticity of motor axons in Drosophila mutants with altered excitability. J Neurosci *10*, 3754-3768.

Buschow, S.I., Nolte-'t Hoen, E.N., van Niel, G., Pols, M.S., ten Broeke, T., Lauwen, M., Ossendorp, F., Melief, C.J., Raposo, G., Wubbolts, R*., et al.* (2009). MHC II in dendritic cells is targeted to lysosomes or T cell-induced exosomes via distinct multivesicular body pathways. Traffic *10*, 1528-1542.

Cajal, R.S. (1906). The structure and connexions of neurons. Nobel Lectures.

Cantera, R., and Nassel, D.R. (1992). Segmental peptidergic innervation of abdominal targets in larval and adult dipteran insects revealed with an antiserum against leucokinin I. Cell Tissue Res *269*, 459-471.

Caricasole, A., Bakker, A., Copani, A., Nicoletti, F., Gaviraghi, G., and Terstappen, G.C. (2005). Two sides of the same coin: Wnt signaling in neurodegeneration and neuro-oncology. Biosci Rep *25*, 309-327.

Chivet, M., Hemming, F., Pernet-Gallay, K., Fraboulet, S., and Sadoul, R. (2012). Emerging role of neuronal exosomes in the central nervous system. Front Physiol *3*, 145. Epub 2012 May 2028.

Ciani, L., Krylova, O., Smalley, M.J., Dale, T.C., and Salinas, P.C. (2004). A divergent canonical WNT-signaling pathway regulates microtubule dynamics: dishevelled signals locally to stabilize microtubules. J Cell Biol *164*, 243-253.

Collingridge, G.L., Kehl, S.J., and McLennan, H. (1983). Excitatory amino acids in synaptic transmission in the Schaffer collateral-commissural pathway of the rat hippocampus. J Physiol *334*.

Collins CA, W.Y., Johnson SL, DiAntonio A. (2006). Highwire restrains synaptic growth by attenuating a MAP kinase signal. Neuron *51*, 57-69.

Coudreuse, D.Y., Roel, G., Betist, M.C., Destree, O., and Korswagen, H.C. (2006). Wnt gradient formation requires retromer function in Wnt-producing cells. Science *312*, 921-924.

De Belle, J.S., and Heisenberg, M. (1994). Associative odor learning in Drosophila abolished by chemical ablation of mushroom bodies. . Science *263*, 692-695.

De Felipe, J. (2002). Sesquicentenary of the birthday of Santiago Ramon Y Cajal, the father of Modern Neuroscience. . Trends in Neurosciences *25*, 481-484.

De Ferrari, G.V., and Inestrosa, N.C. (2000). Wnt signaling function in Alzheimer's disease. Brain Res Brain Res Rev *33*, 1-12.

De Ferrari, G.V., and Moon, R.T. (2006). The ups and downs of Wnt signaling in prevalent neurological disorders. Oncogene *25*, 7545-7553.

de Gassart, A., Geminard, C., Fevrier, B., Raposo, G., and Vidal, M. (2003). Lipid raft-associated protein sorting in exosomes. Blood *102*, 4336-4344.

Dean, C., Liu, H., Dunning, F.M., Chang, P.Y., Jackson, M.B., and Chapman, E.R. (2009). Synaptotagmin-IV modulates synaptic function and long-term potentiation by regulating BDNF release. Nat Neurosci *12*, 767-776.

Eaton, B.A., and Davis, G.W. (2005). LIM Kinase1 controls synaptic stability downstream of the type II BMP receptor. Neuron *47*, 695-708.

Fang, Y., Wu, N., Gan, X., Yan, W., Morrell, J.C., and Gould, S.J. (2007). Higher-order oligomerization targets plasma membrane proteins and HIV gag to exosomes. PLoS Biol *5*, e158.

Faure, J., Lachenal, G., Court, M., Hirrlinger, J., Chatellard-Causse, C., Blot, B., Grange, J., Schoehn, G., Goldberg, Y., Boyer, V*., et al.* (2006). Exosomes are released by cultured cortical neurones. Mol Cell Neurosci *31*, 642-648.

Feinberg, E.H., Vanhoven, M.K., Bendesky, A., Wang, G., Fetter, R.D., Shen, K., and Bargmann, C.I. (2008). GFP Reconstitution Across Synaptic Partners (GRASP) defines cell contacts and synapses in living nervous systems. Neuron *57*, 353-363.

Ferguson, G.D., Vician, L., and Herschman, H.R. (2001). Synaptotagmin IV: biochemistry, genetics, behavior, and possible links to human psychiatric disease. Mol Neurobiol *23*, 173-185.

Fevrier, B., and Raposo, G. (2004). Exosomes: endosomal-derived vesicles shipping extracellular messages. Curr Opin Cell Biol *16*, 415-421.

Fjose, A., Ellingsen, S., Wargelius, A., and Seo, H.C. (2001). RNA interference: mechanisms and applications. Biotechnol Annu Rev *7*, 31-57.

Franch-Marro, X., Wendler, F., Guidato, S., Griffith, J., Baena-Lopez, A., Itasaki, N., Maurice, M.M., and Vincent, J.P. (2008). Wingless secretion requires endosome-to-Golgi retrieval of Wntless/Evi/Sprinter by the retromer complex. Nat Cell Biol *10*, 170-177.

Franciscovich, A.L., Mortimer, A.D., Freeman, A.A., Gu, J., and Sanyal, S. (2008). Overexpression screen in Drosophila identifies neuronal roles of GSK-3 beta/shaggy as a regulator of AP-1-dependent developmental plasticity. Genetics *180*, 2057-2071.

Franco, B., Bogdanik, L., Bobinnec, Y., Debec, A., Bockaert, J., Parmentier, M.L., and Grau, Y. (2004). Shaggy, the homolog of glycogen synthase kinase 3, controls neuromuscular junction growth in Drosophila. J Neurosci *24*, 6573-6577.

Futter, C.E., Pearse, A., Hewlett, L.J., and Hopkins, C.R. (1996). Multivesicular endosomes containing internalized EGF-EGF receptor complexes mature and then fuse directly with lysosomes. J Cell Biol *132*, 1022-1023.

Gagliardi, M., Piddini, E., and Vincent, J.P. (2008). Endocytosis: a positive or a negative influence on Wnt signalling? Traffic *9*, 1-9.
Gogel, S., Wakefield, S., Tear, G., Klambt, C., and Gordon-Weeks, P.R. (2006). The Drosophila microtubule associated protein Futsch is phosphorylated by Shaggy/Zeste-white 3 at an homologous GSK3beta phosphorylation site in MAP1B. Mol Cell Neurosci *33*, 188-199.
Gomez-Ospina, N., Tsuruta, F., Barreto-Chang, O., Hu, L., and Dolmetsch, R. (2006). The C terminus of the L-type voltage-gated calcium channel Ca(V)1.2 encodes a transcription factor. Cell *127*, 591-606.
Goodman, R.M., Thombre, S., Firtina, Z., Gray, D., Betts, D., Roebuck, J., Spana, E.P., and Selva, E.M. (2006). Sprinter: a novel transmembrane protein required for Wg secretion and signaling. Development *133*, 4901-4911.
Gorczyca, M., Augart, C., and Budnik, V. (1993). Insulin-like receptor and insulin-like peptide are localized at neuromuscular junctions in Drosophila. J Neurosci *13*, 3692-3704.
Gorczyca, M.a.B., V. (2006). Appendix: Anatomy of the larval body wall muscles and NMJs in the third instar larval stage. International Review of Neurobiology *75*, 367-373.
Gordon, M.D., and Nusse, R. (2006). Wnt signaling: multiple pathways, multiple receptors, and multiple transcription factors. J Biol Chem *281*, 22429-22433.
Gould, T.D., and Manji, H.K. (2002). The Wnt signaling pathway in bipolar disorder. Neuroscientist *8*, 497-511.
Greco, V., Hannus, M., and Eaton, S. (2001). Argosomes: a potential vehicle for the spread of morphogens through epithelia. Cell *106*, 633-645.
Grumbling G, S.V. (2006). FlyBase: anatomical data, images and queries. Nucleic Acids Res *34*, 484-488.
Harder, B., Schomburg, A., Pflanz, R., Küstner, K., Gerlach, N., and Schuh, R. (2008). TEV protease-mediated cleavage in Drosophila as a tool to analyze protein functions in living organisms. Biotechniques *44*, 765-772.

Harding, C., Heuser, J., and Stahl, P. (1983). Receptor-mediated endocytosis of transferrin and recycling of the transferrin receptor in rat reticulocytes. . J Cell Biol *97*, 329-339.
Harterink, M., and Korswagen, H.C. (2012). Dissecting the Wnt secretion pathway: key questions on the modification and intracellular trafficking of Wnt proteins. Acta Physiol (Oxf) *204*, 8-16.
Hausmann, G., Banziger, C., and Basler, K. (2007). Helping Wingless take flight: how WNT proteins are secreted. Nat Rev Mol Cell Biol *8*, 331-336.
Hebb, D.O. (1949). The Organization of Behavior; a Neuropsychological Theory. Wiley, New York, (reprinted by Lawrence Erlbaum Associates, 2002).
Heisenberg, M., Borst, A., Wagner, S., and Byers, D. (1985). Drosophila mushroom body mutants are deficient in olfactory learning. . J Neurogenet *2*, 1-30.
Hoogenraad, C.C., Milstein, A.D., Ethell, I.M., Henkemeyer, M., and Sheng, M. (2005). GRIP1 controls dendrite morphogenesis by regulating EphB receptor trafficking. Nat Neurosci *8*, 906-915.
Hsu, C., Morohashi, Y., Yoshimura, S., Manrique-Hoyos, N., Jung, S., Lauterbach, M.A., Bakhti, M., Gronborg, M., Mobius, W., Rhee, J.*, et al.* (2010). Regulation of exosome secretion by Rab35 and its GTPase-activating proteins TBC1D10A-C. J Cell Biol *189*, 223-232.
Hutagalung, A.H., and Novick, P.J. (2011). Role of Rab GTPases in membrane traffic and cell physiology. Physiol Rev *91*, 119-149.
Inestrosa, N., De Ferrari, G.V., Garrido, J.L., Alvarez, A., Olivares, G.H., Barria, M.I., Bronfman, M., and Chacon, M.A. (2002). Wnt signaling involvement in beta-amyloid-dependent neurodegeneration. Neurochem Int *41*, 341-344.
Ito, M., and Kano, M. (1982). Long-lasting depression of parallel fiber-Purkinje cell transmission induced by conjunctive stimulation of parallel fibers and climbing fibers in the cerebellar cortex. Neurosci Lett *33*.
James, W. (1890). The principles of psychology (London, MacMillan).
Jan, L.Y., and Jan, Y.N. (1976a). L-glutamate as an excitatory transmitter at the Drosophila larval neuromuscular junction. J Physiol (Lond) *262*, 215-236.

Jan, L.Y., and Jan, Y.N. (1976b). Properties of the larval neuromuscular junction in Drosophila melanogaster. J Physiol (Lond) *262*, 189-214.
Jan, L.Y., and Jan, Y.N. (1982). Antibodies to horseradish peroxidase as specific neuronal markers in Drosophila and in grasshopper embryos. Proc Natl Acad Sci U S A *79*, 2700-2704.
Jia, X.X., Gorczyca, M., and Budnik, V. (1993). Ultrastructure of neuromuscular junctions in Drosophila: comparison of wild type and mutants with increased excitability [published erratum appears in J Neurobiol 1994 Jul;25(7):893-5]. J Neurobiol *24*, 1025-1044.
Johansen, J., Halpern, M.E., Johansen, K.M., and Keshishian, H. (1989). Stereotypic morphology of glutamatergic synapses on identified muscle cells of Drosophila larvae. J Neurosci *9*, 710-725.
Johnson, M.L., and Rajamannan, N. (2006). Diseases of Wnt signaling. Rev Endocr Metab Disord *7*, 41-49.
Johnstone, R.M., Mathew, A., Mason, A.B., and Teng, K. (1991). Exosome formation during maturation of mammalian and avian reticulocytes: evidence that exosome release is a major route for externalization of obsolete membrane proteins. J Cell Physiol *147*, 27-36.
Kadowaki, T., Wilder, E., Klingensmith, J., Zachary, K., and Perrimon, N. (1996). The segment polarity gene porcupine encodes a putative multitransmembrane protein involved in Wingless processing. Genes Dev *10*, 3116-3128.
Keshishian, H., Chiba, A., Chang, T.N., Halfon, M.S., Harkins, E.W., Jarecki, J., Wang, L., Anderson, M., Cash, S., Halpern, M.E.*, et al.* (1993). Cellular mechanisms governing synaptic development in Drosophila melanogaster [published erratum appears in J Neurobiol 1993 Aug;24(8):1130]. J Neurobiol *24*, 757-787.
Keshishian, H., and Kim, Y.S. (2004). Orchestrating development and function: retrograde BMP signaling in the Drosophila nervous system. Trends Neurosci *27*, 143-147.

Kim, E., Niethammer, M., Rothschild, A., Jan, Y.N., and Sheng, M. (1995). Clustering of Shaker-type K+ channels by interaction with a family of membrane-associated guanylate kinases. Nature *378*, 85-88.

Koh, Y.H., Popova, E., Thomas, U., Griffith, L.C., and Budnik, V. (1999). Regulation of DLG localization at synapses by CaMKII-dependent phosphorylation. Cell *98*, 353-363.

Koles, K., Nunnari, J., Korkut, C., Barria, R., Brewer, C., Li, Y., Leszyk, J., Zhang, B., and Budnik, V. (2012). Mechanism of evenness interrupted (Evi)-exosome release at synaptic boutons. J Biol Chem *287*, 16820-16834.

Komada, M., Masaki, R., Yamamoto, A., and Kitamura, N. (1997). Hrs, a tyrosine kinase substrate with a conserved double zinc finger domain, is localized to the cytoplasmic surface of early endosomes. J Biol Chem *272*, 20538-20544.

Koon, A.C., Ashley, J., Barria, R., Dasgupta, S., Brain, R., Waddell, S., Alkema, M.J., and Budnik, V. (2011). Autoregulatory and paracrine control of synaptic and behavioral plasticity by octopaminergic signaling. Nat Neurosci *14*, 190-199.

Koon, A.C., and Budnik, V. (2012). Inhibitory control of synaptic and behavioral plasticity by octopaminergic signaling. J Neurosci *32*, 6312-6322.

Koppen, T., Weckmann, A., Muller, S., Staubach, S., Bloch, W., Dohmen, R.J., and Schwientek, T. (2011). Proteomics analyses of microvesicles released by Drosophila Kc167 and S2 cells. Proteomics.

Korkut, C., Ataman, B., Ramachandran, P., Ashley, J., Barria, R., Gherbesi, N., and Budnik, V. (2009). Trans-synaptic transmission of vesicular Wnt signals through Evi/Wntless. Cell *139*, 393-404.

Korkut, C., and Budnik, V. (2009). WNTs tune up the neuromuscular junction. Nat Rev Neurosci *10*, 627-634.

Korkut, C., Li, Y., Brewer, C., Koles, K., Ashley, J., Yoshihara, M., and Budnik, V. (2012). Regulation of postsynaptic retrograde signaling by presynaptic exosome release.

Krylova, O., Herreros, J., Cleverley, K.E., Ehler, E., Henriquez, J.P., Hughes, S.M., and Salinas, P.C. (2002). WNT-3, expressed by motoneurons, regulates

terminal arborization of neurotrophin-3-responsive spinal sensory neurons. Neuron *35*, 1043-1056.

Lachenal, G., Pernet-Gallay, K., Chivet, M., Hemming, F.J., Belly, A., Bodon, G., Blot, B., Haase, G., Goldberg, Y., and Sadoul, R. (2011). Release of exosomes from differentiated neurons and its regulation by synaptic glutamatergic activity. Mol Cell Neurosci *46*, 409-418.

Lai, S.L., and Lee, T. (2006). Genetic mosaic with dual binary transcriptional systems in Drosophila. Nat Neurosci *9*, 703-709.

Landgraf, M., Bossing, T., Technau, G.M., and Bate, M. (1997). The origin, location, and projections of the embryonic abdominal motorneurons of Drosophila. J Neurosci *17*, 9642-9655.

Landgraf, M., and Thor, S. (2006). Development and structure of motoneurons. Int Rev Neurobiol *75*, 33-53.

Lang, C., Barco, A., Zablowe, K., Kandel, E.R., Siegelbaum, S.A., and Zakharenko, S.S. (2004). Transient expansion of synaptically connected dendritic spines upon induction of hippocampal long-term potentiation. Proc Natl Acad Sci U S A *101*, 16665-16670.

Lässer, C., Eldh, M., and Lötvall, J. (2012). Isolation and characterization of RNA-containing exosomes. J Vis Exp *9*.

Laulagnier, K., Motta, C., Hamdi, S., Roy, S., Fauvelle, F., Pageaux, J.F., Kobayashi, T., Salles, J.P., Perret, B., Bonnerot, C.*, et al.* (2004). Mast cell- and dendritic cell-derived exosomes display a specific lipid composition and an unusual membrane organization. Biochem J *380*, 161-171.

Leenders, A.G., and Sheng, Z.H. (2005). Modulation of neurotransmitter release by the second messenger-activated protein kinases: implications for presynaptic plasticity. Pharmacol Ther *105*, 69-84.

Li, F., Chong, Z.Z., and Maiese, K. (2005). Vital elements of the Wnt-Frizzled signaling pathway in the nervous system. Curr Neurovasc Res *2*, 331-340.

Liebl, F.L., Wu, Y., Featherstone, D.E., Noordermeer, J.N., Fradkin, L., and Hing, H. (2008). Derailed regulates development of the Drosophila neuromuscular junction. Dev Neurobiol *68*, 152-165.

Lin, D.M., Fetter, R.D., Kopczynski, C., Grenningloh, G., and Goodman, C.S. (1994). Genetic analysis of Fasciclin II in Drosophila: defasciculation, refasciculation, and altered fasciculation. Neuron *13*, 1055-1069.

Lin, D.M., and Goodman, C.S. (1994). Ectopic and increased expression of Fasciclin II alters motoneuron growth cone guidance. Neuron *13*, 507-523.

Lin, S.Y., Makino, K., Xia, W., Matin, A., Wen, Y., Kwong, K.Y., Bourguignon, L., and Hung, M.C. (2001). Nuclear localization of EGF receptor and its potential new role as a transcription factor. Nat Cell Biol *3*, 802-808.

Littleton, J.T., Serano, T.L., Rubin, G.M., Ganetzky, B., and Chapman, E.R. (1999). Synaptic function modulated by changes in the ratio of synaptotagmin I and IV. Nature *400*, 757-760.

Lloyd TE, A.R., Wu MN, Zhou Y, Pennetta G, Bellen HJ. (2002). Hrs regulates endosome membrane invagination and tyrosine kinase receptor signaling in Drosophila. Cell *108*, 261-269.

Lloyd, T.E., and Taylor, J.P. (2010). Flightless Flies: Drosophila models of neuromuscular disease. Ann N Y Acad Sci *1184*, 1-20.

Logan, C.Y., and Nusse, R. (2004). The Wnt signaling pathway in development and disease. Annu Rev Cell Dev Biol *20*, 781-810.

Lu, B., and Figurov, A. (1997). Role of neurotrophins in synapse development and plasticity. Rev Neurosci *8*, 1-12.

Lucas, F.R., Goold, R.G., Gordon-Weeks, P.R., and Salinas, P.C. (1998). Inhibition of GSK-3beta leading to the loss of phosphorylated MAP-1B is an early event in axonal remodelling induced by WNT-7a or lithium. J Cell Sci *111*, 1351-1361.

Lucas, F.R., and Salinas, P.C. (1997). WNT-7a induces axonal remodeling and increases synapsin I levels in cerebellar neurons. Dev Biol *192*, 31-44.

Luo, L., Liao, Y.J., Jan, L.Y., and Jan, Y.N. (1994). Distinct morphogenetic functions of similar small GTPases: Drosophila Drac1 is involved in axonal outgrowth and myoblast fusion. Genes Dev *8*, 1787-1802.

Lynch, G., Larson, J., Kelso, S., Barrionuevo, G., and Schottler, F. (1983). Intracellular injections of EGTA block induction of hippocampal long-term potentiation. . Nature *305*, 719-721.

Lynch, M.A. (2004). Long-term potentiation and memory. Physiol Rev *84*, 87-136.

Lyu, J., Yamamoto, V., and Lu, W. (2008). Cleavage of the Wnt receptor Ryk regulates neuronal differentiation during cortical neurogenesis. Dev Cell *15*, 773-780.

Malenka, R.C., Kauer, J.A., Zucker, R.S., and Nicoll, R.A. (1988). Postsynaptic calcium is sufficient for potentiation of hippocampal synaptic transmission. Science *242*, 81-84.

Marques, G. (2005). Morphogens and synaptogenesis in Drosophila. J Neurobiol *64*, 417-434.

Marsh, M., and van Meer, G. (2008). Cell biology. No ESCRTs for exosomes. Science *319*, 1191-1192.

Mathew, D., Ataman, B., Chen, J., Zhang, Y., Cumberledge, S., and Budnik, V. (2005). Wingless signaling at synapses is through cleavage and nuclear import of receptor DFrizzled2. Science *310*, 1344-1347.

Mathew, D., Popescu, A., and Budnik, V. (2003). Drosophila amphiphysin functions during synaptic Fasciclin II membrane cycling. J Neurosci *23*, 10710-10716.

Matsuo, H., Chevallier, J., Mayran, N., Le Blanc, I., Ferguson, C., Faure, J., Blanc, N.S., Matile, S., Dubochet, J., Sadoul, R.*, et al.* (2004). Role of LBPA and Alix in multivesicular liposome formation and endosome organization. Science *303*, 531-534.

McCabe, B.D., Hom, S., Aberle, H., Fetter, R.D., Marques, G., Haerry, T.E., Wan, H., O'Connor, M.B., Goodman, C.S., and Haghighi, A.P. (2004). Highwire regulates presynaptic BMP signaling essential for synaptic growth. Neuron *41*, 891-905.

McGuire, S.E., Mao, Z., and Davis, R.L. (2004). Spatiotemporal gene expression targeting with the TARGET and gene-switch systems in Drosophila. Sci STKE *2004*, pl6.

Mendoza-Topaz, C., Urra, F., Barria, R., Albornoz, V., Ugalde, D., Thomas, U., Gundelfinger, E.D., Delgado, R., Kukuljan, M., Sanxaridis, P.D.*, et al.* (2008). DLGS97/SAP97 is developmentally upregulated and is required for complex adult behaviors and synapse morphology and function. J Neurosci *28*, 304-314.

Miech, C., Pauer, H.U., He, X., and Schwarz, T.L. (2008). Presynaptic local signaling by a canonical wingless pathway regulates development of the Drosophila neuromuscular junction. J Neurosci *28*, 10875-10884.

Mikels, A.J., and Nusse, R. (2006). Wnts as ligands: processing, secretion and reception. Oncogene *25*, 7461-7468.

Monastirioti, M., Gorczyca, M., Rapus, J., Eckert, M., White, K., and Budnik, V. (1995). Octopamine immunoreactivity in the fruit fly Drosophila melanogaster. J Comp Neurol *356*, 275-287.

Morris, R.G., Anderson, E., Lynch, G.S., and Baudry, M. (1986). Selective impairment of learning and blockade of long-term potentiation by an Nmethyl- D-aspartate receptor antagonist, AP5. . Nature *319*, 774-776.

Neumann, C.J., and Cohen, S.M. (1997). Long-range action of Wingless organizes the dorsal-ventral axis of the Drosophila wing. Development *124*, 871-880.

Nusse, R., and Varmus, H.E. (1982). Many tumors induced by the mouse mammary tumor virus contain a provirus integrated in the same region of the host genome. Cell *31*, 99-109.

Nusslein-Volhard, C., Kluding, H., and Jurgens, G. (1985). Genes affecting the segmental subdivision of the Drosophila embryo. Cold Spring Harb Symp Quant Biol *50*, 145-154.

Ostrowski, M., Carmo, N.B., Krumeich, S., Fanget, I., Raposo, G., Savina, A., Moita, C.F., Schauer, K., Hume, A.N., Freitas, R.P.*, et al.* (2010). Rab27a and Rab27b control different steps of the exosome secretion pathway. Nat Cell Biol *12*, 19-30; sup pp 11-13.

Packard, M., Koo, E.S., Gorczyca, M., Sharpe, J., Cumberledge, S., and Budnik, V. (2002). The Drosophila wnt, wingless, provides an essential signal for pre- and postsynaptic differentiation. Cell *111*, 319-330.

Packard, M., Mathew, D., and Budnik, V. (2003). Wnts and TGF beta in synaptogenesis: old friends signalling at new places. Nat Rev Neurosci *4*, 113-120.

Pan, B.T., Teng, K., Wu, C., Adam, M., and Johnstone, R.M. (1985). Electron microscopic evidence for externalization of the transferrin receptor in vesicular form in sheep reticulocytes. J Cell Biol *101*, 942-948.

Pan, C.L., Baum, P.D., Gu, M., Jorgensen, E.M., Clark, S.G., and Garriga, G. (2008). C. elegans AP-2 and retromer control Wnt signaling by regulating mig-14/Wntless. Dev Cell *14*, 132-139.

Panakova, D., Sprong, H., Marois, E., Thiele, C., and Eaton, S. (2005). Lipoprotein particles are required for Hedgehog and Wingless signalling. Nature *435*, 58-65.

Parnas, D., Haghighi, A.P., Fetter, R.D., Kim, S.W., and Goodman, C.S. (2001). Regulation of Postsynaptic Structure and Protein Localization by the Rho-Type Guanine Nucleotide Exchange Factor dPix. Neuron *32*, 415-424.

Pfeiffer, S., Ricardo, S., Manneville, J.B., Alexandre, C., and Vincent, J.P. (2002). Producing cells retain and recycle Wingless in Drosophila embryos. Curr Biol *12*, 957-962.

Pielage, J., Fetter, R.D., and Davis, G.W. (2005). Presynaptic spectrin is essential for synapse stabilization. Curr Biol *15*, 918-928.

Pittenger, C., and Kandel, E.R. (2003). In search of general mechanisms for long-lasting plasticity: Aplysia and the hippocampus. Philos Trans R Soc Lond B Biol Sci *358*, 757-763.

Port, F., and Basler, K. (2010). Wnt Trafficking: New Insights into Wnt Maturation, Secretion and Spreading. Traffic *3*, 3.

Port, F., Kuster, M., Herr, P., Furger, E., Banziger, C., Hausmann, G., and Basler, K. (2008). Wingless secretion promotes and requires retromer-dependent cycling of Wntless. Nat Cell Biol *10*, 178-185.

Potter, C.J., Tasic, B., Russler, E.V., Liang, L., and Luo, L. (2010). The Q system: a repressible binary system for transgene expression, lineage tracing, and mosaic analysis. Cell *141*, 536-548.

Prokop, A. (2006). Organization of the efferent system and structure of neuromuscular junctions in Drosophila. Int Rev Neurobiol *75*, 71-90.

Raposo, G., Nijman, H.W., Stoorvogel, W., Liejendekker, R., Harding, C.V., Melief, C.J., and Geuze, H.J. (1996a). B lymphocytes secrete antigen-presenting vesicles. J Exp Med *183*, 1161-1172.

Raposo, G., Nijman, H.W., Stoorvogel, W., Liejendekker, R., Harding, C.V., Melief, C.J., and Geuze, H.J. (1996b). B lymphocytes secrete antigen-presenting vesicles. . J Exp Med *183*, 1161-1172.

Raposo, G., Tenza, D., Mecheri, S., Peronet, R., Bonnerot, C., and Desaymard, C. (1997). Accumulation of major histocompatibility complex class II molecules in mast cell secretory granules and their release upon degranulation. Mol Biol Cell *8*, 3631-3645.

Record, M., Subra, C., Silvente-Poirot, S., and Poirot, M. (2011). Exosomes as intercellular signalosomes and pharmacological effectors. Biochem Pharmacol *81*, 1171-1182.

Rijsewijk, F., Schuermann, M., Wagenaar, E., Parren, P., Weigel, D. and Nusse, R. (1987). The Drosophila homolog of the mouse mammary oncogene int-1 is identical to the segment polarity gene wingless. . Cell *50*, 649 -657.

Rosso, S.B., Sussman, D., Wynshaw-Boris, A., and Salinas, P.C. (2005). Wnt signaling through Dishevelled, Rac and JNK regulates dendritic development. Nat Neurosci *8*, 34-42. Epub 2004 Dec 2019.

Ruiz-Canada, C., and Budnik, V. (2006). Introduction on the use of the Drosophila embryonic/larval neuromuscular junction as a model system to study synapse development and function, and a brief summary of pathfinding and target recognition. Int Rev Neurobiol *75*, 1-31.

Salinas, P.C., and Zou, Y. (2008). Wnt signaling in neural circuit assembly. Annu Rev Neurosci *31*, 339-358.

Sanyal, S., Narayanan, R., Consoulas, C., and Ramaswami, M. (2003). Evidence for cell autonomous AP1 function in regulation of Drosophila motor-neuron plasticity. BMC Neurosci *4*, 20.

Savina, A., Fader, C.M., Damiani, M.T., and Colombo, M.I. (2005). Rab11 promotes docking and fusion of multivesicular bodies in a calcium-dependent manner. Traffic *6*, 131-143.

Savina, A., Furlán, M., Vidal, M., and Colombo, M.I. (2003). Exosome release is regulated by a calcium-dependent mechanism in K562 cells. J Biol Chem *278*, 20083-20090.

Schulze, K.L., Broadie, K., Perin, M.S., and Bellen, H.J. (1995). Genetic and electrophysiological studies of Drosophila syntaxin-1A demonstrate its role in nonneuronal secretion and neurotransmission. Cell *80*, 311-320.

Schuster, C.M., Davis, G.W., Fetter, R.D., and Goodman, C.S. (1996). Genetic dissection of structural and functional components of synaptic plasticity. I. Fasciclin II controls synaptic stabilization and growth. Neuron *17*, 641-654.

Selkoe, D.J., Yamazaki, T., Citron, M., Podlisny, M.B., Koo, E.H., Teplow, D.B., and Haass, C. (1996). The role of APP processing and trafficking pathways in the formation of amyloid beta-protein. Ann N Y Acad Sci *777*, 57-64.

Siegfried, E., and Perrimon, N. (1994). Drosophila wingless: a paradigm for the function and mechanism of Wnt signaling. Bioessays *16*, 395-404.

Simons, M., and Raposo, G. (2009). Exosomes--vesicular carriers for intercellular communication. Curr Opin Cell Biol *21*, 575-581.

Simpson, R.J., Jensen, S.S., and Lim, J.W. (2008). Proteomic profiling of exosomes: current perspectives. Proteomics *8*, 4083-4099.

Simpson, R.J., Lim, J.W., Moritz, R.L., and Mathivanan, S. (2009). Exosomes: proteomic insights and diagnostic potential. Expert Rev Proteomics *6*, 267-283.

Song, Y., and Balice-Gordon, R. (2008). New dogs in the dogma: Lrp4 and Tid1 in neuromuscular synapse formation. Neuron *60*, 526-528.

Speese, S.D., and Budnik, V. (2007). Wnts: up-and-coming at the synapse. Trends Neurosci *30*, 268-275.

Stewart, B.A., Atwood, H.L., Renger, J.J., Wang, J., and Wu, C.-F. (1994). Drosophila neuromuscular preparations in haemolymph-like physiological salines. . J Comp Physiol *(A)175*, 179-191.

Subra, C., Laulagnier, K., Perret, B., and Record, M. (2007). Exosome lipidomics unravels lipid sorting at the level of multivesicular bodies. Biochimie *89*, 205-212.

Sudhof, T.C. (2002). Synaptotagmins: why so many? J Biol Chem *277*, 7629-7632.

Sudhof, T.C., and Rizo, J. (1996). Synaptotagmins: C2-domain proteins that regulate membrane traffic. Neuron *17*, 379-388.

Takada, R., Satomi, Y., Kurata, T., Ueno, N., Norioka, S., Kondoh, H., Takao, T., and Takada, S. (2006). Monounsaturated fatty acid modification of Wnt protein: its role in Wnt secretion. Dev Cell *11*, 791-801.

Tamai, K., Tanaka, N., Nakano, T., Kakazu, E., Kondo, Y., Inoue, J., Shiina, M., Fukushima, K., Hoshino, T., Sano, K.*, et al.* (2010). Exosome secretion of dendritic cells is regulated by Hrs, an ESCRT-0 protein. Biochem Biophys Res Commun *399*, 384-390.

Tejedor, F.J., Bokhari, A., Rogero, O., Gorczyca, M., Zhang, J., Kim, E., Sheng, M., and Budnik, V. (1997). Essential role for dlg in synaptic clustering of Shaker K+ channels in vivo. J Neurosci *17*, 152-159.

Thery, C. (2011). Exosomes: secreted vesicles and intercellular communications. F1000 Biol Rep *3*, 15.

Thery, C., Amigorena, S., Raposo, G., and Clayton, A. (2006). Isolation and characterization of exosomes from cell culture supernatants and biological fluids. Curr Protoc Cell Biol *Chapter 3*, Unit 3 22.

Thery, C., Boussac, M., Véron, P., Ricciardi-Castagnoli, P., Raposo, G., Garin, J., and Amigorena, S. (2001). Proteomic analysis of dendritic cell-derived exosomes: a secreted subcellular compartment distinct from apoptotic vesicles. J Immunol *166*, 7309-7318.

Thery, C., Ostrowski, M., and Segura, E. (2009). Membrane vesicles as conveyors of immune responses. Nat Rev Immunol *9*, 581-593.

Thomas, U., Kim, E., Kuhlendahl, S., Koh, Y.H., Gundelfinger, E.D., Sheng, M., Garner, C.C., and Budnik, V. (1997). Synaptic clustering of the cell adhesion molecule fasciclin II by discs-large and its role in the regulation of presynaptic structure. Neuron *19*, 787-799.

Torroja, L., Chu, H., Kotovsky, I., and White, K. (1999). Neuronal overexpression of APPL, the Drosophila homologue of the amyloid precursor protein (APP), disrupts axonal transport. Curr Biol *9*, 489-492.

Trajkovic, K., Hsu, C., Chiantia, S., Rajendran, L., Wenzel, D., Wieland, F., Schwille, P., Brugger, B., and Simons, M. (2008). Ceramide triggers budding of exosome vesicles into multivesicular endosomes. Science *319*, 1244-1247.

Trams, E.G., Lauter, C.J., Salem, N.J., and Heine, U. (1981). Exfoliation of membrane ecto-enzymes in the form of micro-vesicles. Biochim Biophys Acta *645*, 63-70.

Valadi, H., Ekstrom, K., Bossios, A., Sjostrand, M., Lee, J.J., and Lotvall, J.O. (2007). Exosome-mediated transfer of mRNAs and microRNAs is a novel mechanism of genetic exchange between cells. Nat Cell Biol *9*, 654-659.

van Amerongen, R., and Nusse, R. (2009). Towards an integrated view of Wnt signaling in development. Development *136*, 3205-3214.

van den Heuvel, M., Nusse, R., Johnston, P., and Lawrence, P.A. (1989). Distribution of the wingless gene product in Drosophila embryos: a protein involved in cell-cell communication. Cell *59*, 739-749.

van Niel, G., Porto-Carreiro, I., Simoes, S., and Raposo, G. (2006). Exosomes: a common pathway for a specialized function. J Biochem *140*, 13-21.

Vician, L., Lim, I.K., Ferguson, G., Tocco, G., Baudry, M., and Herschman, H.R. (1995). Synaptotagmin IV is an immediate early gene induced by depolarization in PC12 cells and in brain. Proc Natl Acad Sci U S A *92*, 2164-2168.

Widelitz, R. (2005). Wnt signaling through canonical and non-canonical pathways: recent progress. Growth Factors *23*, 111-116.

Willert, K., Brown, J.D., Danenberg, E., Duncan, A.W., Weissman, I.L., Reya, T., Yates, J.R., 3rd, and Nusse, R. (2003). Wnt proteins are lipid-modified and can act as stem cell growth factors. Nature *423*, 448-452.

Wodarz, A., and Nusse, R. (1998). Mechanisms of Wnt signaling in development. Annu Rev Cell Dev Biol *14*, 59-88.

Yang, P.T., Lorenowicz, M.J., Silhankova, M., Coudreuse, D.Y., Betist, M.C., and Korswagen, H.C. (2008). Wnt signaling requires retromer-dependent recycling of MIG-14/Wntless in Wnt-producing cells. Dev Cell *14*, 140-147.

Yoshihara, M., Adolfsen, B., Galle, K.T., and Littleton, J.T. (2005). Retrograde signaling by Syt 4 induces presynaptic release and synapse-specific growth. Science *310*, 858-863.

Zhai, L., Chaturvedi, D., and Cumberledge, S. (2004). Drosophila wnt-1 undergoes a hydrophobic modification and is targeted to lipid rafts, a process that requires porcupine. J Biol Chem *279*, 33220-33227.

Zhang, F., Gradinaru, V., Adamantidis, A.R., Durand, R., Airan, R.D., de Lecea, L., and Deisseroth, K. (2010). Optogenetic interrogation of neural circuits: technology for probing mammalian brain structures. Nat Protoc *5*, 439-456.

Zhang, F., Wang, L.P., Brauner, M., Liewald, J.F., Kay, K., Watzke, N., Wood, P.G., Bamberg, E., Nagel, G., Gottschalk, A.*, et al.* (2007a). Multimodal fast optical interrogation of neural circuitry. Nature *446*, 633-639.

Zhang, J., Schulze, K.L., Hiesinger, P.R., Suyama, K., Wang, S., Fish, M., Acar, M., Hoskins, R.A., Bellen, H.J., and Scott, M.P. (2007b). Thirty-one flavors of Drosophila rab proteins. Genetics *176*, 1307-1322.

Zhao, C., Aviles, C., Abel, R.A., Almli, C.R., McQuillen, P., and Pleasure, S.J. (2005). Hippocampal and visuospatial learning defects in mice with a deletion of frizzled 9, a gene in the Williams syndrome deletion interval. Development *132*, 2917-2927.

Zhong, W. (2008). Going nuclear is again a winning (Wnt) strategy. Dev Cell *15*, 635-636.

Zhong, Y., Budnik, V., and Wu, C.F. (1992). Synaptic plasticity in Drosophila memory and hyperexcitable mutants: role of cAMP cascade. J Neurosci *12*, 644-651.

Zito, K., Fetter, R.D., Goodman, C.S., and Isacoff, E.Y. (1997). Synaptic clustering of Fascilin II and Shaker: essential targeting sequences and role of Dlg. Neuron *19*, 1007-1016.

Zito, K., Parnas, D., Fetter, R.D., Isacoff, E.Y., and Goodman, C.S. (1999). Watching a synapse grow: noninvasive confocal imaging of synaptic growth in Drosophila. Neuron *22*, 719-729.

Zitvogel, L., Regnault, A., Lozier, A., Wolfers, J., Flament, C., Tenza, D., Ricciardi-Castagnoli, P., Raposo, G., and Amigorena, S. (1998). Eradication of established murine tumors using a novel cell-free vaccine: dendritic cellderived exosomes. Nat Med *4*, 594-600.